



Functional characterization of GPI-anchored proteins of the SKU5/SKS gene family

Ke Zhou

► To cite this version:

Ke Zhou. Functional characterization of GPI-anchored proteins of the SKU5/SKS gene family. Plants genetics. Université Paris Sud - Paris XI, 2013. English. NNT : 2013PA112096 . tel-01066888

HAL Id: tel-01066888

<https://theses.hal.science/tel-01066888>

Submitted on 22 Sep 2014

HAL is a multi-disciplinary open access archive for the deposit and dissemination of scientific research documents, whether they are published or not. The documents may come from teaching and research institutions in France or abroad, or from public or private research centers.

L'archive ouverte pluridisciplinaire **HAL**, est destinée au dépôt et à la diffusion de documents scientifiques de niveau recherche, publiés ou non, émanant des établissements d'enseignement et de recherche français ou étrangers, des laboratoires publics ou privés.



Comprendre le monde,
construire l'avenir®



UNIVERSITE PARIS-SUD

ÉCOLE DOCTORALE : SCIENCES DU VÉGÉTAL
Laboratoire de Catherine PERROT-RECHENMANN, ISV, CNRS

DISCIPLINE : BIOLOGIE

THÈSE DE DOCTORAT

Soutenance prévue le 21/06/2013

par

Ke ZHOU

**Functional characterization of GPI-anchored proteins of the
SKU5/SKS gene family**

Composition du jury :

Directeur de thèse :

Rapporteurs :

Examineurs :

Catherine PERROT-RECHENMANN

Sébastien MONGRAND

Pierre CAROL

Dao ZHOU

Jacqui SHYKOFF

DR CNRS

Professeur

Professeur

Professeur

DR CNRS

Abstract:

ABP1 (Auxin Binding Protein1), who can bind auxin, is essential for the development of plants. It was proved to have the ability to bind auxin and transduce auxin signal into the cells. It is supposed to be localized and functions at the outer surface of plasma membrane through unknown component.

In my theiss, we tried to investigate the interaction between ABP1 and the candidate of the unknown component, CBP1 (From maize), which is GPI-anchored and already identified as the binding ability to synthesized C-terminus peptide of ABP1 in 2006.

The orthologous of CBP1 in arabidopsis belongs to a gene family with 19 members, in which only three of them were predicted to be GPI anchored. We did the functional characterisation of these three GPI-anchored members. Data suggested that GPI-anchored SKS proteins were involved in cell orientation, gametophyte and embryo development.

Résumé:

L'ABP1 (auxine Binding protein 1), qui peut se lier à l'auxine, est essentielle pour le développement des plantes. Il a été prouvé d'avoir la capacité de se lier signal d'auxine auxine et transduce en les cellules. Il est supposé être localisée et des fonctions à la surface extérieure du plasma membrane à travers composante inconnue.

Dans mes Theiss, nous avons essayé de investigate l'interaction entre ABP1 et le candidat de le composant inconnu, CBP1 (à partir de maïs), qui est GPI-anchored et déjà identifiée comme étant la capacité de liaison de synthèse peptidique C-terminale du ABP1 en 2006.

L'orthologue de CBP1 chez Arabidopsis appartient à une famille de gènes avec 19 membres, dont seulement trois d'entre eux ont été predicted être ancré GPI. Nous avons fait le fonctionnel caractérisation de ces trois membres. Les données suggèrent que GPI Protéines SKS ont été impliqués dans l'orientation de la cellule, gamétophyte et le développement de l'embryon.

Acknowledgments

First I would like to thank members of the jury who have accepted to spend some of their time to review my thesis.

I would like to thank Catherine, my supervisor, who teach me and support me a lot along my PhD.

And thank all the members of our group, especially Catherine PRIMARD, who help me a lot both in life and experiment; Philippe MULLER, who did a lot of work for me in gene expression analyses by Real time PCR; and Sebastien PAQUE, Alexandre TROMAS and Anne-Laure QUETTIER, who gave me a lot of scientific advice. Also thank the other members who were in our group or are still in our group.

And thank the CSC (China Scholarship Council), who granted me for three years.

And finally, I want to thank everybody in our institute for helping me such a lot.

TABLE CONTENTS

List of abbreviations.....	- 4 -
Introduction	- 5 -
I-1 Auxin responses and signalling	- 6 -
I-1-1 Auxin in plants.	- 6 -
I-1-2 Auxin Biosynthesis and Storage	- 7 -
I-1-3 Auxin transport.....	- 8 -
I-1-4 Auxin signalling pathway for transcriptional regulation.....	- 9 -
I-2 The role of ABP1 in auxin signalling.....	- 11 -
I-2-1 ABP1 identification.....	- 11 -
I-2-2 ABP1 functions	- 11 -
I-2-3 ABP1 localization and potential ABP1 docking protein.....	- 11 -
I-3 GPI-Anchored Proteins.....	- 13 -
I-3-1 GPI and GPI-anchored proteins	- 13 -
I-3-2 GPI biosynthesis.....	- 14 -
I-3-3 Transport and localization of GAPS	- 17 -
I-3-4 GAPS in Mammals and Yeasts.....	- 19 -
I-3-5 GAPS in Plants	- 19 -
I-4 Thesis project.....	- 23 -
Results.....	- 24 -
Chapter I: <i>In silico</i> analyses	- 25 -
I-1 CBP1 in Maize.....	- 25 -
I-2 Homologous genes of CBP1 in Arabidopsis.	- 28 -
I-2-1 <i>SKU5</i> gene family in <i>Arabidopsis</i>	- 28 -
I-2-2 <i>In Silico</i> Expression Data	- 31 -
I-2-3 <i>SKU5</i> / <i>SKS</i> proteins.....	- 33 -
I-2-4 <i>SKU5</i> / <i>SKS</i> proteins through evolution	- 35 -
Conclusion and Discussion	- 37 -
Chapter II: Investigating the interaction between GPI-anchored <i>SKU5</i>/<i>SKS</i> proteins and ABP1.....	- 42 -
II-1. CBP1 and GPI-anchored <i>SKU5</i> / <i>SKS</i> proteins were candidates for being ABP1 binding or docking proteins.....	- 42 -
II-2. Yeast two Hybrid System.....	- 42 -
II-3 Interaction detection by yeast two hybrid system	- 44 -
II-3.1 Gene cloning and modification for yeast two hybrid.	- 44 -
II-3-2 Yeast transformation and searching for interaction	- 49 -
Conclusion and Discussion:	- 54 -
Chaper III: Functional Analysis of <i>SKS</i> genes by reverse genetic approaches	- 56 -
III-1 Expression analysis of <i>SKS1</i> , <i>SKS2</i> , <i>SKU5</i> in <i>Arabidopsis thaliana</i> :.....	- 56 -
III-2 Characterization of <i>skS1</i> , <i>skS2</i> and <i>sku5</i> null mutants.	- 58 -
III-2-1 <i>sku5/sks</i> single null mutants	- 58 -
III-2-2 Generating double and triple mutants for <i>skS1</i> , <i>skS2</i> and <i>sku5</i>	- 61 -
III-2-3 <i>SKS1</i> , <i>SKS2</i> and <i>SKU5</i> expression in mutant plants.....	- 63 -
III-2-4 Analyses of <i>skS1</i> , <i>skS2</i> and <i>sku5</i> single and double mutants	- 64 -
III-2-5 Analyses of <i>skS1</i> , <i>skS2</i> , <i>sku5</i> triple mutant.....	- 69 -
III-3 Functions of <i>SKU5</i> , <i>SKS1</i> and <i>SKS2</i> in auxin responses and cell cycle.	- 76 -
Conclusion and Discussion	- 81 -

Chapter IV: <i>SKS1</i>, <i>SKS2</i> and <i>SKU5</i> are required for fertilization and embryogenesis	- 82 -
IV-1 Introduction to fertilization, pollen tube guidance and embryogenesis.....	- 82 -
IV-1-1 Male and female gametophytes	- 82 -
IV-1-2 Pollen tube guidance	- 84 -
IV-1-3 Double fertilization of flowering plants	- 86 -
IV-1-4 Arabidopsis embryogenesis.....	- 87 -
IV-1-5 seed maturation and dessication	- 88 -
IV-2 Absence of <i>SKS1</i> , <i>SKS2</i> and <i>SKU5</i> affect fertilization and embryogenesis.	- 90 -
IV-2-1 <i>SKS1</i> , <i>SKS2</i> , <i>SKU5</i> in fertilization	- 93 -
IV-2-2 <i>SKS1</i> , <i>SKS2</i> and <i>SKU5</i> in embryogenesis.	- 100 -
Conclusion and Discussion	- 105 -
Chapter V. Functions of GPI-anchored SKS and the roles of GPI anchors by overexpression analyses	- 107 -
V-1 Tools for transient assay and SKS overexpression	- 107 -
V-1-1 <i>SKS9</i> was cloned from Arabidopsis.....	- 107 -
V-1-2 SKS genes modifications	- 108 -
V-1-3 Vectors for SKS overexpressors	- 111 -
V-2 GPI-anchors for localization by transient assay.....	- 112 -
V-3 Overexpressors in <i>Ws</i> background acquisition and analyses.....	- 114 -
V-3-1 Overexpressors acquisition.	- 114 -
V-3-2 Expression levels of SKS Overexpressors in <i>Ws</i> background.....	- 115 -
V-3-3 Phenotype analyses of overexpressors.....	- 118 -
V-4 Overexpressors in <i>skl1</i> , <i>sku5</i> background acquisition.....	- 119 -
Conclusion and Discussion	- 120 -
ChapterVI Discussion and Perspectives	- 121 -

List of abbreviations

ABP1: Auxin Binding Protein 1

IAA: Indole 3 acetic acid

GAP: GPI-anchored protein

GPI: GlycosylPhosphatidylInositol

PT: Pollen tube

Introduction

I-1 Auxin responses and signalling

I-1-1 Auxin in plants.

The word ‘Auxin’ was generated from a Greek word which means ‘to grow’. Its function was firstly described by Charles and Francis Darwin in ‘The Power of Movement in Plants’ in 1880 (Darwin and Darwin, 1880). Long-term studies revealed that auxin is the most important plant hormone and functions as a key morphogen in regulating plant growth and development.

Several native auxins were found in plants. According to the chemical structures of native auxin, several chemicals were synthesized and functioned in plants (Simon and PetrÅĳek, 2011). Some of the native and synthetic auxins were shown in Table I-1.

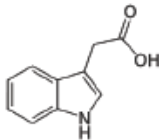
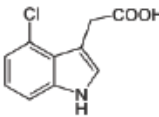
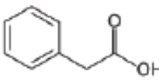
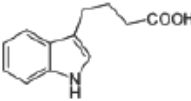
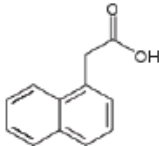
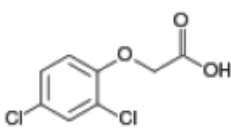
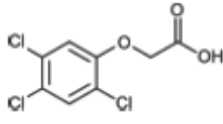
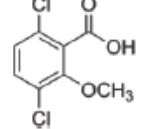
Resource	Name	Structure
Native Auxin	IAA (indole-3-acetic acid)	
	4-Cl-IAA (4chloroindole-3-acetic acid)	
	PAA (2-phenylacetic acid)	
	IBA (Indole-3-butyric acid)	
Synthetic Auxin	NAA (α-Naphthalene acetic acid)	
	2,4-D (2,4-Dichlorophenoxyacetic acid)	
	2,4,5-T (2,4,5-Trichlorophenoxyacetic acid)	
	Dicamba (2-Methoxy-3,6-dichlorobenzoic acid)	

Table I-1 Native and synthetic Auxins.

I-1-2 Auxin Biosynthesis and Storage

Indole-3-acetic acid (IAA) is the main naturally occurring auxin in plants and the best studied. It is biosynthesized through two major routes, from Tryptophan (Trp) using various Trp-dependent pathways and from an indolic Trp precursor via Trp-independent pathways (Woodward and Bartel, 2005; Korasick et al., 2013) (Figure I-1).

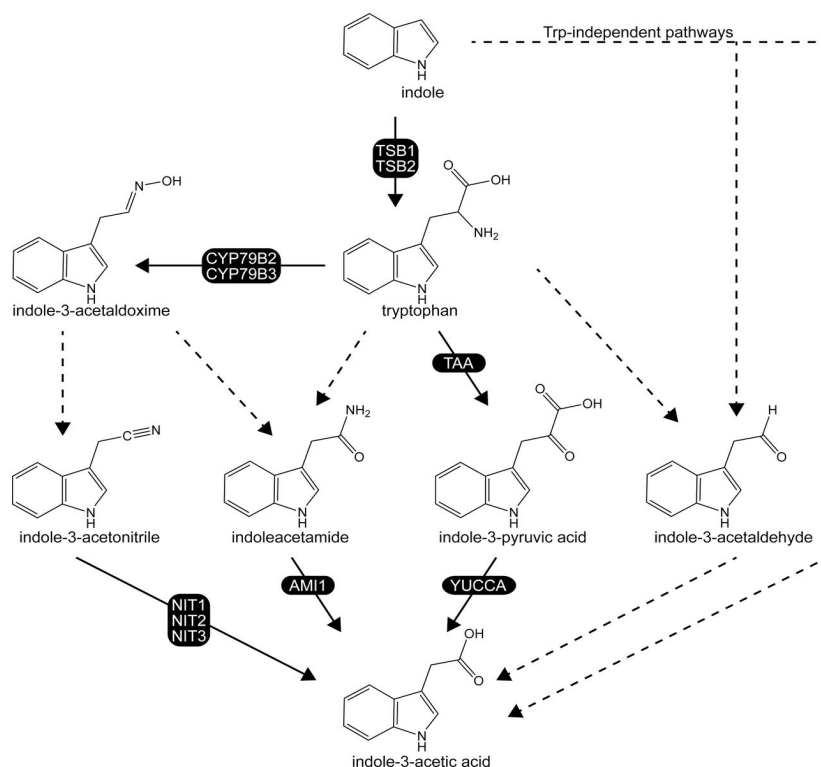


Figure I-1. Potential IAA biosynthetic pathways.

Arrows in pathways for which enzymes have been identified are solid and arrows in pathways that have not been identified are dashed and can represent single or multiple steps. (Korasick et al., 2013)

After the synthesis, IAA is stored in the auxin pool, which includes free auxin, conjugated auxins to amino-acid residues or glucose, inactive auxin precursor IBA and the inactive methyl ester form of IAA, MeIAA; but only a small fraction of auxin exists as free active signalling molecule (Korasick et al., 2013) (Figure I-2).

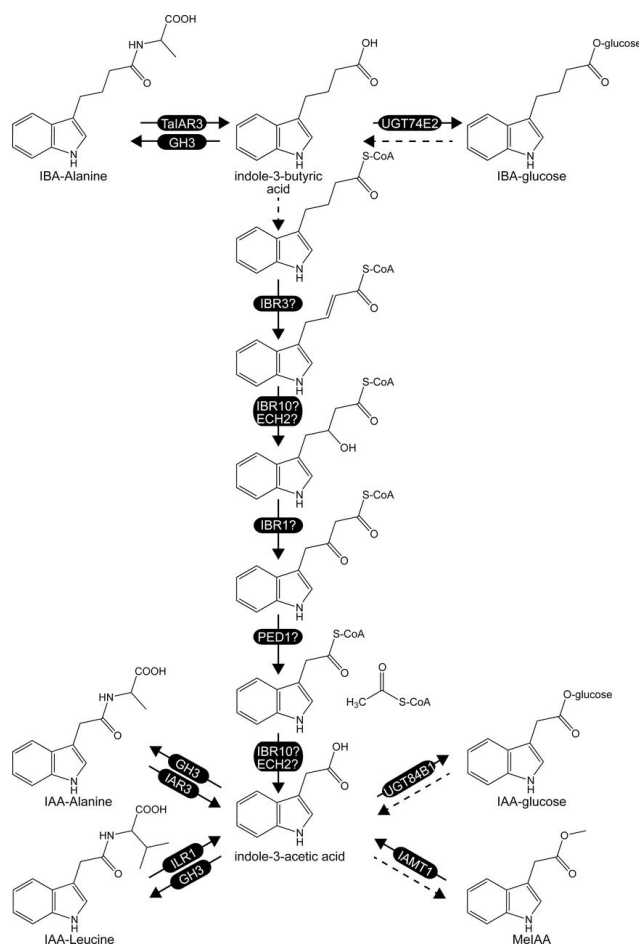


Figure I-2. Potential IAA storage form pathways.

Arrows at steps for which enzymes have been identified are solid and arrows in pathways that have not been identified are dashed and may be single or multiple steps. (Korasick et al., 2013)

I-1-3 Auxin transport

IAA is weak acid with the pKa 4.85. In plants, the pH at the apoplast is approximately 5.5, where the IAA is 83% dissociated and 17% protonated. In the cytosol, the pH is approximately 7, where the almost entire IAA is shifted to dissociated form. Proton-associated IAA molecule can enter the cell by lipophilic diffusion, but dissociated IAA anion cannot go across the plasma membrane (Robert et al., 2010). So the auxin carriers are necessary for the movement of auxin and are responsible for short distance oriented transport of auxin. In Arabidopsis, AUXIN1/LIKE-AUX1 (AUX1 and LAX) family of auxin transporters are major auxin influx carriers whereas PIN-FORMED (PIN) and P-GLYCOPROTEIN (PGP) family members are major auxin efflux carriers (Ugartechea-Chirino et al., 2012).

In Arabidopsis, *AUX1* belongs to a small multigene family comprising four highly conserved genes, *AUX1*, *LAX (LIKE AUX1)1*, *LAX2* and *LAX3*; they show well conserved gene structure. *AUX1/LAX* has 11 transmembrane segments with N-terminal residing inside the cell and C-terminal outside. All proteins they encoded display auxin uptake functions and

bind IAA with PH dependence; the maximal binding takes place between pH5 and 6 (Peret et al., 2012; Swarup and Peret, 2012).

In Arabidopsis, eight *PIN* genes were identified to encode PIN proteins with a similar structure; they all have amino- and carboxy-terminal hydrophobic membrane-spanning domains separated by a central hydrophilic domain (Krecek et al., 2009). They mainly differ by the hydrophilic loop, in terms of sequence and length. *PIN-FORMED 1 (PIN1)* gene, named as naked and pin-like inflorescences with its mutation, was found as the first member of the *PIN* gene family (Okada et al., 1991).

PIN-LIKE genes(*PILs*), identified on the basis of their similarity with a subclass of *PIN* genes, encode proteins containing auxin carrier domain; evidence showed that they were involved in auxin transports but possibly in the endoplasmic reticulum (Barbez et al., 2012)

Auxin transport could be blocked by various chemicals. Auxin transport inhibitor N-1-naphthylphthalamic acid (NPA) was identified as a compound able to inhibit polar auxin transport and at the cell level was shown to block auxin efflux. NPA treatment arrests lateral root development by blocking primordium initiation ; the initiation could be recovered by additional NAA treatment (Casimiro et al., 2001). At a later stage of development application of NPA to the plant can mimick the phenotype of the *pin1* mutant.

I-1-4 Auxin signalling pathway for transcriptional regulation

TIR1 was first identified from the *tir1* mutant that exhibited a weak resistance to the auxin inhibitor NPA. Later on, TIR1 identified as an auxin receptor (Dharmasiri et al., 2005; Kepinski and Leyser, 2005), the mechanism by which it works is much clearer than for ABP1 (Figure I-3).

Auxin response factors (ARF) are transcription factors that regulate the expression of auxin response genes and Aux/IAAs are transcriptional repressors. With the binding of Aux/IAAs and other co-repressors as TOPLESS (TPL) to ARF, the transcription is repressed (Guilfoyle and Hagen, 2007; Causier et al., 2012).

TIR1 and the related auxin F-box (*AFBs*) genes encode F-box proteins that are part of E3 ubiquitine ligase complexes names $SCF^{TIR1/AFBs}$. Auxin promotes the interaction between TIR1/AFBs and Aux/IAAs , acting as a molecular glue (Tan et al., 2007). TIR1/AFBs and Aux/IAA form auxin co-receptors. Aux/IAAs are polyubiquitinated by $SCF^{TIR1/AFBs}$ complexes and then enter the ubiquitin-proteasome degradation pathway (Santner and Estelle, 2011). After the removal of Aux/IAA repressors, ARFs promote the transcription of auxin response genes.

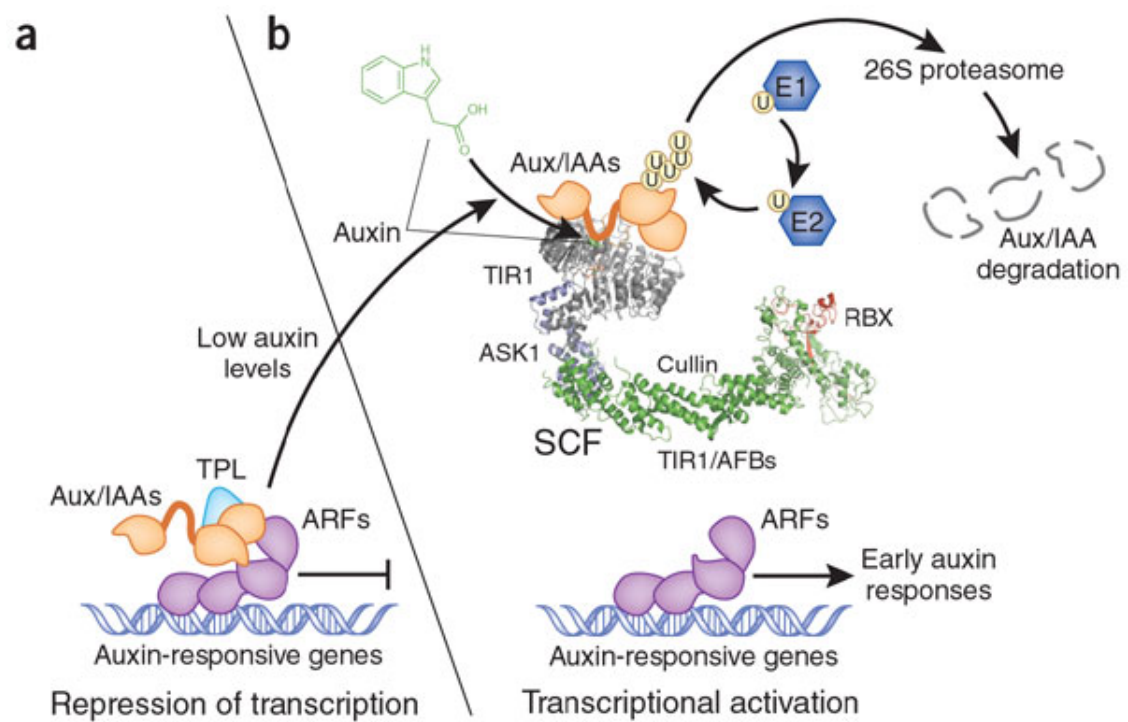


Figure I-3. SCF^{TIR1} and related SCF complexes bind auxin and target Aux/IAA proteins for degradation. **(a)** At low cellular levels of auxin, transcription of auxin response genes is repressed by the Aux/IAAs. **(b)** When auxin cellular levels increase, auxin binds to TIR1 and Aux/IAAs, and promotes their ubiquitination and subsequent degradation, thus permitting the ARF proteins to promote transcription. (Santner et al., 2009)

I-2 The role of ABP1 in auxin signalling

I-2-1 ABP1 identification

AUXIN BINDING PROTEIN 1 (ABP1) was identified on its auxin binding activity nearly 30 years ago (Lobler and Klambt, 1985). Although the binding activity was confirmed by biochemical methods or co-crystallization with auxin (Jones and Venis, 1989; Woo et al., 2002), the mechanism of how it work was still largely unclear.

I-2-2 ABP1 functions

A lot of efforts were made to perform functional analyses of *ABP1*. The importance of *ABP1* is generally revealed. Exogenous ABP1 protein and synthesized C-terminus peptide of ABP1 were shown to induce an hyperpolarization response of tobacco protoplasts (Leblanc et al., 1999b; Leblanc et al., 1999a). ABP1 was involved in auxin-induced protoplast swelling, the antibody to ABP1 and C-terminus peptide could prevent the auxin-induced swelling (Steffens et al., 2001), ABP1 is also essential for the control of the cell cycle; with inactivation of ABP1 by conditional immunomodulation, the cell cycle was arrested in BY2 cells in culture (David et al., 2007).

ABP1 is essential for embryogenesis and null mutation of *abp1-2* causes embryo lethality (Chen et al., 2007). ABP1 functional inactivation was obtained and studied using conditional immunomodulation of ABP1 function in Arabidopsis generated by the controlled production (ethanol induction) of recombinant antibodies blocking the protein (Braun et al., 2008). By this tool, ABP1 was found to be essential at all stages of post-embryonic development. Knockdown for ABP1 results in severe alterations of leaf initiation and growth, as well as inhibition of primary root growth (Braun et al., 2008; Tromas et al., 2009). These defects result from default in cell division and cell expansion. Recently was protein was also shown to control clathrin dependent endocytosis and to alter recycling of plasma membrane proteins, including PIN efflux carriers (Robert et al., 2010; Chen et al., 2012). Whereas the recycling of PIN is potentially affected by ABP1 inactivation, no significant effect was reported on the polar localisation of PIN or on the auxin gradient formed at the root apex (Tromas et al., 2009)

I-2-3 ABP1 localization and potential ABP1 docking protein

The localization of ABP1 is an interesting aspect. *ABP1* genes in different plants species encode soluble proteins with N-terminal signal peptides allowing synthesis to the ER. In flowering plants, a KDEL ER-retention signal is also found at the C-terminus suggesting that

the protein could be retained within the lumen of the ER (Tomas et al., 2010). This KDEL sequence seems however to be recent as it is not present in non-flowering plants (Panigrahi et al., 2009). Despite the absence of hydrophobic domain or post-translational modification allowing interaction with membrane fractions, ABP1 is always found to be associated with membranes. In addition, all functional evidences point out a localization of ABP1 at the plasma membrane (Tomas et al., 2010). The hypothesis that ABP1 might interact with a membrane protein or a protein complex was proposed (Schiebl et al., 1997)(Figure I-4).

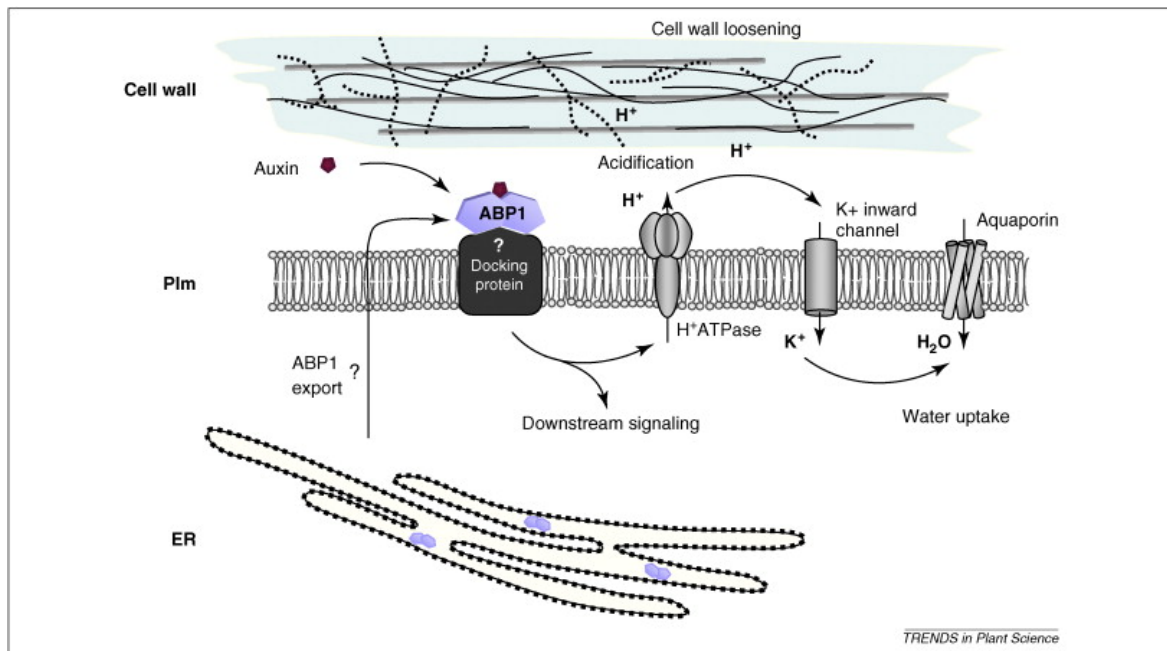


Figure I-4. Rapid auxin responses mediated by ABP1.

Auxin is perceived at the outer face of the plasma membrane (Plm) by ABP1 which interacts with an unknown membrane-associated protein or protein complex (docking protein). Binding of auxin to ABP1 activates a cascade of events including activations of the Plm proton pump ATPase and of potassium inward rectifying channels. The activation of the H⁺ ATPase induces hyperpolarization of the Plm and acidification of the extracellular space which contributes to cell wall loosening. The increase of intracellular K⁺ contributes to the uptake of water which is essential for cell expansion. It is not known whether these early events are part of a signaling cascade controlling downstream ABP1-mediated cellular responses (Tomas et al., 2010).

To identify the putative “docking protein”, a photoaffinity crosslinking study was performed using a synthetic peptide corresponding to the C-terminus of the maize ABP1. GPI-anchored protein C-TERMINAL PEPTIDE BINDING PROTEIN 1 (CBP1) was identified as exhibiting the capacity to bind the synthetic C-terminus peptide of ABP1 (Shimomura, 2006).

Interestingly, GPI-anchor is a structure which can associate protein to the outer face of the plasma membrane. However, no more evidence confirmed the direct interaction between ABP1 and CBP1.

I-3 GPI-Anchored Proteins

I-3-1 GPI and GPI-anchored proteins

Proteins following the secretory pathway can be associated to the plasma membrane by various mechanisms. Proteins exhibiting hydrophobic transmembrane domains can be integrated in the plasma membrane bilayer. Proteins without transmembrane region can be attached to the membrane through post-translational lipid modifications occurring in the lumen of the endoplasmic reticulum. One of the best characterized process is the attachment of glycosylphosphatidylinositol (GPI) anchor that allows tethering the modified protein to the to external surface of the plasma membrane (Ferguson et al., 1988b, 1988a). This glycolipid modification includes a fatty acid tail anchored in the inner membrane leaflet of the endoplasmic reticulum (lumen side) then within the outer leaflet of the plasma membrane bilayer after secretion of the modified protein (Figure.I-5A). GPI moiety from different species exhibit conserved core structure. Mannose residues are linked to the carboxyl-terminus of the protein through an amide bond with ethanolamine phosphate group (Holder and Cross, 1981; Holder, 1983). Glucosamine and phosphatidylinositol make the junction between sugar residues and the fatty acid that can be diacylglycerol or ceramide (Ferguson et al., 1988a) (Figure.I-5B). GPI modification is present among lower and higher eukaryotes, about 0.5% of total proteins are predicted to be GPI anchored proteins (GAPs) (Eisenhaber et al., 2001).

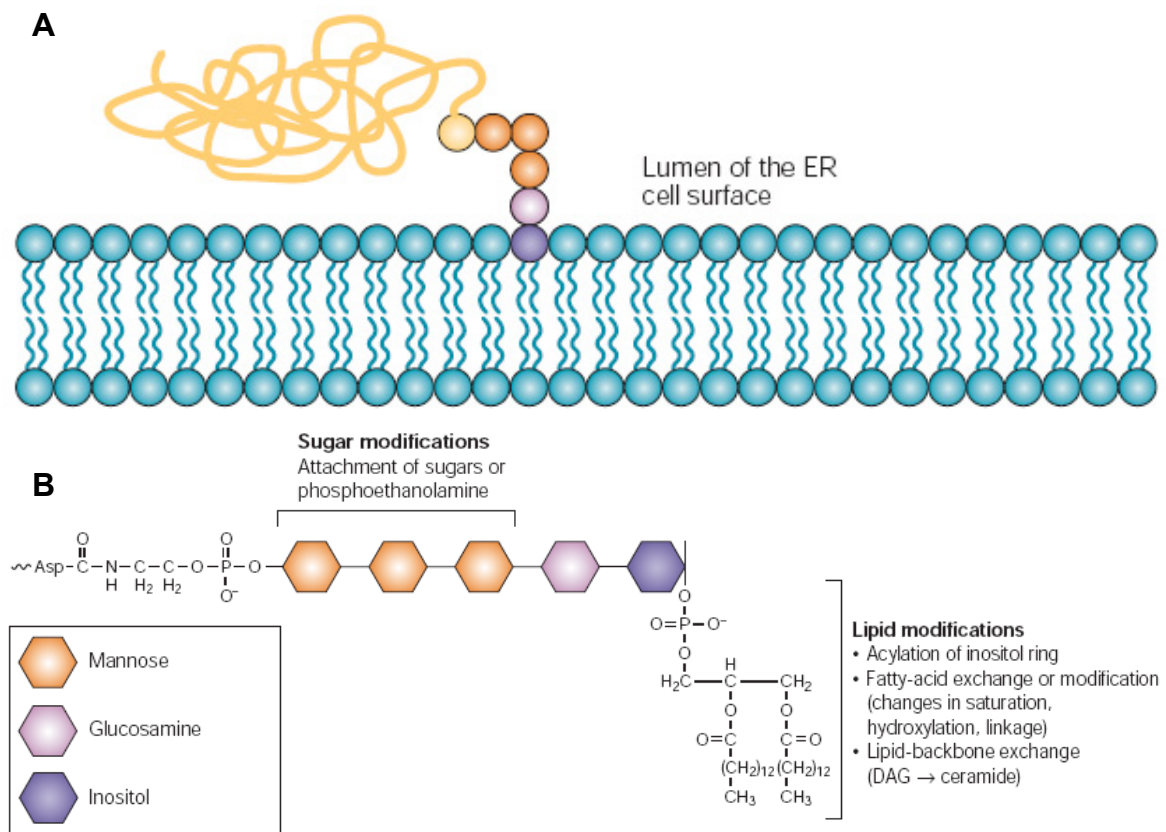


Figure I-5. GAP and Core structure of GPI moiety (from Mayor and Riezman, 2004).

A | GPI-anchored proteins are embedded in the extracellular or luminal leaflet of membranes through their glycolipid moieties and are not directly accessible from the cytosolic face of the membrane. B | The GPI core structure is shown. The conserved core consists of ethanolamine phosphate in an amide linkage to the carboxyl terminus of the protein, three mannose residues (orange), glucosamine (blue) and phosphatidylinositol (purple). It can be modified and is subject to various remodelling reactions of the lipid moiety. Variations can occur by addition of extra sugars or ethanolamine phosphates to the mannose residues; acylation of the inositol ring; changes in the fatty acids (length, saturation, hydroxylation), or their types of linkage to the glycerol backbone (acyl to alkyl); or remodelling of the entire diacylglycerol to ceramide.

I-3-2 GPI biosynthesis

The GPI anchor biosynthesis is decided by the special amino acid sequence of the precursors of non-mature GPI-anchored proteins. All the GAPs are encoded with a cleavable hydrophobic signal peptides at N-terminus and hydrophobic GPI-anchoring signal at carboxy-terminus (Figure I-6) (Caras et al., 1987; Caras and Weddell, 1989; Mayor and Riezman, 2004). The N-terminal hydrophobic signal lead the precursors enter the ER lumen and the carboxy-terminal hydrophobic GPI-anchoring signal forms the transmembrane region when the precursor synthesized passing through the ribosome into the lumen of ER. The signal peptidase recognize and cleave the N-terminal signal peptide and GPI protein transamidase

recognizes and cleaves this region at ω -site, and then link the free –COOH of the mature protein to the synthesized GPI moiety (Mayor and Riezman, 2004).

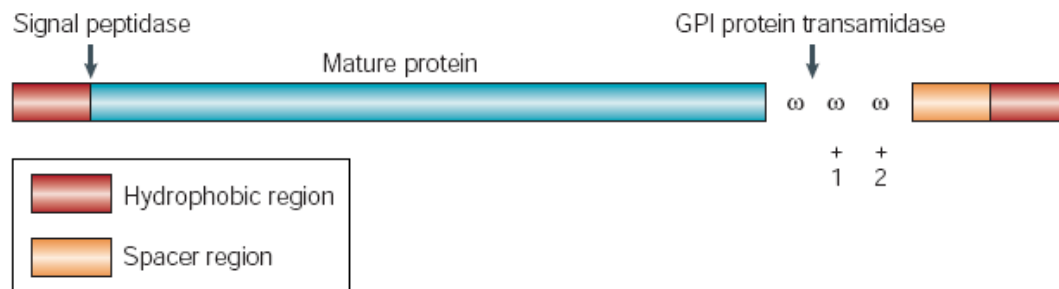


Figure I-6 Structure of GPI-anchor-protein precursor (Mayor and Riezman, 2004).

GPI-anchored proteins are synthesized as precursors with a cleavable, hydrophobic amino-terminal signal sequence that targets the protein to the lumen of the endoplasmic reticulum (ER) and a cleavable, carboxy-terminal signal sequence that directs GPI anchoring. The GPI-anchoring signal consists of a hydrophobic region separated from the GPI-attachment site (ω -site) by a hydrophilic spacer region. Amino-acid residues with small side chains are highly preferred for the two amino acids that follow the ω -site.

When GPI protein transamidase recognizes the precursors, the biosynthesis of GPI moiety begins. The diacyl-PI of lipid bilayer, which is present at the cytoplasmic side of the ER membrane, would flip into the luminal side of the endoplasmic reticulum membrane, where later biosynthesis and linkage to the protein occur (step 1-11 in Figure. I-7); a series of enzymes were identified for their contribution to the different steps of this complex progress in various species (Fujita and Kinoshita, 2010). Table I-2 summarizes identified enzymes in mammals, *Saccharomyces cerevisiae* and *Arabidopsis*.

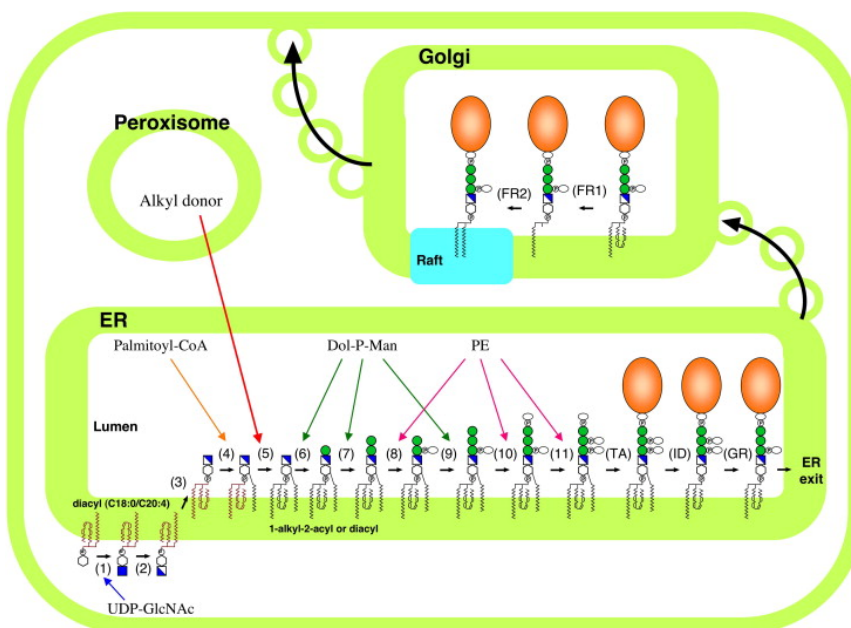


Figure I-7. Biosynthesis and remodeling of mammalian GAPs. (Fujita and Kinoshita, 2010)

Steps 1–11, TA, ID, GR, FR1, and FR2 correspond to those shown in Table 1. TA, transamidation; ID, inositol deacylation; GR, glycan remodeling; FR, fatty acid remodeling; Dol-P-Man, dolichol-phosphate-mannose; PE, phosphatidylethanolamine.

Step		Donor substrate	Mammals	<i>S. cerevisiae</i>	<i>Arabidopsis</i>
1	GPI-GlcNAc transferase (GPI-GnT)	UDP-GlcNAc	<i>PIG-A</i>	<i>GPI3</i>	<i>SETH1</i>
			<i>PIG-C</i>	<i>GPI2</i>	<i>SETH2</i>
			<i>PIG-H</i>	<i>GPI15</i>	AT4G35530
			<i>PIG-P</i>	<i>GPI19</i>	AT1G61280 AT2G39445
			<i>PIG-Q</i>	<i>GPI1</i>	–
			<i>PIG-Y</i>	<i>ERI1</i>	–
			<i>DPM2</i>	–	–
2	GlcNAc-PI de-N-acetylase		<i>PIG-L</i>	<i>GPI12</i>	–
3	Flippase		Not identified	<i>ARV1?</i>	–
4	Inositol acyltransferase	Palmitoyl-CoA	<i>PIG-W</i>	<i>GWT1</i>	–
5	PI remodeling enzyme	?	Not identified	–	–
6	α 1-4mannosyltransferase I (GPI-MT I)	Dol-P-Man	<i>PIG-M</i>	<i>GPI14</i>	<i>PNT1</i> <i>PNT2</i> <i>PNT3</i> <i>PNT4</i>
			<i>PIG-X</i>	<i>PBN1</i>	AT5G46850
			<i>PIG-V</i>	<i>GPI18</i>	AT1G11880
7	α 1-6mannosyltransferase II (GPI-MT II)	Dol-P-Man	–	<i>PGA1</i>	–
8	EtNP transferase I (GPI-ET I)	PE	<i>PIG-N</i>	<i>MCD4</i>	–
9	α 1-2mannosyltransferase III (GPI-MT III)	Dol-P-Man	<i>PIG-B</i>	<i>GPI10</i>	–
M4	α 1-2mannosyltransferase IV (GPI-MT IV)	Dol-P-Man	<i>PIG-Z (SMP3)</i>	<i>SMP3</i>	–
10	EtNP transferase III (GPI-ET III)	PE	<i>PIG-O</i>	<i>GPI13</i>	–
			<i>PIG-F</i>	<i>GPI11</i>	AT1G16040
11	EtNP transferase II (GPI-ET II)	PE	<i>PIG-G (GPI7)</i>	<i>GPI7</i>	–
			<i>PIG-F</i>	<i>GPI11</i>	AT1G16040
			<i>PIG-K</i>	<i>GPI8</i>	–
			<i>GAA1</i>	<i>GAA1</i>	AT5G19130
			<i>PIG-S</i>	<i>GPI17</i>	AT3G07180
TA	GPI transamidase		<i>PIG-T</i>	<i>GPI16</i>	–
			<i>PIG-U</i>	<i>GAB1</i>	AT1G12730 AT1G63110
ID	Inositol deacylase		<i>PGAP1</i>	<i>BST1</i>	AT2G44970 AT3G27325 AT3G52570
GR	2nd EtNP phosphoesterase		<i>PGAP5</i>	<i>CDC1</i> <i>TED1</i>	–
FR1	GPI-phospholipase A2		<i>PGAP3</i>	<i>PER1</i>	–
FR2	Lyso-GPI acyltransferase I	Stearyl-CoA	<i>PGAP2</i>	<i>CWH43-N?</i>	–
			Not identified	<i>GUP1</i>	–
CR	Ceramide remodelase	Ceramide?		<i>CWH43</i>	–
FR3	GPI phospholipase A1		–	–	–
FR4	Lyso-GPI acyltransferase II		–	–	–

Table I-2. Genes required for biosynthesis and remodeling of GPI anchor (Fujita and Kinoshita, 2010).

I-3-3 Transport and localization of GAPs

After the GAPs were synthesized inside the ER, they will be packaged into ER-derived vesicles, which are distinct from the other secreted proteins, and exit endoplasmic reticulum through the Golgi to the surface of plasma membrane (Muniz et al., 2001). In animal cells, GAPs are present at the plasma membrane surface as monomers and a smaller fraction were reported to be associated to nanoscale cholesterol-sensitive clusters (Sharma et al., 2004).

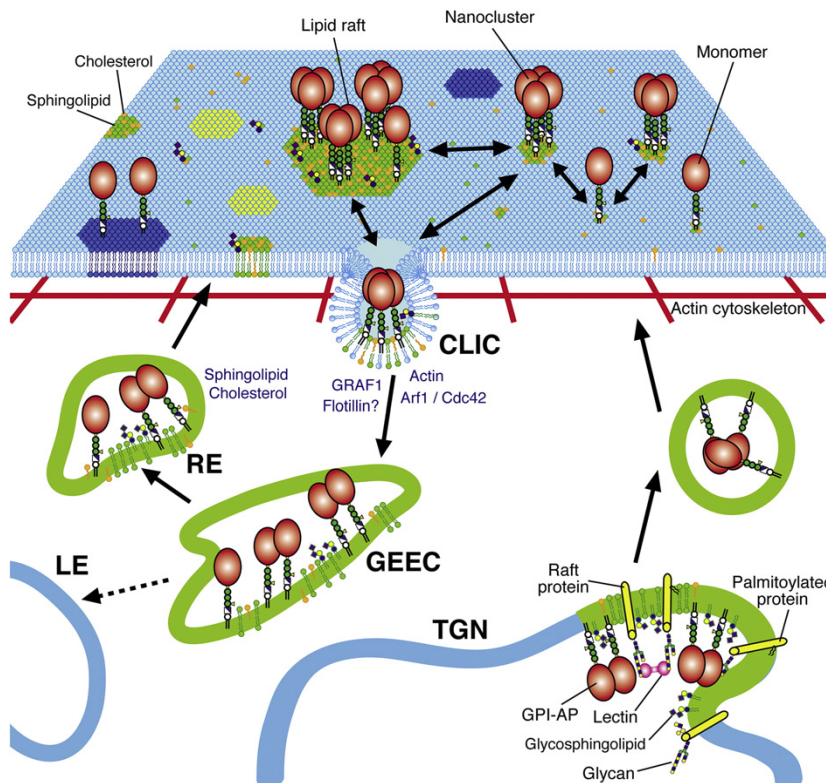


Figure I-8. Trafficking and dynamics of GPI-APs on the membrane in mammalian cells. (extracted from(Fujita and Kinoshita, 2012)). (1) From the TGN to the plasma membrane. GPI-APs are sorted and clustered into lipid-mediated carriers at the TGN. Sorting of raft-associated proteins, such as palmitoylated proteins and lipids, including glycosphingolipid and cholesterol, and exclusion of non-raft components, would occur. Oligomer formation of GPI-APs would be required for apical targeting. Luminal lectins, may help this sorting. (2) At the plasma membrane. The plasma membrane appears to be compartmentalized by a cortical actin cytoskeleton. GPI-APs exist as monomers and as lipid assembled nanoclusters (5–10 nm) that are small and dynamic. In response to external signals, they can be actively induced to form large-scale rafts (40–300 nm). Signaling molecules are then recruited to the domains. The plasma membrane also appears as a mosaic of membrane domains, including caveolae and transient confinement zones. (3) Endocytosis. At steady state, GPI-APs are internalized as clathrin-independent carriers (CLICs) that seem to be regulated by Arf1, Cdc42, actin, and GRAF1. They are then incorporated into GEECs (GPI-APs enriched early endosomal compartment). GPI-APs are subsequently transported to the recycling endosomes (RE), followed by recycling back to the plasma membrane, which is regulated by sphingolipids and cholesterol. Alternatively, GEECs are trafficked to the late endosomes (LE).

Interestingly, the transport efficiency of GAP is dependent on the presence of GPI anchor; without GPI-anchoring signal, the precursor of GAPs display the normal secretory protein pathway, for protein also having a signal peptide at the N-terminus and being targeted to the outer face of the plasma membrane; the absence of the GPI anchor reduces the secretion of the GAPs from the ER to the outer surface. (McDowell et al., 1998)

Although GPI-anchor is supposed to localize protein at the plasma membrane, actually it is not strictly true. In animal cells, the GPI-anchor of plasma membrane located GAPs can be cleaved by PI-specific phospholipase thus releasing the protein as a soluble protein in the medium of mammal cells in culture (McDowell et al., 1998). In yeast, only few GAPs reside permanently at the plasma membrane, a majority of them gets further processed and integrated into the cell wall by a covalent attachment to cell wall glucans (Pittet and Conzelmann, 2007). Several annotations of Arabidopsis genes suggest that PI-specific phospholipase exist also in plants. There is however no functional characterization of these genes confirming their putative role in the cleavage of GPI anchors *in vivo*. Plant GAPs were detected at the plasma membrane and also at the cell wall, however mis-localization of reporter proteins cannot be ruled out (Roudier et al., 2005).

GPI anchor is not only important for the localization but also the functions of GAPs. The GPI anchor cleavage by GPI-PLC could change the antigenicity of Variant Surface Glycoprotein (VSG), which suggests that GPI lipid moiety affect the major conformation of VSG (Butikofer et al., 2001). And when the GPI anchor is replaced by a transmembrane (TM) region, the lymphocyte function-associated antigen 3 (LFA3) isoform TM FLA3 could reduce the *Jurkat* cell adhesion to planer bilayer (Tozeren et al., 1992).

I-3-4 GAPs in Mammals and Yeasts

In mammals and yeasts, GAPs play various and important roles in many biological processes, such as :

1. cell surface receptors: folate receptor in mammal cells participates in the cellular accumulation of 5-methyltetrahydrofolic acid in a number of epithelial cells *in vitro* through the process of caveolin-dependent potocytosis (Weitman et al., 1992); CD14, the first identified Pattern Recognition Receptor (PRR) in mammals, acts as a co-receptor (along with the Toll-like receptor TLR 4 and MD-2 signalling complex) for the detection of bacterial lipopolysaccharide (LPS) and endocytosis (Zanoni et al., 2011).

2. cell adhesion molecules isoforms: fasciclin I directly mediates homophilic drosophila cells adhesion (Elkins et al., 1990), and the Algal-CAMs, which contain the homological repeat of fasciclin I and were found in *Volvox* plant, are also involved in cell adhesion (Huber and Sumper, 1994). But no GPI anchor was predicted in Algal-CAMs.

3. cell surface hydrolases.

4. GPI linked PrPC and PrPSc to plasma membrane, and surface conversion of PrPC to PrPSc requires PrPC, but not PrPSc to be GPI anchored (Radford and Mallucci, 2010).

And so on.

As GPI-anchored proteins play that many important roles, the defect of GPI anchor biosynthesis gene could result in severe phenotypes; the defect of X-linked GPI anchor biosynthesis gene PIG-A, could result in paroxysmal nocturnal hemoglobinuria (PNH) disease (an acquired disorder that leads to the premature death and impaired production of blood cells), and it causes a lethal effect if the defect occurs in embryos (Kawagoe et al., 1996).

I-3-5 GAPs in Plants

248 potential GAPs are predicted by proteomic and genomic analysis, and classified as several families in Arabidopsis, including classical AGPs (arabinogalactan proteins), AG peptides, Fasciclin-like AGPs, COBRA family, SKU5 family, or receptor-like GAPs (Borner et al., 2002; Borner et al., 2003). 47 of them are expressed in pollen, in which 15 of them are detected specifically in flowers and pollens; the defect of GPI anchor biosynthesis pathway specifically block male transmission and pollen function (Lalanne et al., 2004). Plant GAP proteins were shown to be implicated in cell wall synthesis and morphogenesis (Gillmor et al., 2005). However not so many of these proteins have been studied in plant to date.

A large proportion of predicted GAPs (about 40%) are potentially also modified by O-linked arabinogalactans (AGPs)(Figure I-9) (Borner et al., 2003; Eisenhaber et al., 2003; Ellis

et al., 2010). AGPs are one of the most complex families in plants because of the high diversity of glycans that is decorating protein backbone (Ellis et al., 2010).

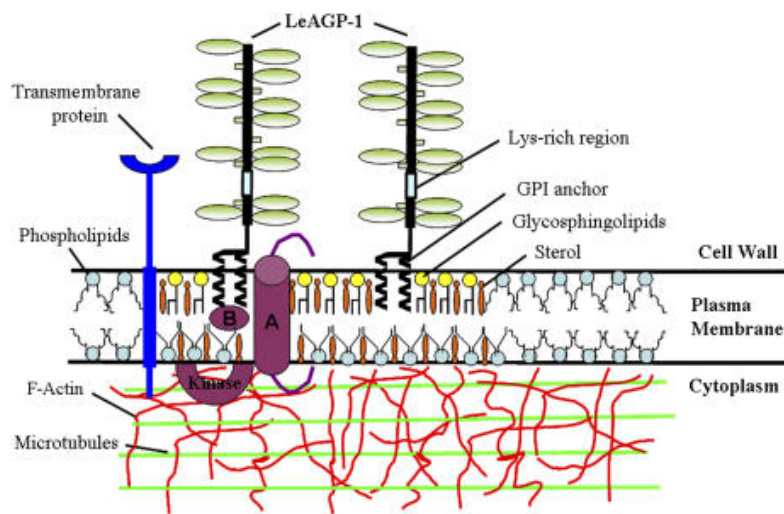


Figure I-9 extracted from (Sardar et al., 2006).

A hypothetical cell surface network model involving interactions between LeAGP-1 and the cytoskeleton (i.e. MTs and F-actin). GPI-anchored LeAGP-1 is localized to lipid rafts, which contain lipids such as glycosphingolipids and sterols (such as stigmasterol, campesterol, and β -sitosterol), and interacts with MTs and F-actin in the cytoplasm either by a transmembrane protein (in the phospholipid bilayer) or by molecules (A and B) associated with the lipid rafts. GPI-anchored LeAGP-1 in lipid rafts may mediate interactions in two possible ways: A, binding of LeAGP-1 to a transmembrane receptor in the lipid microdomain mediates the interactions; and B, ligand-LeAGP-1 receptor complex-induced translocation of a signal molecule outside the lipid raft to activate a cytoplasmic kinase. Also shown are the different constituents of LeAGP-1 that include a Pro/Hyp-rich protein backbone decorated with arabinogalactan polysaccharides, short arabinosides, and an unglycosylated Lys-rich peptide region.

According to their protein backbone, 13 classical AGPs, 10 AG (acid glycoprotein) peptides, 21 Fasciclin-like AGPs, and 3 Lys-rich AGPs are classified in *Arabidopsis* through bioinformatic analysis (Schultz et al., 2002). They are proved to be involved into many processes of growth and development, such as cell adhesion, cell wall composition, pollen tube guidance, cell division and programmed cell death (Seifert and Roberts, 2007).

Salt Overly Sensitive5 (SOS5), also called fasciclin-like AGPs4 (FLA4), was suggested to play a role in cell-to-cell adhesion; the absence of this gene causes thinner cell walls, swelling of root cells and increased sensitivity to salt stress (Shimomura, 2006).

POWDERY MILDEW RESISTANT 6 (PMR6) in *Arabidopsis* encodes a pectate lyase-like protein, which is required for susceptibility to Powdery Mildew. The *pmr6* mutant shows altered leaf morphology and decreased size, and alterations of cell wall composition that were proposed to activate defense response. PMR6 represents an interesting link between the cell wall and pathogen resistance, however the mode of action is unknown (Vogel et al., 2002).

COBRA belongs to a multigene family consisting of 12 members in Arabidopsis, all predicted to be GAP. Analysis of COBRA mutants (*cob*) revealed that the protein is essential for anisotropic expansion in most organs. Further studies suggested that COBRA Elongating cells of *cob* mutants, especially in fast elongating zone as in root or hypocotyl, expand radially instead of longitudinally thus resulting in very severe phenotypes (Schindelman et al., 2001; Roudier et al., 2002). The complete loss of function of COBRA causes severe growth and developmental defects, like cell swelling and extreme dwarfism through the whole plant body (Ko et al., 2006). COBRA protein was found to be localized in limited domains of the plasma membrane and only at the lateral side of elongating cells (perpendicular to the axis of elongation). The patterning of COBRA is dependent on cortical microtubule organization (Roudier et al., 2005) and reciprocally COBRA was proposed to be required for orientation of cellulose microfibrils (Roudier et al., 2005). GPI-anchored COBRA-like proteins are also found in other species. The absence of Brittle culm1 in rice, Brittle stalk2 in maize, provoke alterations of cell wall composition and structure of secondary cell wall affecting mechanism strength of the tissues, resistance to bending (Sindhu et al., 2007; Panigrahi et al., 2009). In tomato, SICOBRA-like was also reported to play an important role on fruit cell wall architecture and fruit development (Cao et al., 2012).

LORELEI belongs to a small plant-specific family containing 4 GPI-anchored members, LORELEI, LLG1, 2 and 3. In Arabidopsis, *LORELEI* encodes a putative GPI-anchor-containing membrane protein involved in signaling mechanisms at the synergid cell membrane by which the female gametophyte recognizes the arrival of a compatible pollen tube and promotes sperm release (Capron et al., 2008). LORELEI was shown to have a role in double fertilization and early seed development (Tsukamoto et al., 2010). Loss of function results in mostly failure of fertilization, which is mainly caused by pollen tubes continuing to grow after reaching the embryo sac and embryo sac continuing to attract additional pollen tubes (Capron et al., 2008; Tsukamoto et al., 2010). Despite a delay in the initiation of embryo development, the embryos recover and complete embryo development; no significant defect is detected in seedling and root development (Tsukamoto and Palanivelu, 2010).

SKU5 family belongs to a family of 19 highly conserved members, but only 3 members, SKU5, SKS1 (SKU5-similar 1) and SKS2 (SKU5-similar 2) are predicted to be modified by a GPI anchor (Borner et al., 2003). Among these, SKU5 was shown to be modified by a GPI.

The protein was released from the microsomal membrane fraction by action of a phosphatidylinositol-specific phospholipase C that cleaves the lipid of the anchor (Sedbrook et al., 2002).

To date, SKU5 is the only GPI-anchored member of this family that was studied. Loss-of-function mutant has twisted roots and exhibits directional growth defects compared to wild type. The expression of the protein was correlated with expanding cells and the protein was localized at the plasma membrane and in the cell wall (Sedbrook et al., 2002). SKS6, a non-GPI-anchored member of this family, participates in cotyledon vascular patterning; the T-DNA insertion mutants have decreased numbers of full vascular loops in their cotyledon (Jacobs and Roe, 2005).

I-4 Thesis project

In my thesis, three questions were going to be addressed:

1. Whether GPI-anchored SKS proteins are ABP1 binding/docking proteins.
2. If not, the functions of GPI-anchored *SKS* in Arabidopsis are still interesting for us.
3. The role GPI anchors play in localization and function of GPI-anchored SKS proteins.

To solve these questions, experiments were designed.

1. Yeast two hybrid system were utilized for investigating the interaction between ABP1 and GPI-anchored SKS protein *in vitro*.
2. *Null* mutant of GPI-anchored SKS genes were ordered and crossed to investigating the function of them.
3. The omega-domain, which is the signal for GPI synthesis, was cleaved from *SKS* genes and visualized by fluorescent proteins to investigate the function of GPI in localization and function.

Results

Chapter I: *In silico* analyses

I-1 *CBP1* in *Maize*.

As mentioned in the introduction, GPI-anchored protein C-terminal peptide-binding protein 1 (CBP1) from maize was identified through its capacity to bind synthetic C-terminal peptides of ABP1 *in vitro* and was thus proposed to be an ABP1 binding or docking protein in *Maize* (Shimomura, 2006).

CBP1 encodes a precursor protein with a signal peptide at the N-terminus and a hydrophobic C-terminal domain preceded by an ω -site. The leader peptide leads CBP1 to be addressed into the ER during synthesis. The C-terminal hydrophobic domain anchors the protein in the inner face of the ER membrane before its cleavage at the ω -site and replacement by a GPI anchor. The protein is then predicted to enter the secretion pathway and to be localized at the outer surface of the plasma membrane by its GPI anchor (Figure I-1).

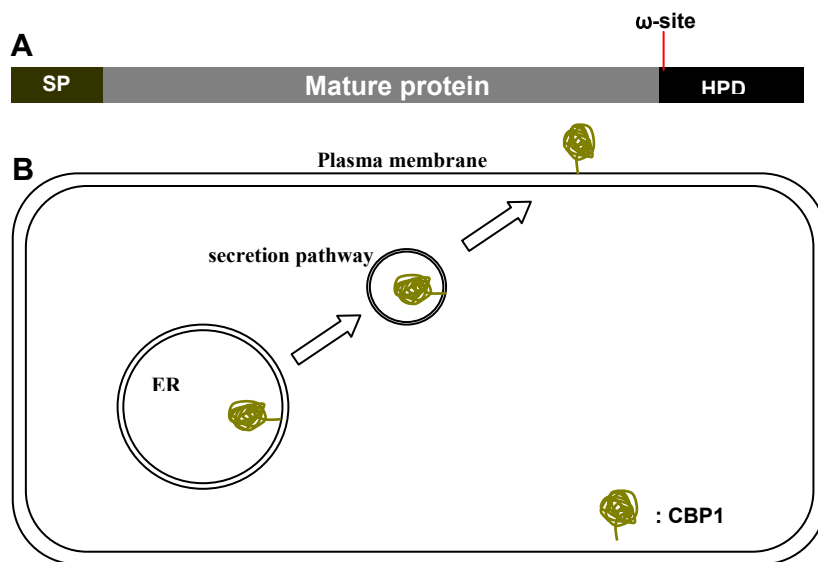


Figure I-1. GPI-Anchored Protein CBP1.

A- CBP1 protein scheme. CBP1 has a signal peptide at the N-terminus (SP) and a hydrophobic domain (HPD) at the C-terminus with a cleavage site named ω -site. B- CBP1 is synthesized and targeted into the ER. After cleavage of the C-terminus and addition of a GPI anchor, the protein is entering the secretion pathway and is located at the outer surface of the plasma membrane.

The mature protein of CBP1 is predicted to exhibit conserved domains showing high similarities with multicopper oxidases, ascorbate oxidase and laccase (by NCBI Conserved Domain Database). The multi-domain consists of three domains, which are distributed along the sequence and are related to multicopper-oxidase of Cu-oxidase type 3, type 1 and type 2 (from N-ter to C-ter), respectively. All are structurally related to COX2 (Cytochrome c oxidase subunit 2) superfamily (Figure I-2), which is the second subunit of cytochrome c oxidase. It provides the substrate-binding site and contains a copper centre called Cu(A) that transfers electrons from cytochrome c to the catalytic subunit 1 (Capaldi et al., 1983).

In this series of proteins, Ascorbate oxidase (AO) has been studied deeply. It is proved to have copper binding and oxidase enzymatic activities. Comparison between CBP1 and AO was performed and it revealed that most critical residues of copper binding center motifs are absent or mutated in CBP1. These residues are labeled as * in figure I-2 (Messerschmidt and Huber, 1990). It suggests that copper binding to these centers in CBP1 is very unlikely.

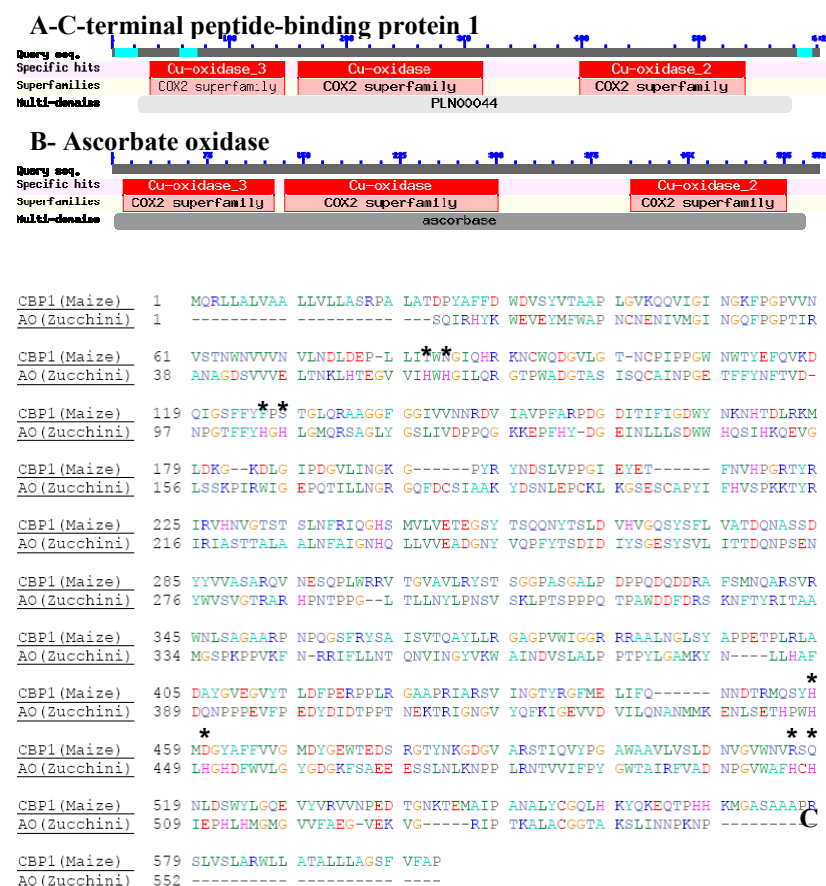


Figure I-2. Putative conserved domains of CBP1 (*Maize*) and ascorbate oxidase (*Zucchini*), and copper binding center.
A, B- Conserved domains of CBP1 and AO
C- Amino acid alignment and copper binding sites
Figures A and B are from Conserved Domain Database of NCBI. Grey bars: amino acid sequence; Cyan fragments: compositionally biased regions not used for domain database search; conserved domains and superfamilies are indicated in dark red and pink bars; PLN00044 and ascorbase are the name of multidomains.
The Histidine residues in copper binding centers of CBP1 are mostly absent (pointed by *) (Messerschmidt and Huber, 1990)

CBP1 has several homologous genes in *Maize* (Figure I-3). Only several of them are predicted to encode GPI-anchored proteins (Table I-1), but none of them has been described.

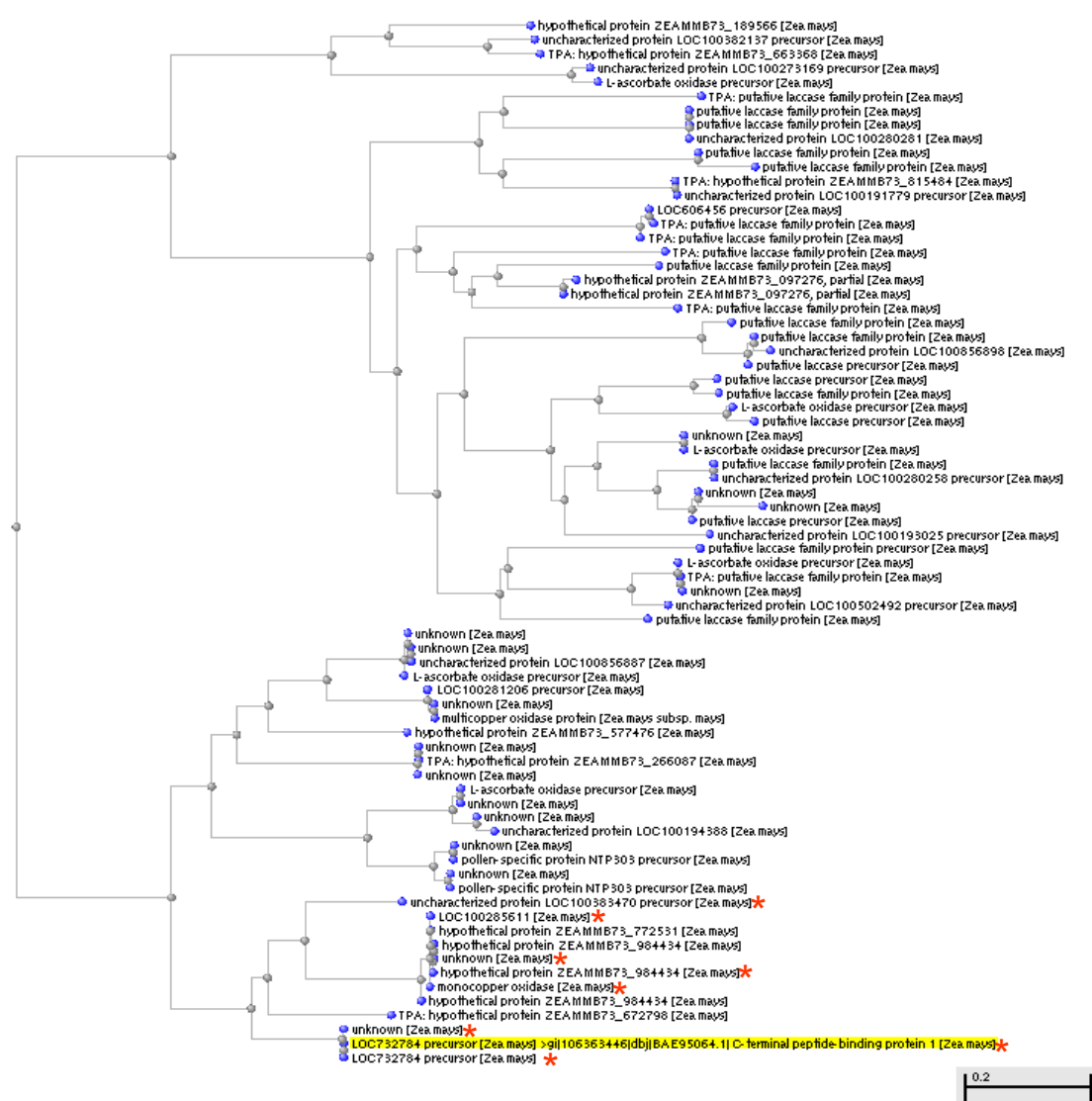


Figure I-3. Phylogenetic tree of proteins encoded by CBP1 and its homologous genes in Maize .

73 Proteins from *Maize* were identified through amino acid residues BLAST; and phylogenetic tree was calculated by COBALT tool.

By GPI-anchor predictor PredGPI calculation, some of them are predicted to have GPI anchors (Table I-1) and labeled as * in the figure).

CBP1 is underlined in yellow , bar is 0.2 billion years.

Table I.1. GPI-anchor prediction by PredGPI tool.

Highly probable	8
Probable	9
Weakly probable	5
Not GPI-anchored	76

I-2 Homologous genes of *CBP1* in *Arabidopsis*.

Homologous genes of *CBP1* were identified in *Arabidopsis* and utilized for our research. By amino acid sequence BLAST in NCBI database, *SKU5* was identified as the closest homologous gene of *ZmCBP1* because it encodes a protein showing 68% identities and only 13 gaps in amino acid sequence (Figure I-4).

CBP1	1	MQRLLALVAALLVLLASRPALATDPYAFFDWDVSYVTAAPLGVKQQVIGINGKFPGPVNVSTNWNVNVNLDLDEPLL	80
SKU5	1	MDLFKILLVFFVNISF--CFAADPYSFYNFVSYITASPLGVPQQVIAINGKFPGPPTINVTTNENLVNVNRNKLDEGLL	78
CBP1	81	ITWNGIQHRKNCWQDGLTNCPIPPGWNWTFYFQVKDQIGSFFYPFSTGLQRAAGGFGGIVVNNRDIIVPFARPDGDI	160
SKU5	79	LHWNGIQRRVSWQDGLTNCPIPPKWNWTFYFQVKDQIGSFFYPFSLHFQASGGFGSFVVPRAIIPVFPSTPDGDI	158
CBP1	161	TIFIGDWYNKNHTDLRKMLEDKGLDLPDGLVINGKGPYRYNDSLVPFGIEYETFNVHPGRTYRIRVHNVTSTSLNFRI	240
SKU5	159	TVTIGDWYIRNHTALRKALDDGKDLGMPDGLVINGKGPYRYNDTLVADGIDFETITVHPGKTYRLRVSNVGISTSLNFRI	238
CBP1	241	QGHSMVLVETEGSYTSQQNYTSLDVHVQSYSLVATDQNASDDYYVVASARQVNESQPLWRRVTGVAVLRYSTSGGPAS	320
SKU5	239	QGHNLVLAESEGSYTVQQNYTSLDIHVQSYSLVTMDQNASDDYYIVASARVVNET--IWRRTVGVGILKYTNSKSKAK	316
CBP1	321	GALFDPQDQDDRAFSMNQARSVRWNLSAGAARPNPQGSFRYSATSVTQAYLLRGAGPVWIGGRRRAALNGLSYAPPETP	400
SKU5	317	GQLFPQPQDEFDKTFSMNQARSIRWNVASAGARPNPQGSFKYGSINVTDVYVLRNMPPTISGKRRTTLNGISFKNPSTP	396
CBP1	401	LRLADAYGVEGVYTLDFPERPPLRGAAFPRIARSVINGTYRGFMELIFQNNDRMQSYHMDGYAFFVVGMDYGEWTEDSRG	480
SKU5	397	IRLADKLKVKDVYKLDFFPKR-PLTGPA-KVATSIINGTYRGFMEVVLQNNDRMQSYHMSGYAFFVVGMDYGEWTENSRG	474
CBP1	481	TYNKGDGVARSTIQVYPGAWAAVLVSLDNVGVWNVRSQNLDSWYLGQEVYVRVVPEDTGNKTEMAIPANALYCGQLHKY	560
SKU5	475	TYNKWDGIARSTIQVYPGAWSAIILSLDNPGAWNLRTEENLDSWYLGQETVYVRVVP-DENNKTEFGHPDNVLYCGALSKL	553
CBP1	561	OKEQTPHHKMGASAAAPRSLVSLARWLLATALLLAGSFVFAP	602
SKU5	554	QKPQ----KVSSASKSIGFTSLSMVVMALVMM-----MLQH	587

Figure I-4. Amino acid alignment between CBP1 and SKU5.

Proteins are indicated on the left and the consensus residues are in red; different amino acid residues are in blue and gaps are in black.

SKU5 was firstly described via the characterisation of a null *sku5* mutant in *Arabidopsis*, it was reported to affect two directional growth processes, especially in root growth (Sedbrook et al., 2002).

I-2-1 *SKU5* gene family in *Arabidopsis*

18 genes were identified as homologous genes of *SKU5* in *Arabidopsis thaliana*. They are named *SKU5*-similar (*SKS*) genes and form the *SKU5/SKS* gene family. Members of this family encode proteins showing high identities. They were compared to *SKU5* by BLAST analysis, and in which *SKS1*, *SKS2* and *SKS3* encode proteins with the highest identities with *SKU5* (Table I-2).

Accession number (Gene name)	Percent identity	Percent coverage
AT4G12420 (SKU5)	100	100
AT4G25240 (SKS1)	67	95
AT5G51480 (SKS2)	66	96
AT5G48450 (SKS3)	60	98
AT4G22010 (SKS4)	51	92
AT1G76160 (SKS5)	49	92
AT1G41830 (SKS6)	48	92
AT1G21860 (SKS7)	49	93
AT1G21850 (SKS8)	49	92
AT4G38420 (SKS9)	48	92
AT4G28090 (SKS10)	48	91
AT3G13390 (SKS11)	49	91
AT1G55570 (SKS12)	47	93
AT3G13400 (SKS13)	46	93
AT1G55560 (SKS14)	46	94
AT4G37160 (SKS15)	49	93
AT2G23630 (SKS16)	49	90
AT5G66920 (SKS17)	48	89
AT1G75790 (SKS18)	45	93

Table I-2. *SKS* genes products are highly similar to SKU5 at the protein level.

SKS genes are found in all Arabidopsis chromosomes, however chromosomes 1 and 4 exhibit most of them with 7 and 6 *SKS* genes, respectively. Several genes localize as neighbors in the same chromosome, such as *SKS7* and *SKS8*, *SKS11* and *SKS13*, *SKS12* and *SKS14* (Figure I-5). *SKS7* and *SKS8* genes have the same transcriptional direction, but *SKS11* and *SKS13*, *SKS12* and *SKS14* have the opposite transcriptional direction. These pairs exhibit similar gene structures with 8 exons for *SKS7* and *SKS8*, whereas *SKS11*, *12*, *13*, *14* have only 3 exons. Such distribution and high similarity between these pairs suggest rather recent events of duplication. Within the *SKU5/SKS* family, gene structure varies in a large range as shown table I-3, with 3 to 10 exons according to the member of the family.

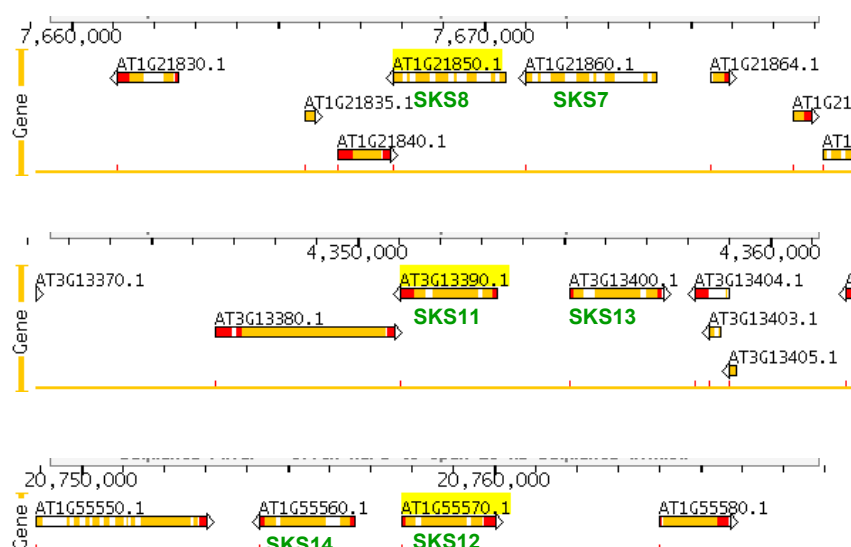


Figure I-5. Some genes are neighbors in the same chromosome. *SKS7* and *SKS8*, *SKS11* and *SKS13*, *SKS12* and *SKS14* are close to each other in the same chromosome. *SKS7* and *SKS8* genes have the same transcriptional direction, but *SKS11* and *SKS13*, *SKS12* and *SKS14* have the opposite transcriptional direction. Genes are indicated in the figure; Yellow: exons; Red: UTR; white: introns.

Table I-3. Heterogeneity in gene structure within the *SKU5/SKS* family

Number of exons	Gene name
10	<i>SKS3</i>
9	<i>SKU5</i> , <i>SKS1</i> , <i>SKS2</i>
8	<i>SKS5</i> , <i>SKS6</i> , <i>SKS7</i> , <i>SKS8</i> , <i>SKS15</i> , <i>SKS16</i> , <i>SKS18</i>
7	<i>SKS9</i> , <i>SKS10</i> , <i>SKS17</i>
6	<i>SKS4</i>
3	<i>SKS11</i> , <i>SKS12</i> , <i>SKS13</i> , <i>SKS14</i>

cDNA phylogenetic tree calculated by DNA maximum likelihood program with molecular clock confirmed the short evolutionary distance between *SKS7* and *SKS8*, *SKS11*, *SKS12*, *SKS13* and *SKS14* (Figure I-6), which suggests that *SKS7* and *SKS8*, *SKS11*, *SKS12*, *SKS13* and *SKS14* could be the duplications to each other respectively. Then the duplicated *SKS11*, *SKS13* in chromosome 3 duplicated in chromosome 1 as *SKS12*, *SKS14*.

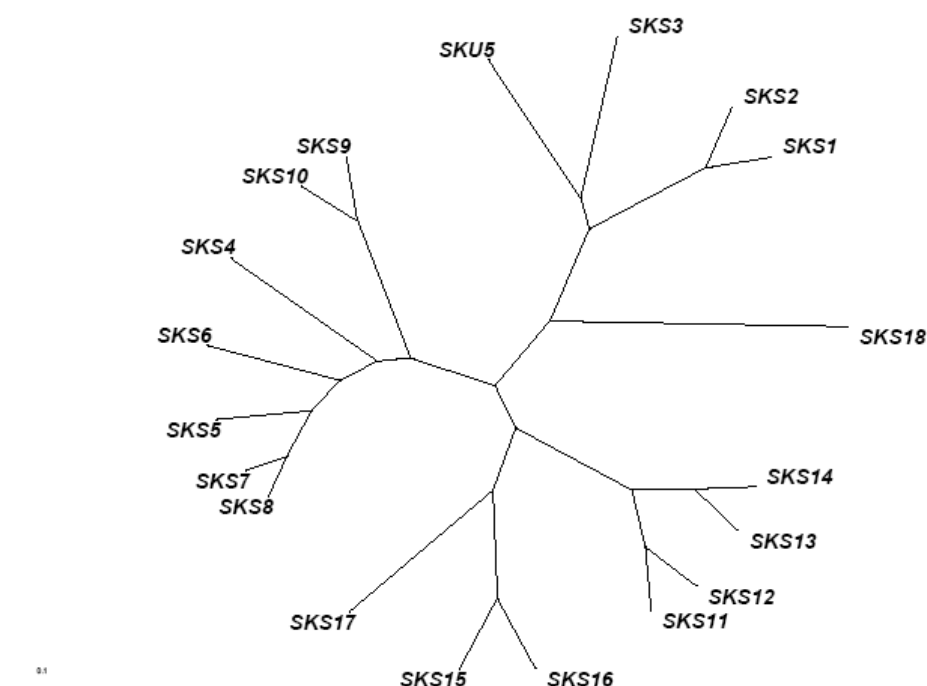


Figure I-6. cDNA unrooted phylogenetic tree calculated by DNA maximum likelihood program with molecular clock.

Gene names are indicated. The length of the lines means the evolutionary distance between different cDNA. Bar is 0.1 billion years.

I-2-2 *In Silico* Expression Data

AtGenExpress Visualization Tool (AVT) analysis shows that about half of these genes (*SKS2*, *SKS7*, *SKS8*, *SKS10*, *SKS11*, *SKS12*, *SKS13*, *SKS14*, and *SKS18*) are highly expressed in reproductive organs whereas they are not significantly detected in other organs (Figure I-7A). Six members, including *SKU5* (*SKU5*, *SKS3*, *SKS4*, *SKS5*, *SKS6* and *SKS17*) are expressed broadly all over the whole plant except in senescing leaves and mature seeds (Figure I-7B). *SKS15* and *SKS16* exhibit a far more specific pattern of expression as they were found to be only expressed in roots (Figure I-7C). *SKS1* is also strongly expressed in roots but is also found in the shoot apex (before and after bolting) and at the early stages of silique and seed development (Figure I-7D). This gene is not significantly expressed in leaves, floral organs and mature seeds. Interestingly, *SKS9* exhibits a complementary profile of expression as it is mostly expressed in leaves and floral organs and not significantly expressed in roots, shoot apex, siliques and seeds (Figure I-7) (Schmid et al., 2005).

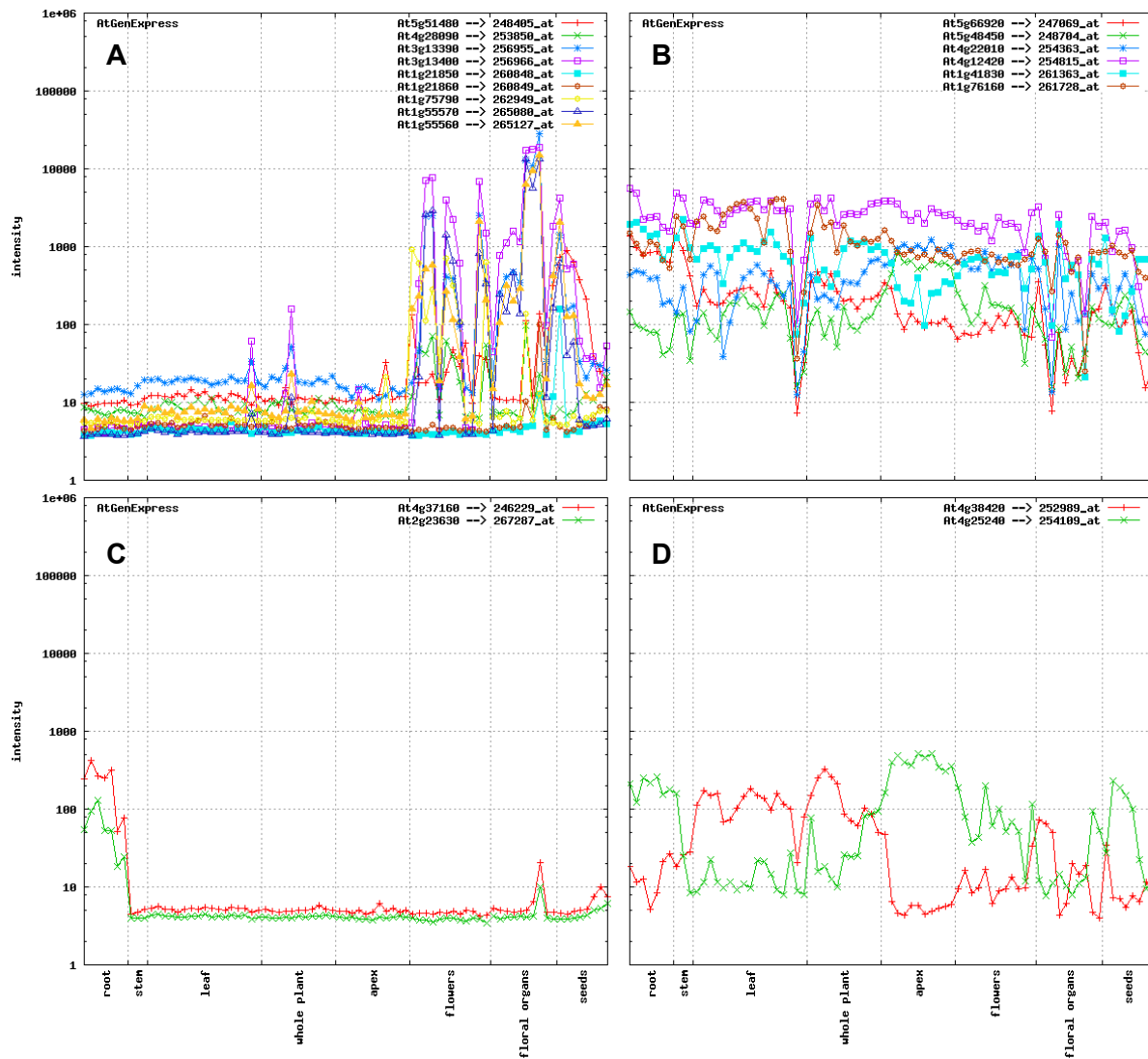


Figure I-7. AtGenExpress Visualization Tool (AVT) analysis of SKS family members.

Genes exhibiting rather similar profiles of expression were grouped within the same graphs (A-C); SKS1 and SKS9 showed nearly opposite patterns as illustrated in D. These data were extracted from the developmental set of microarray data (Schmid et al, 2005)

The values are absolute values from micro array. And the organs are indicated in X-axis. Genes' IDs are indicated in figures.

I-2-3 SKU5/SKS proteins

All *SKS* gene members encoded proteins consist of 3 conserved domains identified as Cu-oxidase type 3, type 1 and type 2 (from N-ter to C-ter). According to multi-domain predictions, SKU5, SKS1, SKS2 and SKS3 are predicted to be multi-copper oxidase-related proteins whereas the others are predicted more generally to belong to oxidoreductases and pectinesterase (Table I-4). Further domain analysis of the distinct proteins using NCBI Conserved Domain Database prediction revealed however the presence of the Cu-oxidase domains of type 3, 1 and 2 in all members of the family (Figure I-8).

Table I-4. *SKS* genes encode proteins with different multi-domains

Multi-Domains	
PLN00044 (multi-copper oxidase-related protein)	SKU5, SKS1, SKS2, SKS3
PLN02991 (oxidoreductase)	SKS4, SKS5, SKS6, SKS7, SKS8
PLN02792 (oxidoreductase)	SKS9, SKS10
PLN02354 (copper ion binding / oxidoreductase)	SKS11, SKS12, SKS13, SKS14
PLN02835 (oxidoreductase)	SKS15, SKS16, SKS17
PLN02168 (copper ion binding / pectinesterase)	SKS18

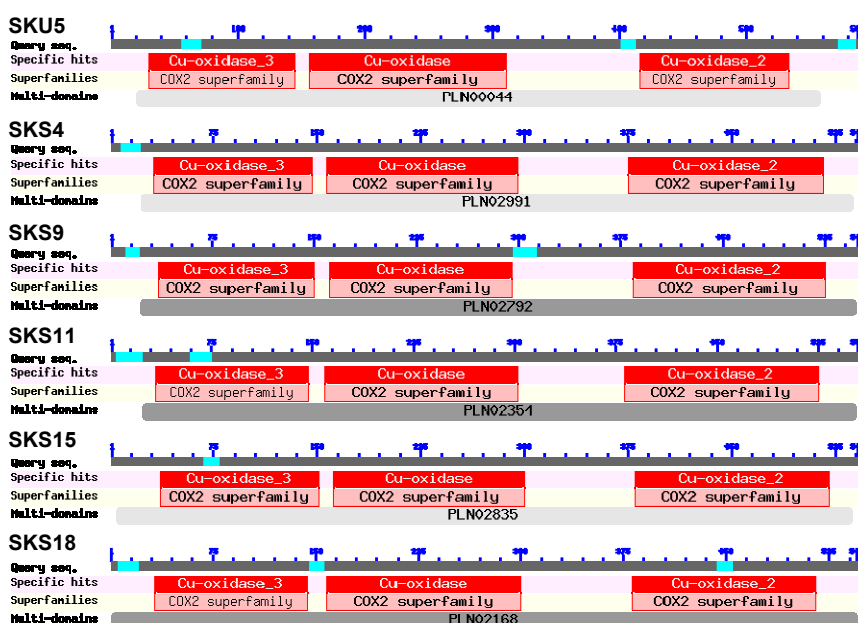


Figure I-8. General structure of predicted SKS proteins.

6 proteins were selected as examples. They all include the highly conserved Cu-oxidases 3, 1 and 2 (from N-ter to C-ter) which are indicated in the figure.

When comparing SKU5/SKS sequences to the ascorbate oxidase from *Zucchini*, which has the copper binding activity, none of SKS members was found to have enough conservation for maintenance of an active copper binding center. Within the SKS members, critical residues of

copper binding center motifs are absent or mutated suggesting that copper binding to these centers is very unlikely as previously observed for maize CBP1 (Figure I-2).

Whereas gene structure was varying in a large range, SKU5 and SKS proteins share common features. In addition to the above mentioned multi-domains, they all include a leader peptide of rather divergent sequences at the N-terminus that is cleaved after biosynthesis of the protein (predicted by SignalP4.1 tool (Emanuelsson et al., 2007)). ClustalW multiple alignment analysis of amino acid sequences (Thompson et al., 1994) shows the conservation between members of the SKU5/SKS family (ANNEXE 1). The major difference within the SKU5/SKS members is observed at the C-terminus as only 3 members, including SKU5, exhibit a hydrophobic region preceded by an ω -domain as in CBP1. This C-terminal domain is susceptible to be cleaved and replaced by a GPI anchor for SKU5, SKS1 and SKS2 using various GPI anchor prediction tools (Eisenhaber et al., 2004; Poisson et al., 2007; Pierleoni et al., 2008). (Figure I-9).

```
SKU5  515  FGHPDNVLYC  GALSKLLQKPQ  ---KVSSA  -SKSIGFTSL  SMVVMALVMM  MMLQH
                                     *
```

```
SKS1  518  MDPPDNVLYC  GALKNLLQKEQ  ---HSAAT  -SILNGHLKL  ML--LMVLLA  SVFRFC
                                     *
```

```
SKS2  518  MDPPENVMYC  GALQAMLQKEQ  ---HSSAT  KSMTNGQLIL  IFSMMVLLS  SFSSFC
                                     *
```

```
SKS3  509  NSVPKNSIYC  GRLSPLLQKDQ  AQRVNFSGSQ  RSIFVTSRGI  LLALFAILVN  -INRLCNTKK  ILDSTAKAQT
      DLSLVETDRI  SEKNRDRISY
```

```
SKS4  498  YPPPKNALMC  GRAKGRHTRP  F
```

```
SKS5  498  YPIPKNALLC  GRASGRSTRP  L
```

```
SKS6  499  YPIPKNSRLC  GRARGRHTRP  L
```

```
SKS7  498  YLIPKNALLC  GRASSSHR
```

```
SKS8  498  YLIPKNALLC  GRATGHHTTT  PGPLSEGSER  F
```

```
SKS9  507  YLLPKNALLC  GRASNKHT--  -TP
```

```
SKS10 502  YPLPKNALLC  GRASNKNMSI  ITP
```

```
SKS11 507  YNMPETSLQC  GLVKGTPKPN  PYAGA
```

```
SKS12 508  YNMPETSLQC  GLVKGKPKVN  PYAGA
```

```
SKS13 505  YNIPLNTNLC  GIVKGLPLPT  PYTI
```

```
SKS14 504  YNIPLNTNLC  GIVKGLPLPA  HYS
```

```
SKS15 502  AEPPLNVLYC  GKAKRPL
```

```
SKS16 500  SEPPVNVLFC  GKAKHPRLI
```

```
SKS17 506  YNPPDNLQLC  GKAVGRHV
```

```
SKS18 503  NPIPGNVIRC  GKVR
```

Figure I-9. Comparison of SKU5/SKS C-terminus.

Only SKU5, SKS1 and SKS2 are predicted to have an ω -site at C-terminus, (pointed with *) and an hydrophobic C-terminus. SKS3 has additional amino acid residues at the C-terminus but cannot be predicted to be further modified by GPI-tail because of the good water solubility of the C-terminus. The other members missed these additional peptide, are not predicted to have an ω -site and to be modified with a GPI anchor.

In addition to the C-terminus differences, short sequences inserted or deleted in few sequences contribute to increase the divergences, as for example at positions 210-223 or 313-317 (ANNEXE 1). These differences support identification of various clades (Table I-5).

Table I-5. SKS members exist in different clades of phylogenetic tree.

CLADES	1	2	3	4	5	6	7	8
SKS GENES	SKU5	SKS 3	SKS 11	SKS 4	SKS 5	SKS 9	SKS 15	SKS 18
	SKS1		SKS12		SKS 6	SKS 10	SKS 16	
	SKS2		SKS13		SKS 7		SKS 17	
			SKS14		SKS 8			

By proteomic and genomic analysis, SKU5 and SKS1 were confirmed to be associated with plasma membrane fraction and to have the GPI anchor in *Arabidopsis* (Borner et al., 2003). And by searching the Plant Proteome Database, SKS2 is also identified to be localized at the plasma membrane as a GPI-anchored protein. Considering the low expression level of SKS2 in most plant organs or cells in culture, it is possible that SKS2 was not confirmed by proteomic analysis because it was under the detection level. SKS2 has the required domains to be a GPI protein as SKU5 and SKS1. SKU5 is the sole member for which the presence of the GPI was established; accordingly, by using translational fusion with the GFP (Green Fluorescent protein), SKU5 was found to be localized at the plasma membrane and at least partly in the cell wall (Sedbrook et al, 2002). It is however difficult to know whether this dual localization reflects the distribution of the endogenous protein or results from the overexpression of the transgene (as a 35SCaMv promoter was used). Cleavage of the GPI anchor for a SKU5 protein associated at the plasma membrane might be a mechanism regulating the relative abundance of the protein at the surface of the PM.

I-2-4 SKU5/SKS proteins through evolution

Comparative analysis of the SKU5/SKS sequences by using BLAST tools against available genome sequence databases of land plants, allowed to identify genes exhibiting *SKS-like* sequences in mosses, club-mosses, conifers, monocot plants and eudicot plants. The phylogenetic tree of the deduced proteins was calculated by COBALT tool (Figure I-10). Clades for the SKS members are labelled by their numbers accordingly to Table I-5. The distance between different SKS genes in *Arabidopsis* is even larger than that of homologous genes between different divisions. It suggests that members of the SKS family is a group of ancient genes which might have diverged very early, that they existed before the diversity of

higher plants and evolved in their own ways to acquire specific functions and potentially play different roles in plants.

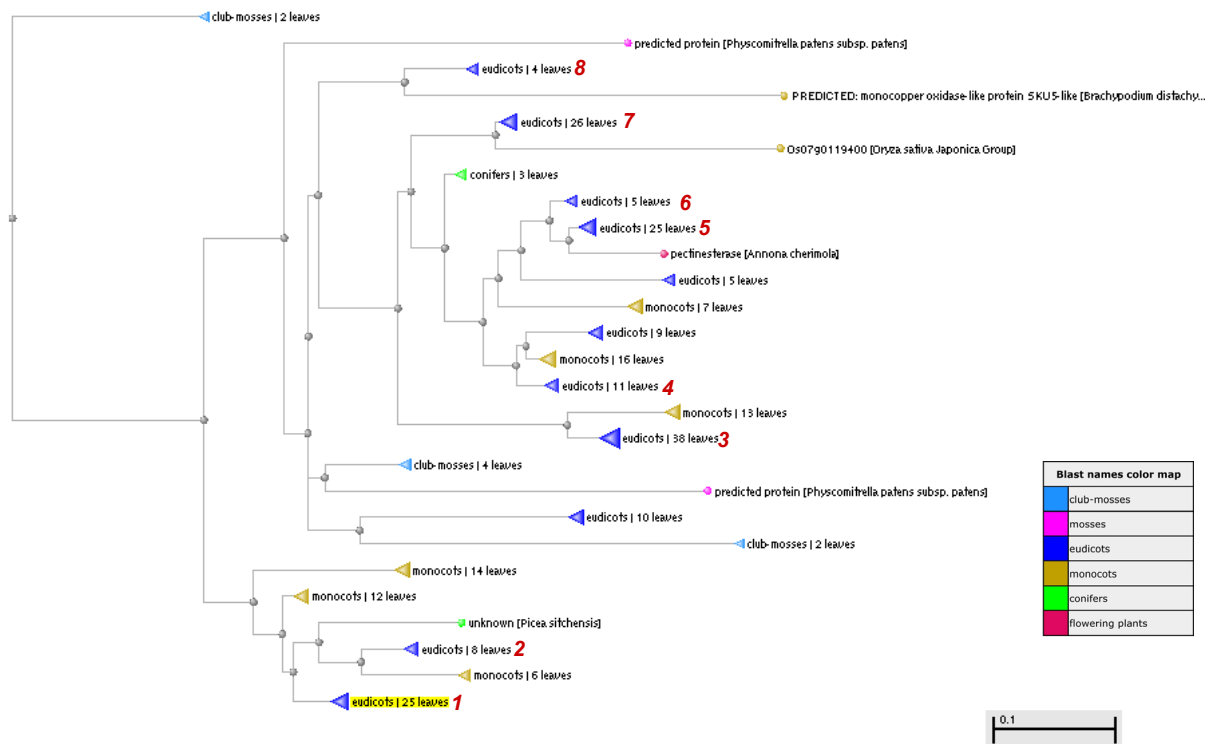


Figure I-10. COBALT phylogenetic analysis of proteins encoded by homologous genes of the SKU5/SKS family.

250 proteins encoded by *SKS* putative homologous genes were identified by BLAST analysis (BLASTP 2.2.27+) (Altschul et al., 1997; Altschul et al., 2005) and phylogenetic tree was calculated by COBALT tool. In this phylogenetic tree, genes were classified by divisions as mosses, club-mosses, conifers, monocot plants and eudicot plants in different colour codes. The size of triangles depends on numbers of homologous proteins (labelled as leaves) inside one clade.

Data shows that *SKS* genes exist through all higher plants. The distance between different members of *SKS* gene family in *Arabidopsis* is even larger than that of homologous genes between different divisions.

Parameter utilized: Fast Minimum Evolution, Max Seq different is 0.85. Bar is 0.1 billion years. .

Conclusion and Discussion

CBP1 is a GPI-anchored maize protein that was identified as a possible interactor of ABP1. *SKU5* and *SKS* are homologous genes of *CBP1* in *Arabidopsis*. They belong to a rather ancient gene family. In *Arabidopsis*, this family contains 19 members. They encode proteins with conserved amino acid sequences and domains but include mutations impairing copper-binding and oxidase activity. *SKU5*, *SKS1*, *SKS2* and *SKS3* encode proteins with the highest similarities with CBP1. *SKU5*, *SKS1*, *SKS2* are the only three members predicted to be modified at their C-terminus by substitution of the hydrophobic domain by a GPI anchor as CBP1. Other members are unlikely to get this post-translational modification and thus to be associated with the plasma membrane. I started to be interested into this protein family as CBP1 was shown to be interacting with ABP1 C-terminus. It was hypothesized that CBP1 could act as a carrier helping ABP1 to reach and be positioned at the outer surface of the plasma membrane or to be directly part of an auxin receptor complex. The output of the *in silico* analysis performed on the *SKU5/SKS* gene family in *Arabidopsis* is that despite the relatively high homology between the members, only 3 genes are putative GPI-anchored proteins. Further work was mainly focused on *SKU5*, *SKS1* and *SKS2* genes.

ANNEXE 1. Alignment of SKS proteins.

	10	20	30	40	50	60	
1	
1	-----	MDLFKI	LLLVFFVNIS	FCFAADPYSF	YNFEVSYITA	SPLGVPQQVI	SKU5
1	-----	MAATCSLLAS	FLLCFALLSA	VSFAADPFVS	YDFRVSYLTA	SPLGVPQQVI	SKS1
1	-----	MAAT-DFFFA	FVFSFALIFG	FSFAGDPYVS	YDFTLSYITA	SPLGVPQQVI	SKS2
1	-----	MRCFPPPLWC	TSLVVFLSVT	GALAADPYVF	FDWTVSYLSA	SPLGTRQQVI	SKS3
1	-----	MRGSCVK	SIVLLLLVLIN	GVLGDNPYRF	FTWKITYGDI	YPLGVKQQGI	SKS4
1	-----	MAGSASFAS	ALFIGLSLLF	AVTAEDPYRF	FEWNITYGDI	YPLGVRQQGI	SKS5
1	-----	MMAVGRSGGT	ILLFCLSFSA	AVTAESPYRF	FDWNVTYGDI	YPLGVRQQGI	SKS6
1	-----	MKVKSMNTRA	MITTLLFLIS	LAFADPYRF	FEWVITYGNI	SPLGVAQQGI	SKS7
1	-----	MEVKSVENTTA	MILGLFFLIS	FVAAEDPYKF	FEWVITYGNI	SPLKVAQQGI	SKS8
1	-----M	CWWLNGAVWT	MMMTTISIIS	FVQADDPYRF	FDWRVITYGNI	SPLGIPQGGI	SKS9
1	-----M	EWLWNGGVW-	MMMTTTTIIIS	FVKAEDTL-F	YNWRVITYGKI	ALDTLPRGGI	SKS10
1	-----	MRG-VKLLAA	CLYLAATAATV	VVRAEDPYFH	HVWNVITYGTV	SPLGVPQQVI	SKS11
1	-----	MKGGVKLLAV	CLCVATATVM	MVQADPYFH	HVWNVITYGTA	SPLGVPQQVI	SKS12
1	-----	-MQGGRLLTV	LVCLAS-TVA	LVSAGDPYFY	YTWNVITYGTA	APLGIPQQVI	SKS13
1	-----	-MEG-RLLTV	LVCLVS-TVA	IVNAGDPYFF	HTWNVITYGTA	SPLGVPQKVI	SKS14
1	-----MKQTN	LLVCKLFTGA	LFWLG---SV	LVNAEDPYMF	YTWTVITYGTR	SPLGVPQQVI	SKS15
1	-----MKQKH	LLLLGFLI-A	YCFSS---VF	VINAEDPYLF	FTWTVITYGTR	SPLGVPQQVI	SKS16
1	-----MKMASRKTTS	LLNHLLLGA	LTLSS--LV	IVKGESPYKF	YTWTVITYGII	SPLGVPQQVI	SKS17
1	-----	--MRHFVFEV	LVLISLVILE	LSYAFAPISS	YQWVVSYSQR	FILGGNKQVI	SKS18
	70	80	90	100	110	120	
47	
51	AINGKFPGP	INVTNENLV	VNVNKLDEG	LLLHWNGIQQ	RRVSWQDGL	GTNCPIPPKW	SKU5
51	AVNGQFPGP	LNATTNINV	VNVFNHLEP	LLLTWPGIQM	RRNSWQDGL	GTNCPIPPRW	SKS1
50	AVNGKFPGP	INATTNINV	VNVFNHLEP	LLLTWPGVQM	RRNSWQDGL	GTNCPIPPW	SKS2
51	GINGQFPGP	LNVTNWNV	MNVKNNLEP	LLLTWNGIQH	RKNSWQDGL	GTNCPIPSGW	SKS3
48	LINGQFPGP	IDAITNDNI	ISVFNYLKEP	FLISWNGVQQ	RKNSWQDGV	GTTCPIPPGK	SKS4
50	LINGAFPGP	IHSVTNDNI	INVYNSLEP	FLLSWNGIQQ	RRNSFVDGV	GTTCPIPPGK	SKS5
51	LINGQFPGP	VNSTNDNI	INVYNSLEP	FLISWNGVQN	RRNSYVDGM	GTTCPIPPRS	SKS6
51	LINGKFPGP	IISITNDNI	INVFNHLEP	FLLSWNGIRN	WKNFQDGV	GTMCPIPPGK	SKS7
51	LINGKFPGP	IAAVTNDNI	INVFNHLEP	FLISWSGIRN	WRNSYQDGV	GTTCPIPPGK	SKS8
52	LINGQYPGP	IYSVTNDNI	INVFNHLEP	FLLSWNGVQL	RKNSYQDGV	GTTCPIPPGK	SKS9
50	LINGQFPGP	IRSLTNDNI	INVQNDLDDP	FLLSWNGVHM	RKNSYQDGV	GTNCPIPPGK	SKS10
50	LINGQFPGP	VNSTNNVI	INVFNHLEP	FLLTWNQIQH	RKNCWQDGT	GTMCPIMPGT	SKS11
51	LINGQFPGP	INSTNNVI	VNVFNHLEP	FLITWAGIQH	RKNCWQDGT	GTMCPIPPGQ	SKS12
49	LINGQFPGP	LNSTNNV	INVFNHLEP	FLLTWSGLQH	RKNSWQDGT	GTSCPIAGT	SKS13
48	LINGQFPGP	LNSTNNV	INVFNHLEP	FLLTWSGIQH	RKNCWQDGT	GTSCPIAGQ	SKS14
53	LINGQFPGP	IEAVTNNIV	VNLINKLDEP	FLITWNGVKQ	RRTSWQDGL	GTNCPIQPNS	SKS15
52	LINGQFPGP	IEGVNNIV	VNVINKLDEP	FLITWNGIKQ	RKMSWQDGL	GTNCPIQPKS	SKS16
59	LINGQFPGP	LEVVTNDNI	LNLINKLQD	FLLTWNQIKQ	RKNSWQDGL	GTNCPIQPNS	SKS17
49	VINDMFPGP	LNATANDI	VNIFNNLEP	FLMTWNGLQL	RKNSWQDGV	GTNCPILPGT	SKS18
	130	140	150	160	170	180	
107	
111	NWTFYQFQKD	QIGSFFFYFSP	LHFQASGGF	GSEFVNPRAI	IPVPFSTPDG	DITVTIGDWY	SKU5
111	NFTYQFQKD	QIGSFFFYSPS	LNHFQASGGF	GPIVINNRDI	IPVPFPQPDG	ELIFIIGDWY	SKS1
110	NFTYDFQLKD	QIGSYFYFSPS	LNHFQASGGF	GALIINNRLD	VPVPFTEPDG	EIIFIIGDWY	SKS2
111	NWTFYQFQKD	QIGSFFFYFSP	TNFQASGGY	GGIIVNNRAI	IPVPFALPDG	DVTLFISDWY	SKS3
108	NFTYVIQVKD	QIGSFFFYFSP	LAFHKAAGAF	GAIRVWSRPR	IPVPFSPPDG	DFWLLAGDWY	SKS4
110	NYTYILQMKD	QIGSFFFYFSP	LGFKHKAAGGF	GGIRILSRPR	IPVPFPDPAG	DTTVLIGDWY	SKS5
111	NYTYILQVKD	QIGSFFFYFSP	LAFHKAAGGF	GGIRILSRPG	IPVPFADPAG	DYTVLIGDWY	SKS6
111	NYTYALQVKD	QIGSFFFYFSP	LGFKHKAAGGF	GGIRISSRAL	IPVPFPTPAD	DYTLVIGDWY	SKS7
111	NYTYALQVKD	QIGSFFFYFSP	LGFKHKAAGGF	GAIRISSRPR	IPVPFPAPAG	DYTVLIGDWY	SKS8
112	NYTYAIQVKD	QIGSFFFYFSP	LAVHKAAGGF	GGFRILSRPR	IPVPFPEPAG	DFTFLIGDWF	SKS9
110	NYTYDFQVKD	QVGSFYFYFSP	LAVQKAAGGY	GSRLIYSLPR	IPVPFPEPAE	DFTFLVNDWY	SKS10
110	NYTYHFQPKD	QIGSYFYFSP	TAMHRSAGGF	GGLRVNSRLL	IPVPYADPED	DYTVLIGDWY	SKS11
111	NFTYHFQPKD	QIGSYFYFPT	TAMHRAAGGF	GGLRVNSRLL	IPVPYADPED	DYTVLINDWY	SKS12
109	NFTYHFQPKD	QIGSYFYFSP	TALHRSAGGF	GGLRVNSRLL	IPVPYADPED	DYTVLINDWY	SKS13
108	NFTYHFQPKD	QIGSYFYFPT	TSLHRSAGGF	GGLRVNSRLL	IPVPYADPED	DYTVLIGDWY	SKS14
113	NWTFYQFQKD	QIGTYTYFAS	TSLHRSAGAF	GALNINQSV	ITTPYPTPDG	DFTLLVSDWF	SKS15
112	SWTYHFQPKD	QIGTYTYFAS	TSMHRSAGAF	GALNVNQSV	IFVPYKPKDA	DFTLLVSDWF	SKS16
119	NFTYKFQTKD	QIGTFNYFSP	TAFHKAAGGF	GAINVYARPG	IPVPYPLPTA	DFTLLVSDWF	SKS17
109	NWTFYQFQKD	QIGSYFYFPT	LLQKAAGGY	GAIRIYPPEL	VPVPFPPDE	EYDILIGDWF	SKS18

	190	200	210	220	230	240	
167	I-RNHTALRK	ALDDGKDLG-	MPDGVLINGK	GPYRYNDTLV	ADGIDFETIT	VHPGKTYRLR	SKU5
171	T-QDHKALRR	ALDSGKELG-	MPDGVLINGK	GPYKYN-SSV	PDGIDYLTFF	VEPGKTYRIR	SKS1
170	T-QNHTALRR	ILDSGKELG-	MPDGVLINGK	GPFKYN-SSV	PDGIEHETVN	VDPGKTYRIR	SKS2
171	T-KSHKKLRK	DVESKNGLR-	PPDGIVINGF	GPFASN----	--GSPFGTIN	VEPGRTYRFR	SKS3
168	K-TNHYVLR	LLEAGRNLP-	NPDGVLINGR	-----	-GWGG-NTFT	VQPGKTYRFR	SKS4
170	K-ANHTDLRA	QLDNGKKLP-	LPDGILINGR	-----	-SSG--ATLN	VEQGKTYRFR	SKS5
171	K-FNHTDLKS	RLDGRGKLP-	SPDGILINGR	-----	-SNG--ATLN	VEQGKTYRLR	SKS6
171	K-TNHKDLKA	QLDNGGKLP-	LPDGILINGR	-----	-SSG--ATLN	IEPGKTYRLR	SKS7
171	K-TNHKDLRA	QLDNGGKLP-	FPDGILINGR	-----	-GSG--ATLN	IEPGKTYRLR	SKS8
172	K-HDHKVLKA	ILDGRGKLP-	LPQGVLINGQ	-----	-GVSYMSSIT	VHKGKTYRFR	SKS9
170	R-RNHTTLKK	ILDGGRKLP-	MPDGVMINGQ	-----	-GVSTVYSIT	VDKGKTYRFR	SKS10
170	T-KSHTQLRK	FLDSGRTLG-	RPDGILINGK	S-----	GK GDGSDAPLFT	LKPGKTYRVR	SKS11
171	T-KSHTQLKK	FLDSGRTIG-	RPDGILINGK	S-----	GK TDGSDKPLFT	LKPGKTYRVR	SKS12
169	A-KSHTALKN	FLDSGRTLG-	SPDGVLINGK	S-----	GK LGGNNAPLFT	MKPGKTYKYR	SKS13
168	T-AGHTALKN	FLDSGRTLG-	LPNGVLINGK	S-----	GK VGGKNEPLFT	MKPGKTYKYR	SKS14
173	SNMTHKDLRK	SLDAGSALP-	LPDALLING-	-----	--VSKGLIFT	GQQGKTYKFR	SKS15
172	K-MGHKELQR	RLDSSRALP-	PPDGLLING-	-----	--ASKGLVFT	GQHGKIYRFR	SKS16
179	K-TNHTTLQ	RLDGGVLP-	FPDGLMING-	-----	--TQ-STFS	GDQGKTYMLR	SKS17
169	Y-LDHTVMRA	SLDAGHSLP-	NPDGILFNGR	-----	--GPEETFFA	FEPGKTYRLR	SKS18

	250	260	270	280	290	300	
225	VSNVGIISTSL	NFRIQGHNLV	LAESGYSYTV	QQNYTSLDIH	VGQSYSLVLT	MDQNASS---	SKU5
228	VHNVGIISTSL	NFRIQNHSL	LVETEGHYTS	QANFTDFDVH	VGQSYSLVLT	MDQDATS---	SKS1
227	VHNVGIISTSL	NFRIQNHKLL	LIETEGRYTS	QMNFTDFDVH	VGQSYSLVLT	MDQNATS---	SKS2
223	VHNSGIATSL	NFRIQNHNL	LVETEGSYTI	QQNYTNMDIH	VGQSFSFLVT	MDQSGSN---	SKS3
214	ISNVGVATSL	NFRIQGHMTK	LVEVEGSHTV	QNIYTSLDIH	LGQSYSLVLT	ANQAPQ----	SKS4
215	ISNVGLQDSL	NFRIQDHMK	VVEVEGHTL	QTFSSLDVH	VGQSYSLVLT	ADQTPR----	SKS5
216	ISNVGLQDSL	NFRIQNHMK	LVEVEGHTL	QTMFSSLDVH	VGQSYSLVLT	ADQSPR----	SKS6
216	ISNVGLQNSL	NFRIQNHMTK	LVEVEGRYTI	QNLFSSLDVH	VGQSYSLVLT	ADQPAK----	SKS7
216	ISNVGLQNSL	NFRIQNHMK	LVEVEGHTI	QTFSSLDVH	VGQSYSLVLT	ADQPAK----	SKS8
219	ISNVGLQHTL	NFRIQGHQMK	LVEVEGHTV	QSMYTSLDIH	VGQSYSLVLT	MDQPDQ----	SKS9
218	VSNVGLQSL	NLEILGHQK	LIEVEGHTV	QTMYSLDIH	VGQTYSLVLT	MDQPPQ----	SKS10
221	ICNVGLKTS	NFRIQNHKLK	LVEMEGSHVL	QNDYDSLVDH	VGQCYGTILT	ANQEAQ----	SKS11
222	ICNVGLKASL	NFRIQNHMK	LVEMEGSHVL	QNDYDSLVDH	VGQCFGVIVT	ADQEPK----	SKS12
220	ICNVGFKSTL	NFRIQGHMK	LVEMEGSHVL	QNDYDSLVDH	VGQCFAVLVT	ADQVAK----	SKS13
219	LCNVGFKSTL	NFRIQNHMK	LVEMEGSHVI	QNDYDSLVDH	VGQCFSVLVT	ANQAAK----	SKS14
219	VSNVGIATSI	NFRIQNHMTS	LIEVEGAHTL	QESYESLDVH	VGQSMTVLVT	LKASVR----	SKS15
217	ISNVGIISTSI	NFRIQGHMTT	LVEVEGSHTL	QEVYESLDIH	VGQSVTVLVT	LKAPVK----	SKS16
223	ISNVGLSSTF	NFRIQGHMTK	VVEVEGSHVI	QTDYDSLVDH	VGQSLAVLVT	LNQSPK----	SKS17
215	ISNVGLKTCL	NFRIQDHMDL	LVETEGTYVQ	KRVYSSLDIH	VGQSYSLVLT	AKTDPVGIYR	SKS18

	310	320	330	340	350	360	
282	DYYIVASARV	VNETIWRVVT	GVGILKYTNS	KGKAKGQLPP	--GPQDEFDK	TFSMNQARSI	SKU5
285	DYYIVASARF	VNETVWQVVT	GVAILHYSNS	KGPVSGPLPV	--PKTDVSSP	WSAMSQPKTI	SKS1
284	DYYIVASARF	VNETVWQVVT	GVGILHYSNS	KGPASGPLPV	--SATDVNHP	WSAMNQPRAI	SKS2
280	DYYIVASPRF	ATS---IKAS	GVAVLRYSNS	QGPASGPLP-	--DPPIELDT	FFSMNQARSL	SKS3
270	DYYIVISSRF	TRK---VLT	TTSLHYSNS	RKGVSGPVP-	---NGPTLDI	ASSLYQARTI	SKS4
271	DYYVVVSSRF	TSN---VLT	TTGIFRYSNS	AGGVSGPIP-	---GGPTIQI	DWSLNQARAI	SKS5
272	DYYVVVSSRF	TDK---IIT	TTGVLRYSGS	STPASGPPI-	---GGPTIQV	DWSLNQARAI	SKS6
272	DYYVVVSSRF	TSK---ILT	TTGVLHYSNS	VAPVSGPIP-	---DGP-IKL	SWSFNQARAI	SKS7
272	DYYIVVSSRF	TSK---ILI	TAGVLHYSNS	AGPVSGPIP-	---EAP-IQL	RWSFDQARAI	SKS8
275	DYDIVVSTKF	VAK---KLL	VSSTIHYSNS	RHSHSSANS	VHVQQPADEL	DWSIKQARSI	SKS9
274	NYSIVVSTRF	INA---EVV	IRATLHYSNS	KGHKIITAR-	---RPDPPDV	EWSIKQAQSI	SKS10
277	DYYMVASSRF	LKS---VIT	TTGLLRYEGG	KGPASSQLP-	---PGPVG-W	AWSLNQFRSF	SKS11
278	DYYMIASRF	LKK---PLT	TTGLLRYEGG	KGPASSQLP-	---AAPVG-W	AWSLNQYRSF	SKS12
276	NYYMVASTRF	LKK---EVS	TVGVMSYEGS	NVQASSDIP-	---KAPVG-W	AWSLNQFRSF	SKS13
275	DYYMVASTRF	LKK---ELS	TVGVIRYEGS	NVQASTELP-	---KAPVG-W	AWSLNQFRSF	SKS14
275	DYFIVASTRF	TKP---VLT	TTASLRYQGS	KNAAYGPLP-	---IGPTYHI	HWSMKQARTI	SKS15
273	DYFIVASTRF	TKP---ILT	TTGILSYQGS	KIRPSHPLP-	---IGPTYHI	HWSMKQARTI	SKS16
279	DYYIVASTRF	IRS---KLS	VMGLLRYSNS	RVPASGDPP-	---ALPPGEL	VWSMRQARTF	SKS17
275	SYIIFATARF	TDS---YLG	GIALIRYPGS	PLDPVGQGP-	---LAPALQDF	GSSVEQALSI	SKS18

	370	380	390	400	410	420	
340	RWNVSASGAR	PNPQGSFYK	SINVTDVYVL	RNMPPVTISG	KRRTTLNGIS	FKNPSTPIRL	SKU5
343	RQNTSASGAR	PNPQGSFYH	QINITNTYIL	RSLPPTIING	ALRATLNGIS	FVNPSTPVRL	SKS1
342	KQNTSASGAR	PNPQGSFYH	QINITRTYIL	RSLPPTKING	KLRATLNGIS	FVNPSTPMRL	SKS2

334 RLNLSSGAAR PNPQGSFKYG QITVTDVYVI VNRPPEMIEG RLRATLNGIS YLPPATPLKL SKS3
322 RRNLASGPR PNPQGSYHYG LIKPGRTIIL AN-SAPWING KQRYAVNGAS FVAPDTPLKL SKS4
323 RTNLSASGPR PNPQGSYHYG MINTTRTIRL AS-SAGQVDG KQRYAVNSVS FKPADTPLKI SKS5
324 RTNLTASGPR PNPQGSYHYG LIPLIRTIVF GS-SAGQING KQRYGVNSVS FVPADTPLKL SKS6
323 RTNLTASGPR PNPQGSYRYG VINITRTRIRL AN-NLGHIEG KQRYAVNSAS FYPADTPLKL SKS7
323 KTNLAASGPR PNPQGTYHYG KIKVTRTIKL AS-SAGNING KQRYAVNSAS FYPTDTPLKL SKS8
331 RTNLTASGPR PNPQGSYHYG RIKISRRLIL ES-SAALVKR KQRYAINGVS FVPGDTPPLKL SKS9
326 RTNLTASGPR TNPQGSYHYG KMKISRRLIL ES-SAALVKR KQRYAINGVS FVPSDTPLKL SKS10
328 RWNLTASAAR PNPQGSYHYG KINITRRIKL VN-TQGVVDG KLRVALNGVS HTDPETPLKL SKS11
329 RWNLTASAAR PNPQGSYHYG KINITRRIKL VN-TQGVVDG KLRVALSGVS HTDPETPLKL SKS12
327 RWNLTASAAR PNPQGSYHYG KINITRRIKL AN-TKNLVNG KVRFGFNGVS HVDTETPLKL SKS13
326 RWNLTASAAR PNPQGSYHYG KINITRRIKL VN-SKSVVDG KVRFGFNGVS HVDTETPLKL SKS14
327 RMNLTANAAR PNPQGSFHYG TIPINRTVL AN-AATLIYG KLRVTNVRIS YINPTPLKL SKS15
325 RLNLTANAAR PNPQGSFHYG TIPINRTVL AN-GRAMING KLRVTNVRIS YVNPATPLKL SKS16
331 RWNLTANAAR PNPQGSFHYG MISPTKTFVF SN-SAPLING KQRYAVNGVS YVKSETPLKL SKS17
328 RMDLNVGAAR SNPQGSYHYG RINVTRTIIL HN-DVMLSSG KLRVTINGVS FVYPETPLKL SKS18

430 440 450 460 470 480
....|....||....||....||....||....||....|
400 ADKLKVKD-V YKLD-FPKRP --LTGPA-KV ATSIINGTYR GFMEVVLQNN DTKMQSYHMS SKU5
403 ADRNKVKG-A YKLD-FPDRP --FNRPL-RL DRSMINATYK GFIQVVFQNN DTKIQSFHVD SKS1
402 ADDHKVKG-D YMLD-FPDRP --LDEKLERL SSSIINATYK GFIQVVFQNN DTKIQSFHID SKS2
394 AQQYNISG-V YKLD-FPKRP --MNRHP-RV DTSVINGTFK GFVEIIFQNS DTTVKSYPHL SKS3
381 ADYFKIPG-V FNLGSIPTSP --SGNGGYL QSSVMAANFR EFIEVVFQNW ENSVQSWHVS SKS4
382 ADYFKIDG-V YRSGSIQYQP --TGG-GIYL DTSVMQVDYR TFVEIIFENS EDIVQSWHLD SKS5
383 ADFFKISG-V YKINSISDKP --TYG-GLYL DTSVLQVDYR TFIEIVFENQ EDIVQSYHLN SKS6
382 VDYFKIDG-V YKPGSISDQP --TNG-AIFP TTSVMQADFR AFVEVIFENS EDIVQSWHLD SKS7
382 ADYFKIAG-V YNPGSIPDQP --THG-AIYP VTSVMQTDYK AFVEIVFENW EDIVQTHWLD SKS8
390 ADYFKIKG-V FKMGSIPDKP --RRGRGMRM ETSVMGAHHR DFLEIIFQNR EKIVQSYHLD SKS9
385 ADHFKIKD-V FKVGTIPDKP --RRGGGIRL DTAVMGAHHR AFLEIIFQNR EKIVQSYHLD SKS10
387 AEYFGVADKV FKYDSTIDNP TPEQIKSIKI VENVLNITHR TFIEVVFENH EKSVQSWHLD SKS11
388 AEYFGVADKV FKYDTISDNP NPDQIKNIKI EPNVLNITHR TFIEVVFENH ERSVQSWHLD SKS12
386 AEYFGMSEKV FKNVNIKDEP -AAKITTLTV EPNVLNITFR TFVEVVFENH EKSMQSFHLD SKS13
385 AEYFQMSEKV FKNVNIKDEP -AAKITALT VQPNVLNITFR TFVEIIFENH EKTMQSFHLD SKS14
386 ADWYNISG-V FDFKTIISTP ---TTGPAHI GTSVIDVELH EFVEIVFQND ERSIQSWHMD SKS15
384 ADWFNIPG-V FNFKTIMNIP ---TPGPSIL GTSVFDVALH EYVEVVFQNN EGSIQSWHLD SKS16
390 ADHFGISG-V FSTNAIQSVP ---SNSPPTV ATSVVQTSHH DFLEIVFQNN EKSMQSWHLD SKS17
387 VDHFQLND-T IIPGMFPVYP ---SNKTPTL GTSVVDIHYK DFHIVFQNP LFGLESYHID SKS18

490 500 510 520 530 540
....|....||....||....||....||....||....|
455 GYAFFVVGMD YGEWTENSRG TYNKWDGIAR STIQVYPGAW SAILISLDNP GAWNLRTEENL SKU5
458 GYSFFVVGMD FGIWSEDKKG SYNNDWAISR STIEVYPGGW TAVLISLDNV GVWNIRVENL SKS1
458 GYAFFVVGMD FGIWSEDRNS SYNNDWAISR STVEVYPGAW TAVLISLDNV GVWNIRVENL SKS2
449 GYAFFVVGMD FGLWTENSRG TYNKGDVAAR STTQVFPGAW TAVLVSLDNA GMWNLRIDNL SKS3
438 GYSFFVVGMD GGQWTPGSRG KYNLRDAVSR STVQVYPRAW TAIYIALDNV GMWNIRSENV SKS4
438 GYSFVVGMD GGQWSPDSRN EYNLRDAVSR CTVQVYPSSW TAILIALDNV GMWNLRSEFW SKS5
439 GYSFVVGMD GGQWKTGSRN GYNLRDAVSR STVQVYPKSW TAIYIALDNV GMWNLRSEFW SKS6
438 GYSFVVGME LGKWSPASRK VYNLNDAILR CTIQVYPRSW TAIYIALDNV GMWNMRSEIW SKS7
438 GYSFFVVGME LGKWSAASRK VYNLNDAVSR CTVQVYPRSW TAIYVSLDNV GMWNLRSEIW SKS8
447 GYSFVVGTD RGTWSKASRK EYNLRDAISR STTQVYVESW TAVYVALDNV GMWNLRSEYW SKS9
442 GYNFVVGIN KGIWSRASRR EYNLKDASIR STTQVYPKSW TAVYVALDNV GMWNLRSQFW SKS10
447 GYSFFAVAVE PGWTTPKRRK NYNLLDAVSR HTVQVYPCW AAILLTFDNC GMWNVRSENS SKS11
448 GYSFFAVAVE PGWTTPKRRK NYNLLDAVSR HTVQVYPCW AAILLTFDNC GMWNIRSENA SKS12
445 GYSFFAVASE PGRWTPEKRN NYNLLDAVSR HTVQVYPCW SAILLTFDNA GMWNIRSENV SKS13
444 GYSFFAVASE PGRWTPEKRE NYNLLDAVSR HTVQVYPCW SAILLTFDNA GMWNIRSENL SKS14
442 GTSAYAVGYG SGTWNMARRR RYNLVDVSR HTFQVYPLSW TTILVSLDNK GMWNLRSQIW SKS15
440 GTSAYVVGYG SGTWNMARRR GYNLVDVSR HTFQVYPLSW TTILVSLDNK GMWNLRSQIW SKS16
446 GYDFVVGFG SGTWTPAKRS LHNLDALTR HTTQVYVESW TTILVSLDNQ GMWNMRSAIW SKS17
443 GYNFVVGYG FGAWSESKA GYNLVDVSR STVQVYPYSW TAILIAMDNQ GMWNVRSQKA SKS18

550 560 570 580 590 600
....|....||....||....||....||....||....|
515 DSWYLGQETY VRVNN-----PDENN-KTE FGHDPDNVLYC GALSCLKQKPQ ----KVSSSA SKU5
518 DRWYLGQETY MRTN-----PEEDG-KTE MDPPDNVLYC GALKNLQKEQ ----HSSAAT SKS1
518 DRWYLGQETY MRIIN-----PEENG-STE MDPPENVMYC GALQAMQKEQ ----HSSAT SKS2
509 ASWYLGQELY LSVNN-----PEIDIDSE NSVPKNSIYC GRLSPLQKDQ AQRVNFSGSQ SKS3
498 ARQYLGQQFY LRVYT-----SSTSY-RDE YPPPKNALMC GRAKGRHTRP F----- SKS4
498 ARQYLGQQLY LRVYT-----PSTSL-RDE YPIPKNALLC GRASGRSTRP L----- SKS5
499 ARQYLGQQLY LRVFT-----SSTSL-RDE YPIPKNSRLC GRARGHTRP L----- SKS6
498 ERQYLGQQFY MRVYT-----TSTSL-RDE YLIPKNALLC GRASSSHR------- SKS7

498	ERQYLGGQFY	MRVYT-----	-PSTSL-RDE	YLIPKNALLC	GRATGHHTTT	PGPLSEGSE	SKS8
507	ARQYLGGQFY	LRVYS-----	-PTHSL-RDE	YLLPKNALLC	GRASNKHT--	-TP-----	SKS9
502	ARQYLGGQFY	LRVHS-----	-PNHSP-KDE	YPLPKNALLC	GRASNKNMSI	ITP-----	SKS10
507	ERRYLGGQLY	ASVLS-----	-PEKSL-RDE	YNMPETSLQC	GLVKGTPKPN	PYAGA-----	SKS11
508	ERRYLGGQLY	ASVLS-----	-PEKSL-RDE	YNMPETSLQC	GLVKGKPKVN	PYAGA-----	SKS12
505	ERRYLGGQLY	VSVLS-----	-PEKSL-RDE	YNIPLNTNLC	GIVKGLPLPT	PYTI-----	SKS13
504	ERKYLGEQLY	VSVLS-----	-PEKSL-RDE	YNIPLNTNLC	GIVKGLPLPA	HYS-----	SKS14
502	SRRYLGGELY	VRVWN-----	-DEKSL-YTE	AEPPLNVLVC	GKAKRPI---	-----	SKS15
500	SRRYLGGELY	VRVWN-----	-NEKSL-YTE	SEPPVNVLC	GKAKHPRLI-	-----	SKS16
506	ERQYSGQGFY	LKVWN-----	-SVQSL-ANE	YNPPDNLQLC	GKAVGRHV--	-----	SKS17
503	EQWYLGGELY	MRVKGEGEED	PSTIPV-RDE	NPIPGNVIRC	GKVR-----	-----	SKS18

	610	620	630	640	650	660	
	
563	-SKSIGFTSL	SMVVMALVMM	MMLQH-----	-----	-----	-----	SKU5
566	-SIINGLHL	ML--LMVLLA	SVERFC-----	-----	-----	-----	SKS1
567	KSMITNGQLI	IFSMMLVLLS	SFSSFC-----	-----	-----	-----	SKS2
563	RSIFVTSRGI	LLALFAILVN	-INRLCNTKK	ILDSTAKAQT	DLSLVETDRI	SEKNRDRISY	SKS3
541	-----	-----	-----	-----	-----	-----	SKS4
541	-----	-----	-----	-----	-----	-----	SKS5
542	-----	-----	-----	-----	-----	-----	SKS6
538	-----	-----	-----	-----	-----	-----	SKS7
551	F-----	-----	-----	-----	-----	-----	SKS8
549	-----	-----	-----	-----	-----	-----	SKS9
547	-----	-----	-----	-----	-----	-----	SKS10
554	-----	-----	-----	-----	-----	-----	SKS11
555	-----	-----	-----	-----	-----	-----	SKS12
551	-----	-----	-----	-----	-----	-----	SKS13
549	-----	-----	-----	-----	-----	-----	SKS14
541	-----	-----	-----	-----	-----	-----	SKS15
541	-----	-----	-----	-----	-----	-----	SKS16
546	-----	-----	-----	-----	-----	-----	SKS17
545	-----	-----	-----	-----	-----	-----	SKS18

Chapter II: Investigating the interaction between GPI-anchored SKU5/SKS proteins and ABP1

II-1. CBP1 and GPI-anchored SKU5/SKS proteins were candidates for being ABP1 binding or docking proteins.

As described in the general introduction, functional evidences support the role of ABP1 at the plasma membrane. ABP1 is however not an intrinsic membrane protein and was proposed to be associated with the membrane through interaction with a PM protein or a PM protein complex. The domain of interaction with the PM protein or protein complex was predicted to be within the amino acid sequence of ABP1.

GPI-anchored protein C-terminal peptide binding protein 1 (CBP1), as the name suggests, was identified as its capacity to bind the synthetic peptide corresponding to ZmABP1 C-terminus (Shimomura, 2006). The starting hypothesis was that maize CBP1 and related GPI-anchored SKU5/SKS members in Arabidopsis were potential interactors of ABP1 contributing to the targeting of the protein at the PM and/or acting as a docking protein.

In '*in silico analyses*', *SKS1*, *SKS2*, *SKU5* were exhibited to be the closest members and localized in the same clade at the phylogenetic tree. They were the only three members of this family which were predicted to encode GPI-anchored proteins in Arabidopsis. Therefore, they were supposed to be the candidate to act the same role as *CBP1* in Arabidopsis.

In this chapter, the coding sequences for *CBP1*, *ZmABP1* from maize, *SKS1*, *SKS2*, *SKU5* and *AtABP1* from Arabidopsis were cloned. And the interactions between SKU5 and AtABP1 from Arabidopsis, as well as CBP1 and ZmABP1 from maize were investigated by yeast two hybrid system.

II-2. Yeast two Hybrid System

Yeast two hybrid system is a popular tool for testing the direct interaction between two proteins in heterologous conditions. The proteins to be tested as interactors are fused with DBD (Gal4 DNA binding domain) or AD (activating domain) respectively, at the N-terminus of the proteins. Each fusion alone cannot activate the transcription. The DBD domain can bind the DNA of the reporter gene but this binding cannot activate the expression, and the protein fused to the DBD is named the bait. The AD domain is the domain that activates the transcription and the protein that is fused to the AD is called the prey.

Both DBD and AD domains include NLS sequences (nucleus localization signal) which could enrich the potential fused interactive protein into the nucleus for effective transcriptional activation. And the transcription is activated only when the bait and the prey are interacting together, the AD domain is then close enough from the DNA of the reporter gene to bind the RNA polymerase that starts the RNA transcription (Figure II-1).

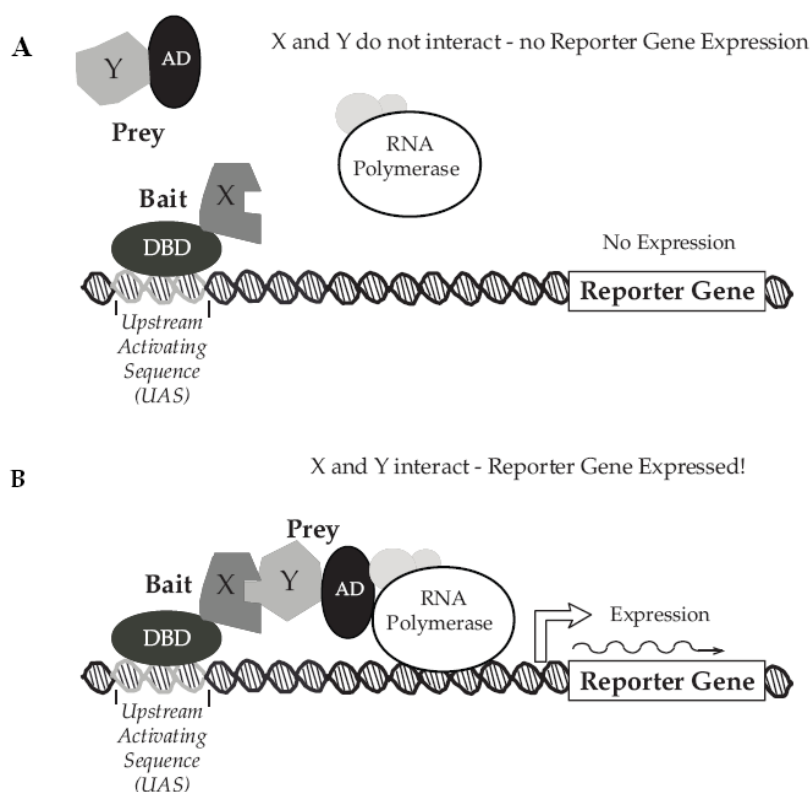


Figure II-1. Interaction detection by Yeast two Hybrid system. (From protocol for yeast two hybrid system, Invitrogen)

(A) the status when there is no interaction between two protein which were tested (X and Y); AD is far away from the reporter gene, and the RNA polymerase cannot start the RNA transcription.

(B) the status when there is interaction between X and Y; AD was close to the reporter gene because of the interaction between X and Y, and the RNA polymerase start the RNA transcription.

For cloning of CBP1/SKU5/SKS1 and ABP1, the ProQuest™ Two Hybrid System with Gateway® Technology from Invitrogen was used. pDEST22 and pDEST32 were utilized as destination vectors (maps are shown in Figure II-2), they confers gentamycin or ampicillin resistance, respectively. Genes were inserted inside these vectors by Gateway cloning technology.

These two constructs were going to be transformed into Mav203 yeast complement cells. pDONR201 that confers a kanamycin resistance (map was shown in Figure II-2) was utilized as a donor vector.

pDEST22 and pDEST32 vectors contain *LEU2* and *TRP1* genes, which were critical in Leu and Trp biosynthesis genes and are lacking in Mav203 Yeast cells. It means that only yeast colonies containing both of these two constructs can survive on medium without Leu and Trp.

The reporter gene includes *HIS3*, which was critical in His biosynthesis genes and also is also lacking in Mav203 cells. It means that only yeast colonies containing both pDEST22 and pDEST32, and where the bait and prey proteins are interacting to each other could survive on medium without His.

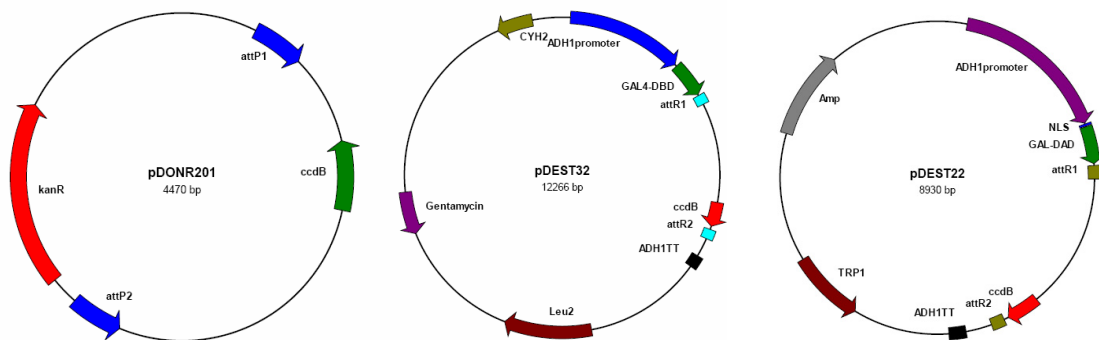


Figure II-2 Vectors utilized for yeast two hybrid analyses.

From left to right, pDONR201, pDEST32, pDEST22 are present respectively. pDEST 32 has DNA binding domain at N-terminus; pDEST22 has DNA activation domain and nucleus localization signal at N-terminus.

II-3 Interaction detection by yeast two hybrid system

II-3.1 Gene cloning and modification for yeast two hybrid.

As described at the beginning of this chapter, *SKS1*, *SKS2* and *SKU5* were suspected to encode the candidates of ABP1 binding/docking protein in Arabidopsis. As well as *AtABP1* in Arabidopsis, *CBP1* and *ZmABP1* in Maize, they were cloned for investigating interactions and further investigation.

RNAs were prepared from seedlings of Arabidopsis and Maize by RNeasy® plant mini kit (QIAGEN), and cDNAs were produced by SuperScript™ III first-strand synthesis system (Invitrogen). Considering *SKS2* was specifically expressed in reproductive organs, cDNA produced from flowers of Arabidopsis was utilized for *SKS2* cloning.

Proper primers were designed for amplifying the full length CDS of each gene. The primers and cDNA resources were indicated in Table II-1. In most cases, 5'-UTR and 3'-UTR were included in the amplification.

GENES	Primers	cDNA Resource	Organs
<i>SKS1</i>	5'-CCTAACTTTATGGCGGCGAC-3' 5'-CCTGGGTCGATCAACATAAAGA-3'	Arabidopsis	Seedlings
<i>SKS2</i>	5'-ACCCGAAGATCATCAACGAAGAAAGCG-3' 5'-AGAGAAACAGAACGAACCCAAGTCTG-3'	Arabidopsis	Flowers
<i>SKU5</i>	5'-AGAAAATGGATTTGTTCAAGATCCT-3' 5'-TTAACAATTTCAATGCTGAAGCATC-3'	Arabidopsis	Seedlings
<i>AtABP1</i>	5'-AAGCATCGAGAAAATGATCGTACT-3' 5'-GCTTTTAGCCTCGGACTTTGC-3'	Arabidopsis	Seedlings
<i>CBP1</i>	5'-GCGGTCCATCTCACTCTCACAGGCT-3' 5'-CCTCGGTGCAGAAGTAACGGTTGCC-3'	Zea.Maize	Seedlings
<i>ZmABP1</i>	5'-TCATTCCACTCCGACATTCA-3' 5'-CAGCAGGATCATGGATGAAG-3'	Zea.Maize	Seedlings

Table II-1 Gene cloning for yeast two hybrid.

Polymerase Chain Reactions (PCR) were then performed at proper conditions with primers and cDNAs as indicated. The fragments containing full length CDS were cloned and recycled by QIAquick® Gel Extraction Kit (QIAGEN). These fragments were cloned into pCR2.1® vectors after adding a 3'-Adenine tail and introduced into DH5α *E.coli* competent cells. 3 colonies with Ampicilline resistance were amplified in cultures for each cloning. Plasmids were prepared from each colony by GENEJET™ plasmid miniprep kit (FERMENTAS) and sequenced to select a plasmid without any mutation.

For investigating interactions with ABP1, these genes should be modified. As described in 'introduction' and '*in silico* analyses' chapters, the signal peptide at the N-terminus and the C-terminus hydrophobic domain are both cleaved during protein maturation *in vivo*. But in yeast two hybrid system, prey and bait should not contain signal peptide at N-terminus but containing Nucleus Localization Signal (NLS) for being transported and localized in nucleus where the reporter gene can be activated. Obviously, without being modified in Endoplasmic Reticulum (ER), the hydrophobic region of GPI modification signal at C-terminus would not be cleaved as well. It means that, for yeast two hybrid system, the hydrophobic region in N-terminus and C-terminus should both be removed.

Similarly, the N-terminal signal peptide of ABP1 should also be removed. As the protein was not supposed to be synthesized in Endoplasmic Reticulum, the KDEL ER-retention signal at the C-terminus was not necessary to be modified.

CBP1 was identified as a binding protein of a synthetic peptide corresponding to the C-terminus of ABP1. In case the absence of interaction would be due to the presence of the

whole protein, we used a truncated ABP1 sequence corresponding to the last 87 AA residues of the maize and Arabidopsis sequences. The sequence is longer than the synthetic peptide originally used but the cleavage occurs within a flexible loop of the protein that was successfully used to introduce a GFP sequence and obtain an ABP1 reporter protein (Robert et al, 2010). This C-terminal sequence contains only the third Cys of ABP1 that is also present in the synthetic peptide.

Gateway® technology was utilized for gene introductions, so the gene modifications could be carried out at amplification for Gateway® BP reaction.

Adapter PCR protocol was used for additional sequence, and the adapter primers were indicated in Table II-2.

Primers for the first amplification with STOP codon (bold) at reverse primers were also indicated in Table II-2. The sequence correspondence to the adapter was in red. The amplified sequence was re-amplified by adapter primers and then cloned into donor vector pDONR201 after BP reaction (Figure II-3) and the recombinant plasmids were introduced into DH5α *E.coli* complement cells.

Table II-2 Primers for Gene Modifications		
Modified Genes	Primers	Templates
<i>SKU5ΔSPΔω</i>	5'- AAAAAGCAGGCT CTGCAGATCCATATTC-3' 5'- AGAAAGCTGGGTGTT ATGAAACCTTCTGTGG-3'	pCR2.1- <i>SKU5</i>
<i>CBP1ΔSPΔω</i>	5'- AAAAAGCAGGCT TCACCGACCCCTACGCC-3' 5'- AGAAAGCTGGGTGTT ACGCCCCCATCTTGTG-3'	pCR2.2- <i>CBP1</i>
<i>AtABP1ΔSP</i>	5'- AAAAAGCAGGCT CTGCTCCTTGTCCTCAT-3' 5'- AGAAAGCTGGGTGTT AAGCTCGTCTTTTGTG-3'	pCR2.1- <i>AtABP1</i>
<i>ZmABP1ΔSP</i>	5'- AAAAAGCAGGCT TCTCCTGCGTGCGAGAT-3' 5'- AGAAAGCTGGGTGTT ATTAGAGTTCGTCTTT-3'	pCR2.1- <i>ZmABP1</i>
<i>Cter-AtABP1ΔSP</i>	5'- AAAAAGCAGGCT TCGCTGAAACACATGGA-3' 5'- AGAAAGCTGGGTGTT AAGCTCGTCTTTTGTG-3'	pCR2.1- <i>AtABP1</i>
<i>Cter-ZmABP1ΔSP</i>	5'- AAAAAGCAGGCT TCGGATCAAGCTCACTA-3' 5'- AGAAAGCTGGGTGTT ATTAGAGTTCGTCTTT-3'	pCR2.1- <i>ZmABP1</i>
<i>Adapter</i>	5'-GGGGACAAGTTTGTACAA AAAAAGCAGGCT -3' 5'-GGGGACCACTTTGTACA AGAAAGCTGGGT -3'	<i>Products of First amplification</i>

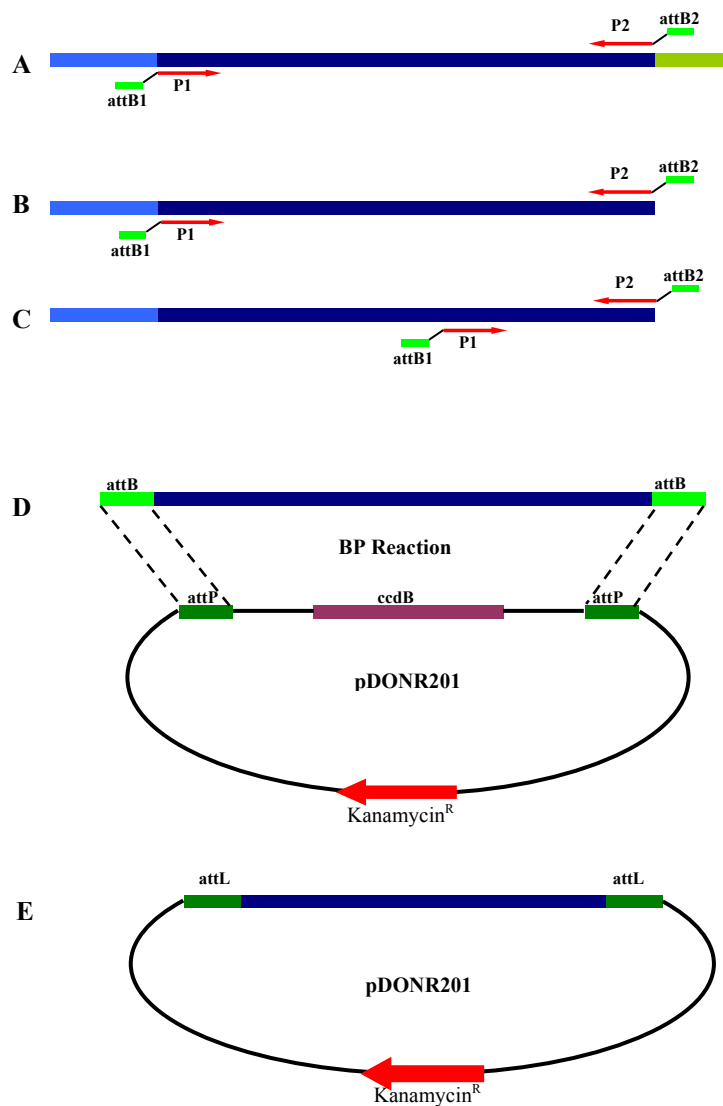


Figure II-3. *SKU5/CBP1* and *At/ZmABP1* genes were modified and cloned into pDONR201 vector. (A) modification of *SKU5* and *CBP1*, (B) modification of *AtABP1* and *ZmABP1*, (C) modification of Cter-ABP1, (D) BP reaction, (E) modified genes were recombined into donor vector pDONR201, Fragments encoding mature proteins were in dark blue, N-terminal signal peptides were in blue, adapters for BP reaction were in green and antibiotics resistant gene was in red.

Colonies with kanamycin resistance were amplified in culture containing kanamycin; and then plasmids were prepared and sequenced, and then utilized for LR reaction together with destination vectors pDEST32 or pDEST22 (Figure II-4). The modified genes were introduced into both pDEST32 and pDEST22. They were named as DBD- or AD- gene name respectively. Then the recombined plasmids were introduced in DH5α *E.coli* complement cells.

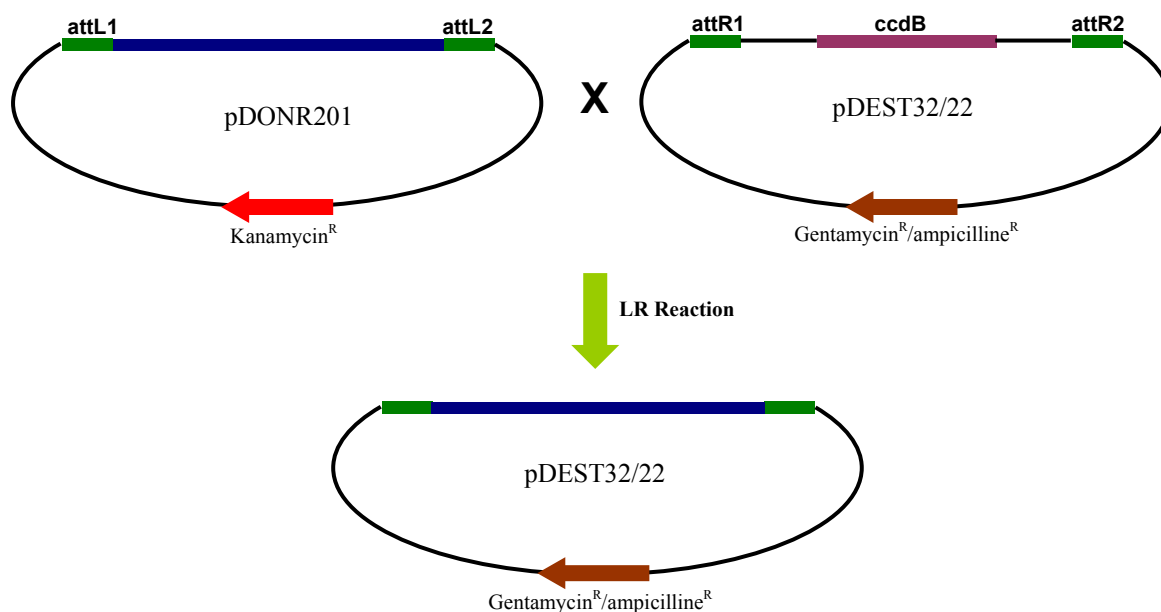


Figure II-6 Recombining genes into destination vectors by LR reaction.
Gene inserted was in dark blue.

Colonies with gentamycin (pDEST32) or ampicilline (pDEST22) resistance were gotten and amplified in LB medium containing proper antibiotics. Plasmids were prepped and the insertions of baits or preys were confirmed by PCR; primers were supplied by Invitrogen (Table II-3).

Table II-3 Primers for confirmation of insertions		
Plasmid	Direction	Primers
Bait	Forward	5'-AACCGAAGTGCGCCAAGTGTCTG-3'
Bait and Prey	Reverse	5'-AGCCGACAACCTTGATTGGAGAC-3'
Prey	Forward	5'-TATAACGCGTTTGAATCACT-3'

The confirmed colonies were amplified in medium with proper antibiotics and the plasmids were prepped for yeast two hybrid transformation.

II-3-2 Yeast transformation and searching for interaction

SKU5 were identified as the *Arabidopsis* genes showing the highest homology with the maize *CBP1*. The objective here was to investigate whether *SKU5* would be able to interact with *AtABP1*. If the interaction could be confirmed between *SKU5* and *ABP1*, interaction investigation would also be performed on the other members.

Following the protocol provided (described in “method”), pairs of plasmids containing baits and preys were co-transformed in Mav203 yeast complement cells and selected on SC medium without Leucine and Tryptophan (SC/-Leu/-Trp). Colonies growing on SC/-Leu/-Trp were supposed to include both bait and prey constructs. Crude DNAs from four colonies of each co-transformants were prepared and gene insertions were confirmed by PCR amplification using primers shown table II-3.

The four colonies were amplified in YPAD medium for few hours and 4µl culture was transferred on SC/-Leu/-Trp plates and cultured at 30°C for 2 days (Figure II-7A). The yeast colonies on SC/-Leu/-Trp plates were transferred and resuspended in 100µl sterilized water, and then 4µl solution was transferred on SC plates without Leucine, Tryptophan and Histidine, but with 0, 25, 50, 100mM 3-Amino-1,2,4-triazole (3AT) (His synthesis inhibitor). Yeasts on SC/-Leu/-Trp/-His+25mM 3AT were cultured at 30°C for three days, when the co-transformants should grow up. In our research, 25mM 3AT was enough to inhibit the background Histidine synthesis and no negative control could grow on these plates.

Unfortunately, none of the yeast co-transformants showed a significant interaction between *ABP1* and *SKU5*, whatever they were used as bait or prey; co-transformation between DBD-Cter*ABP1* and AD-*SKU5* or AD-Cter*ABP1* and DBD-*SKU5* also provided negative data. (Figure II-4). The strong, weak and negative interaction transformants supplied from INVITROGEN were also included in these plates (line #5 in Figure II-4A and 4B).

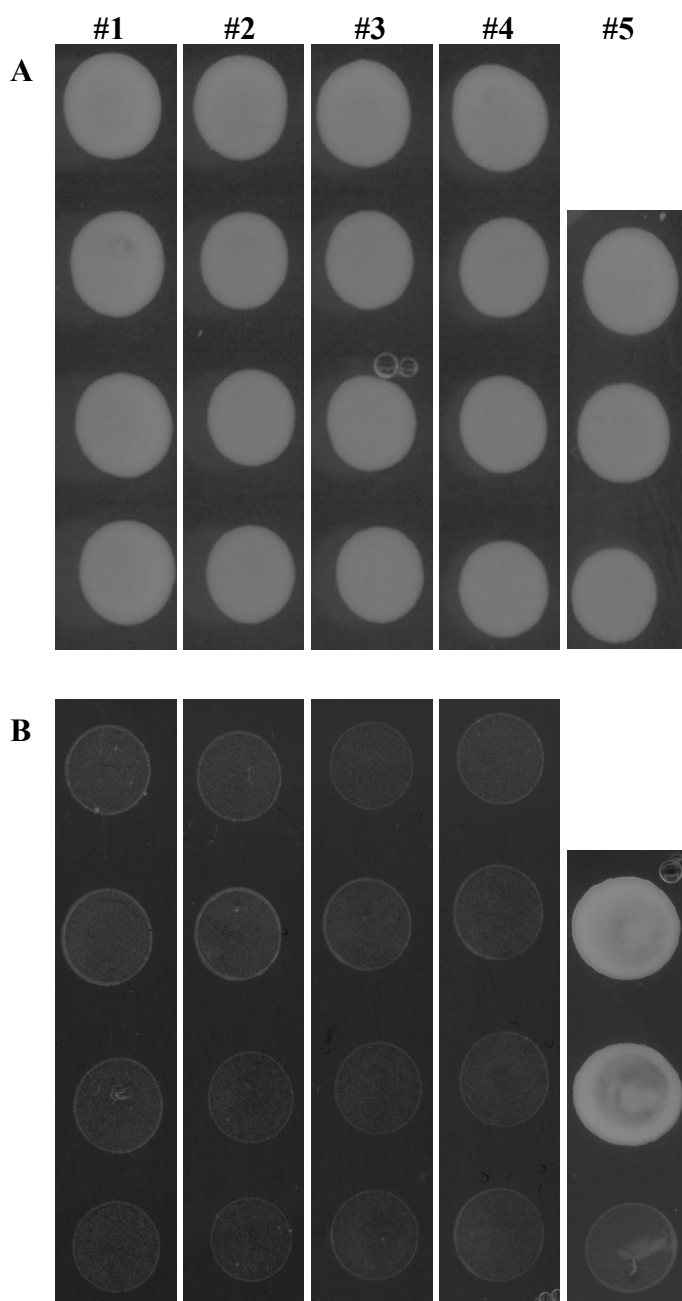


Figure II-7 Interaction detective between SKU5 and ABP1/C-part ABP1.

Yeast co-transformants **(A)** on SC/-Trp/-Leu plate, **(B)** on SC/-Trp/-Leu/-His+25mM 3-AT.

#1: DBD-SKU5 + AD-*AtABP1*

#2: DBD-*AtABP1* + AD-SKU5

#3: DBD-SKU5 + AD -*Cter -AtABP1*

#4: DBD-*Cter -AtABP1* + AD-SKU5

#5: Control, from up to down: strong positive control, weak positive control, and negative control.

In some experiments, a very weak growth was occasionally observed on the triple selective medium but it was not robust enough to conclude on the significance for such interaction. Before making the conclusion that ABP1 is not interacting with SKU5, at least in the heterologous yeast system; we decided to use the maize sequences as the original identification of CBP1 was identified in maize. Interestingly the two C-terminus domains of *AtABP1* and *ZmABP1* differs on several important residues (Figure II-8).

ZmABP1 : ---//---IYDDWSMPHTAAKLKFPYFWDEDCLP-APKDEL

AtABP1 : ---//---IYEDWFMPHTAARLKFPYYWDEQCIQESQKDEL

Figure II-8 Comparison of the C-terminal domains of ZmABP1 and AtABP1

The 12 amino acids forming the synthetic peptide used for the identification of CBP1 are underlined. Residues in common with the Arabidopsis sequence are indicated in red. Strong divergences are observed before the terminal KDEL sequence.

Interactions were checked using co-transformation of Mav203 complement cells with both combinations of constructs: DBD-CBP1 and AD-ZmABP1/AD-Cter-ZmABP1, DBD-ZmABP1/DBD-Cter-ZmABP1 and AD-CBP1. Unfortunately, it was not possible to observe an interaction between CBP1 and either the whole protein or the C-terminal part of ZmABP1 (Figure II-9). There are several possible explanations to these negative results: 1- the folding of CBP1 and Zm-ABP1 in yeast do not allow interaction 2- interaction between CBP1 and ABP1 can only be detected using the last 12 residues of the C-terminus of the protein 3- there is a default of production of at least one of the protein in yeast 4- the proteins are not interacting.

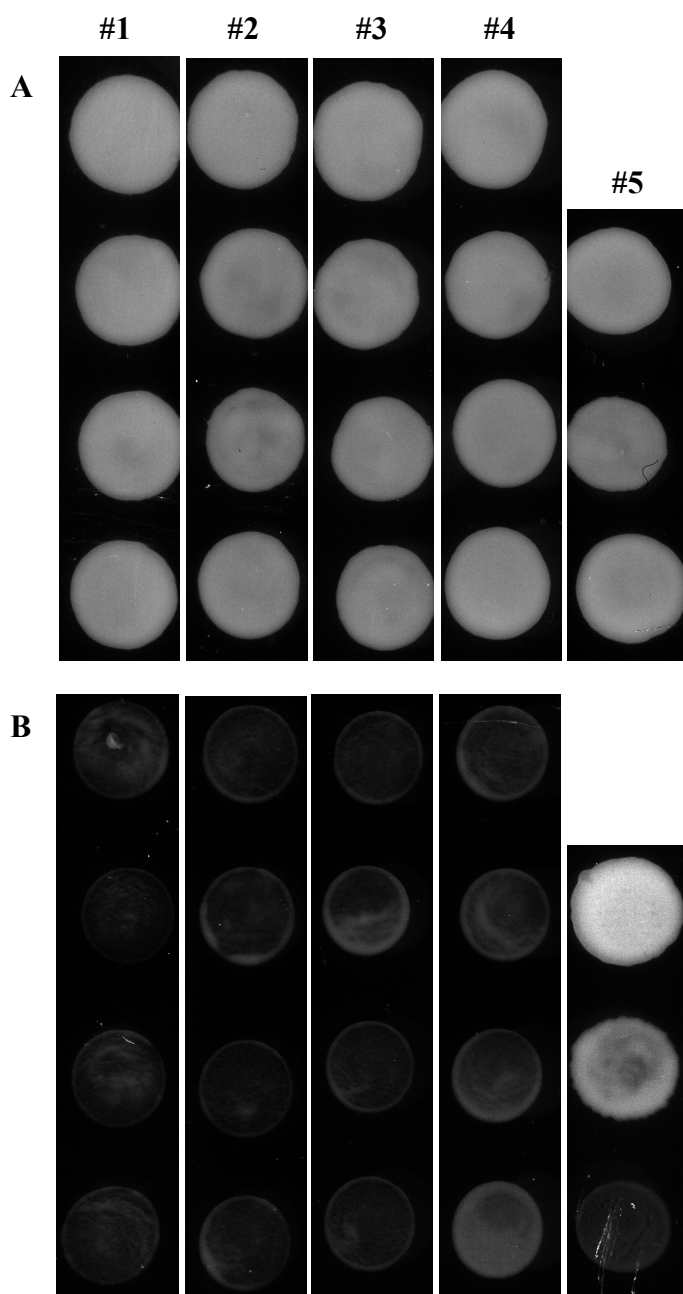


Figure II-9 Interaction detective between CBP1 and ZmABP1/Cter-ZmABP1.

Yeast co-transformants (A) on SC/-Trp/-Leu plate, (B) on SC/-Trp/-Leu/-His+25mM 3-AT.

#1: DBD-*CBP1* + AD-*ZmABP1*

#2: DBD-*ZmABP1* + AD-*CBP1*

#3: DBD-*CBP1* + AD-*Cter-ZmABP1*

#4: DBD-*Cte-ZmABP1* + AD-*CBP1*

#5: Control, from up to down: strong positive control, weak positive control, and negative control.

Finally, the question of the appropriate production of all these proteins in yeast was raised. I first tried to extract the proteins from yeast to perform western blot using commercial antibodies against DBD or AD but the results were not convincing even with the control clones that were growing well on the triple selective media for which we know that the proteins were well produced.

ABP1 was reported to act mainly as a dimer; similarly multi-copper oxidases were also reported to form dimers. A last assay was then performed to see whether ABP1-ABP1, SKU5-SKU5 and CBP1-CBP1 interactions could be detected by Y2H.

In the case of ABP1, the result was not conclusive (Figure II-10), however for CBP1 and SKU5, a weak but significant growth of the co-transformed yeast was detected using DBD-*CBP1* and AD-*CBP1*, DBD-*SKU5* and AD-*SKU5* together (Figure II-11), suggesting that CBP1 and SKU5 might form homodimers and providing also some evidence that the proteins were produced in yeast for both constructs.

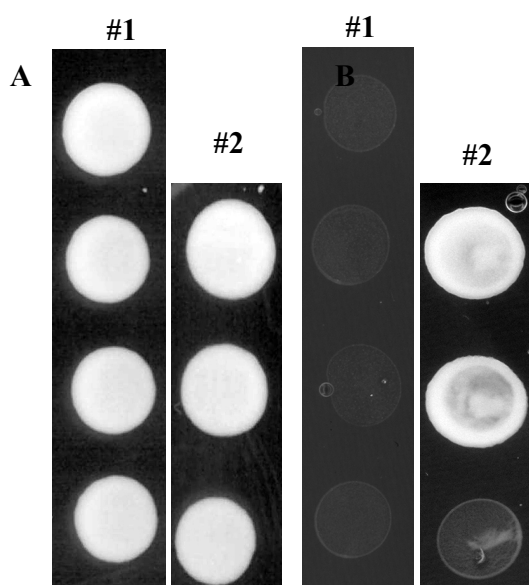


Figure II-10 Interaction detective between ABP1 and ABP1.

Yeast co-transformants (A) on SC/-Trp/-Leu plate, (B) on SC/-Trp/-Leu/-His+25mM 3-AT.

#1: DBD-*AtABP1* + AD-*AtABP1*

#2: Control, from up to down: strong positive control, weak positive control, and negative control.

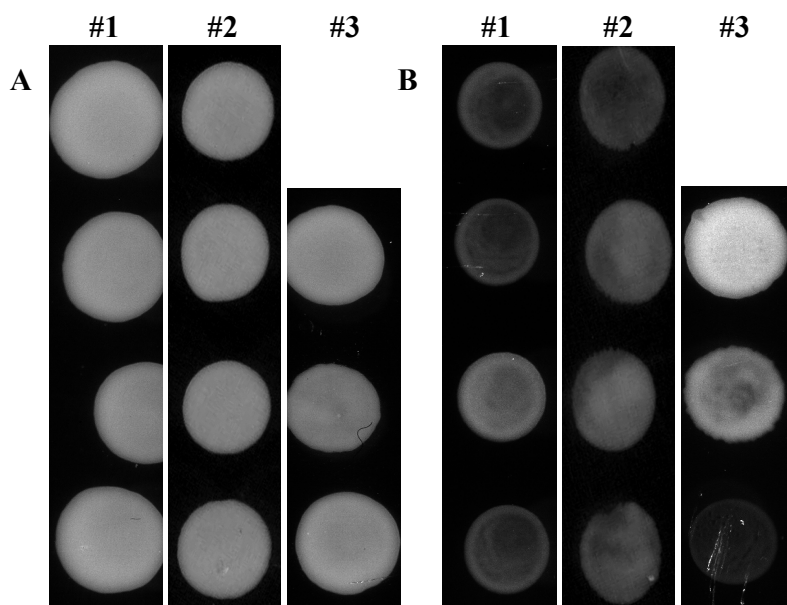


Figure II-11 Interaction detective between CBP1 and SKU5.

Yeast co-transformants (A) on SC/-Trp/-Leu plate, (B) on SC/-Trp/-Leu/-His+25mM 3-AT.

#1: DBD-*CBP1* + AD-*CBP1*

#2: DBD-*SKU5* + AD-*SKU5*

#3: Control, from up to down: strong positive control, weak positive control, and negative control.

Conclusion and Discussion:

Interactions between ABP1 and GPI-anchored members can not be confirmed in heterologous yeast two hybrid system.

There are 4 possibilities:

1. There is no direct interaction between ABP1 and GPI-anchored proteins.

Considering the CBP2, which was also identified with the same ability to bind C-terminus synthesized peptide of ZmABP1, but was not supposed to be the ABP1 binding protein because of its cytosolic localisation, CBP1 also have the chance that it's not the true ABP1 binding protein and the reported interaction was an artefact.

2. The modification of GPI anchor effect the interaction.

As described in 'introduction', the GPI anchors might effect conformation of the whole protein and function of these proteins. In yeast two hybrid system, the GPI anchor had to be cleaved, which might affect the potential ability of binding ABP1.

3. The production or conformation of ABP1 might affect the interaction.

The conformation of ABP1 is changeable, which depends on auxin-binding, pH (David et al., 2001; Woo et al., 2002; Bertosa et al., 2008) . in the nucleus of yeast where the potential interaction happened, the environment must be different from the ER or outer surface of plant cells where the interaction with ABP1 should happen. Especially the redox conditions are often evoked as responsible for alteration of protein folding in yeast.

4. The interactions need the presentation of the third component.

As described in 'introduction', GPI-anchored CBP1 or SKU5/SKS1/SKS2 could not be the only ABP1 binding or docking protein, because plenty of behaviours of ABP1 cannot be explained if it's only binding or docking by GPI-anchored CBP1 or SKU5/SKS1. Very recently, the identification of a series of 4 leucine-rich repeat receptor-like kinase proteins as interactors of ABP1 at the plasma membrane was reported in a commentary following the last auxin meeting in December 2012 (Strader and Nemhauser, 2013). ABP1 and LRR-RLK might form the function receptor unit at the plasma membrane. This does not exclude a contribution of CBP1/SKU5/SKS1 but involves at least a third component in the interaction.

Instead of focusing the work trying to confirm or invalidate the interaction between ABP1 and SKU5/SKS GPI-anchored proteins, the choice was made to develop a genetic approach to learn more about the SKU5/SKS GPI-anchored proteins in Arabidopsis and then investigate

whether molecular or developmental phenotypes would be reminiscent of those observed in ABP1 loss of function. Whatever the result, the characterisation of the SKU5/SKS GPI-anchored proteins would be interesting to be investigated.

Chaper III: Functional Analysis of *SKS* genes by reverse genetic approaches

As mentioned in chapter “*in silico analysis*”, *SKS1*, *SKS2*, *SKU5* are the only 3 members in the *SKU5/SKS* family that are susceptible to be modified with a GPI anchor. Yeast two hybrid approach was not conclusive to confirm a possible interaction between these proteins and ABP1 from *Arabidopsis*, or even between CBP1 and ZmABP1 (see Results, chapter II “interaction between ABP1 and SKS protein”). We decided to develop a genetic approach to explore the role of *SKS1*, *SKS2* and *SKU5*, by selecting null mutants, constructing double and triple mutants, studying their phenotype and response to auxin, and also generating overexpressors (Chapter V). The objectives were firstly to get insight into the role of *SKS1*, *SKS2* and *SKU5* during development and secondly to determine whether specific traits of the mutants could provide experimental evidences supporting a possible interaction with ABP1 or a role in auxin signalling. Investigating the role of these genes is also interesting because there are not so many GPI-anchored proteins that have been identified and studied in plants to date.

III-1 Expression analysis of *SKS1*, *SKS2*, *SKU5* in *Arabidopsis thaliana*:

Specific primers were designed to study the expression levels of *SKS1*, *SKS2* and *SKU5*, by real-time RT-PCR (Table III-1). RNAs were extracted from roots of 5-day old plantlets, 5-day-old whole seedlings, rosette leaves, opened flowers (including sepal, petal, pistil and stamens) and 5 day after fecundation (DAF) siliques of *Arabidopsis* *Ws*-ecotype. The efficiency of each pair of primers was determined by studying the slope and linearity of the amplification for at least three cDNA concentrations over 2 orders of magnitude.

After validation of the primers, semi-quantitative analysis was performed and expression data were expressed relative to *ACTIN2-8* that is used as an internal reference (Figure III-1).

Table III-1 Primers used for Real-time RT-PCR

Genes	Primers	Sequence	Localization on mRNA	Products length
<i>SKS1</i>	SKS1-F	CGGATCACAAACCCCGAGGAGGAT	1722-1892	171bp
	SKS1-R	CACCGAGGCGAGCAACACCATTAG		
<i>SKS2</i>	SKS2-F	ACCCTGAGGAAAACGGAAGTACGG	1784-1887	104bp
	SKS2-R	TGTGGCCGAGCTGTGATGTTGTTTC		
<i>SKU5</i>	SKU5-F	CGAATTCCGACACCCTGACAATGTTC	1875-1975	101bp
	SKU5-R	TGAATCCAATGCTCTTCGATGCCGA		

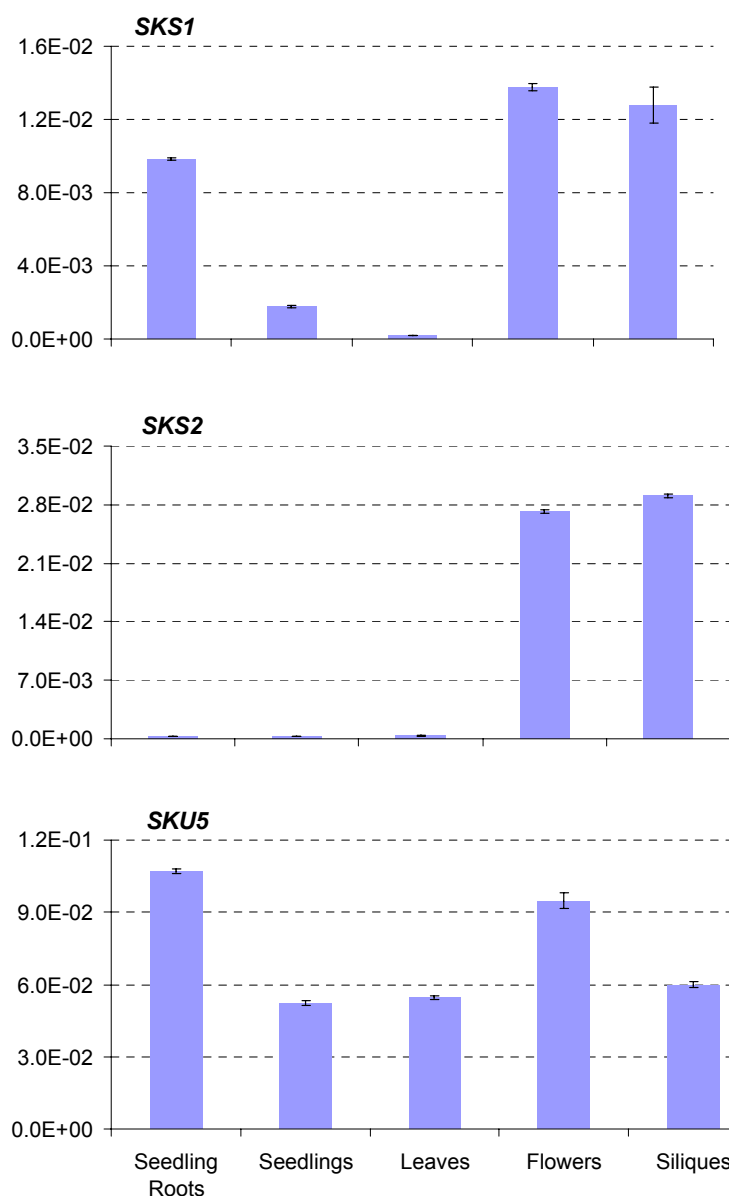


Figure III-1. *SKS1*, *SKS2*, *SKU5* expression levels in different organs of Arabidopsis.

RNAs were extracted from roots of 5-day old plantlets, 5-day-old whole seedlings, rosette leaves, opened flowers (including sepal, petal, pistil and stamens) and 5DAF siliques of Arabidopsis Ws-ecotype.

Genes analyzed were indicated above each chart; x-axis is the organs; y-axis is actin units. The expression tests were repeated technically, and the Error Bars correspond to the standard deviations .

These experimental results are in agreement with the GenExpress data collected from microarray expression data on affymetrix chips: *SKS1* was expressed highly in reproductive organs and roots; *SKS2* was expressed specifically in reproductive organs; *SKU5* was expressed all over the plants with much higher levels than *SKS1* and *SKS2* even in roots and reproductive organs.

Analysis of the effects of hormonal treatments, light conditions, biotic or abiotic treatments did not revealed significant changes in gene expression of *SKU5* and *SKS1* in microarray data and was not investigated here. It was not conclusive for *SKS2* as it is not significantly expressed in young seedlings that were the biological material used for these transcriptomic analyses.

III-2 Characterization of *skt1*, *skt2* and *sku5* null mutants.

Many tools, data and materials are potentially available for the scientific community for the model plant *Arabidopsis*. A reverse genetic approach was feasible after identification, ordering of mutants and their validation. Single mutants were first characterized then double and triple mutants were generated by crosses to *knock-out* two or three GPI-anchored proteins together, respectively.

III-2-1 *sku5/skt* single null mutants

We were interested by knock-out mutants, so we searched for insertion mutants in *Arabidopsis* mutant libraries accessible in TAIR databases. Whenever possible we favoured T-DNA lines exhibiting insertion within an exon. Figure III-2 illustrates *SKS1*, *SKS2*, *SKS3* and *SKU5* genes with insertion sites indicated by green bars. *SKS3* was initially included in a primary analysis as it appeared in the same clade as *SKU5*. However detailed sequence analysis revealed that the protein is unlikely to be modified by a GPI anchor.

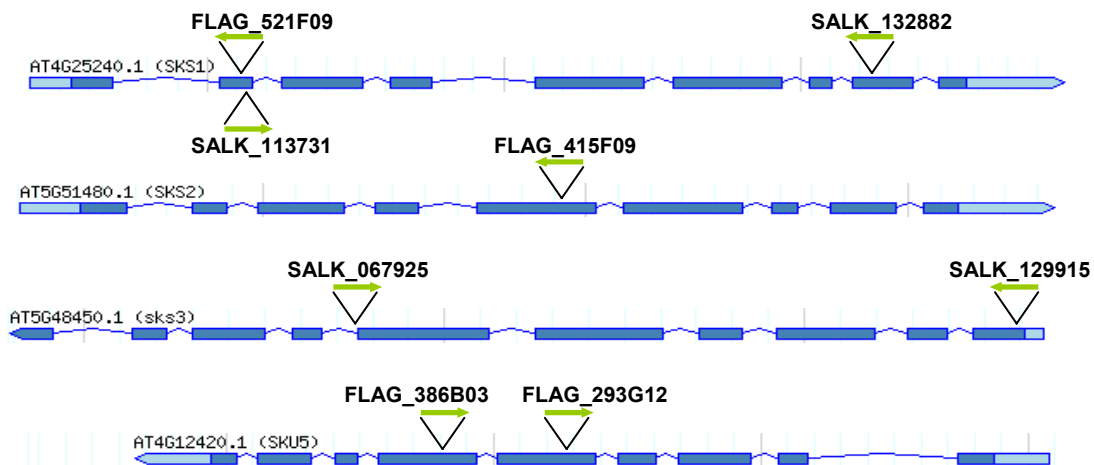


Figure III-2. Maps of ordered *skt* insertion mutants.

Blue bars are *SKS* gene exons, blue lines between exons are introns, and green arrows are T-DNA insertions. Null mutant lines are named by FLAG_ or SALK_.

One to three mutants were ordered for each gene upon their availability. *skt2* and *sku5* mutants were only found in Wassilewskija (*Ws*)-ecotype background (Table III-2). A *Ws* mutant was also selected for *SKS1* in the perspective of generating various combinations of mutants in a homogenous ecotype background.

Table III-2. *sk5/sku5* mutants in different background.

Gene	Predicted GPI anchor	Mutant line	Ecotype Background	Mutant Name
<i>SKS1</i>	YES	FLAG_521F09	<i>Ws</i>	<i>sk5-1-1</i>
		SALK_113731	<i>Col0</i>	<i>sk5-1-2</i>
		SALK_132882	<i>Col0</i>	<i>sk5-1-3</i>
<i>SKS2</i>	YES	FLAG_415F09	<i>Ws</i>	<i>sk5-2-1</i>
<i>SKS3</i>	NO	SALK_067925	<i>Col0</i>	<i>sk5-3-1</i>
		SALK_129915	<i>Col0</i>	<i>sk5-3-2</i>
<i>SKU5</i>	YES	FLAG_293G12	<i>Ws</i>	<i>sku5-2</i>
		FLAG_386B03	<i>Ws</i>	<i>sku5-3</i>

Mutants were ordered at the European Arabidopsis Stock Center (NASC) and at the *Arabidopsis thaliana* Resource Center for genomics of the Institute Jean-Pierre Bourgin (IJPB) for SALK and FLAG mutants, respectively. After receipt, it was first essential to confirm the insertion position for each of them and to verify whether they were homozygous or heterozygous for the T-DNA insertion. The principle is illustrated figure III-3. For each mutant, primers were designed as P1, P2 and P3, P1 being on the T-DNA, P2 and P3 on each side of the insertion within the gene. They were designed for amplification of DNA fragments of distinct sizes between P1-P2 and P3-P2 combinations.

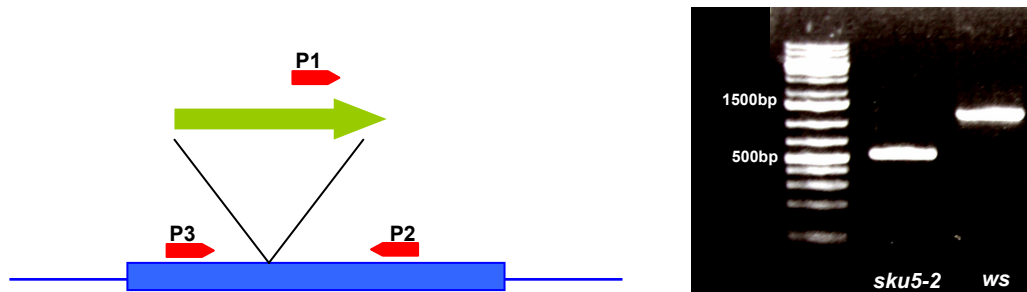


Figure III-3 . Genotyping of *sk5* T-DNA mutants.

A- Principle of mutant genotyping. Primer P1, P2, P3 (red arrow) were designed on the T-DNA insertion (green arrow) and at both sides of the insertion site, on *SKU5/SKS* genes (blue bar). B- Example of amplification products for *sk5-2*. line 1: 1kb ladder marker; line 2, *sku5-2* homozygous amplified by primers P1 and P2 among P1, P2 and P3; line 3, wild type amplified by primers P2 and P3 among P1, P2 and P3.

Resistances are also associated to the T-DNA, they can potentially help to select homozygous mutants. For SALK mutants, pROK2 includes a resistance to kanamycin; but the resistance was often silenced (Alonso et al, 2003). For FLAG mutants, pGKB5 contains two resistances, one to kanamycin and another one to the herbicide Basta (Bouchez et al,1993).

It was then important to control whether these mutants were null for the gene disrupted by the insertion as expected. RNAs were extracted from 5 day-old seedlings of the different *skl*, and *sku5* single mutant lines and from flowers for *skl2*. Real-time RT-PCR was utilized to search for corresponding mRNAs.

As described in chapter ‘*in silico analyses*’, *SKL1*, *SKL2*, *SKL3* and *SKU5* encode extremely conserved proteins, in which *SKL1*, *SKL2* and *SKU5* includes C-terminal omega domain. By analyzing their knock-out mutants, it would be possible to reveal whether they play the same role in plants.

In the original paper of *SKU5* investigation (Sedbrook et al., 2002), the authors found that *sku5* knock-out mutant exhibited twisted roots which caused left slanting on solid medium (containing 1.5% agar). This could be utilized as the iconic phenotype of *SKU5* mutation.

Following the method described in the original paper, the twisted and left slanting roots were investigated. These phenotypes were only found in *sku5-2* and *sku5-3* null mutants (Figure III-5), but never in any alleles of *skl1*, *skl2* or *skl3* mutants. *skl1*, *skl2* and *skl3* null mutant plants didn’t exhibit significant difference in phenotype compared to wild-type (not shown).

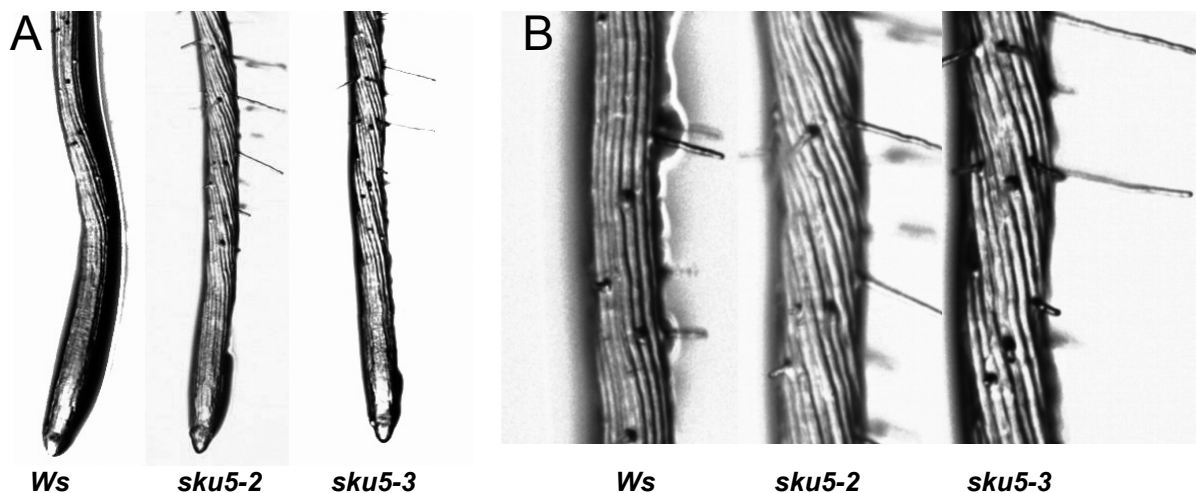


Figure III-5. Skewed roots of *sku5-2* and *sku5-3* single null mutants on medium containing 0.8% agar. (A) Root tips of *Ws*, *sku5-2*, *sku5-3* grew on $\frac{1}{2}$ MS medium containing 0.8% agar for 7 days. In all single null mutant seedlings, only two *sku5* knock out mutant, *sku5-2* and *sku5-3* null mutant have severely skewed roots similarly to previous report by Sedbrook (2002). (B) Close-up of root files of *Ws*, *sku5-2* and *sku5-3*. Twisted files were observed within the 2 alleles of the *sku5* mutant

According to ‘*in silico* analyses’ and real-time RT-PCR data (Figure III-1), *SKS2* gene is specifically expressed in reproductive organs, but no flower defect was observed in flower shapes, or seed set in *sk2* null mutant plants (data not shown).

These primary analyses indicated that although *SKS1*, *SKS2* and *SKS3* have very conserved sequence and structure with *SKU5*, the roles they played in plants might be different or minor compared to *SKU5*.

III-2-2 Generating double and triple mutants for *sk1*, *sk2* and *sku5*.

SKU5, *SKS1* and *SKS2* are the sole members of the family that are susceptible to be modified by a GPI-anchor. Considering the absence of phenotype of *sk1* and *sk2* mutants and the subtle phenotypes of *sku5*, we hypothesized that these proteins might have at least partial redundant functions. *SKU5* is broadly expressed in the plant and can thus be co-expressed with the two other members. The three genes are expressed in flowers and at the early stages of silique and seed development.

We decided to generate double and triple mutants. To avoid being confused by phenotypes resulting from the combination of *Ws* and *Col-0* ecotypes, only mutants in *Ws-ecotype* background were used for crosses. Homozygous *sk1-1* mutant was crossed with homozygous *sk2* and also with *sku5-3* (Figure III-6). *sk2* and *sku5-3* were also crossed together. To facilitate references to these mutants and as only one allele of each was used for crosses, the number of the allele is no longer indicated in the following text and figures.

Although *SKS3* encoded highly conserved protein with *SKS1*, *SKS2* and *SKU5*, no GPI anchor was predicted and the *sk3* knock-out mutants were only found in *Col-0* background. Therefore, the *sk3* knockout mutants were not included in the crosses and for further investigation.

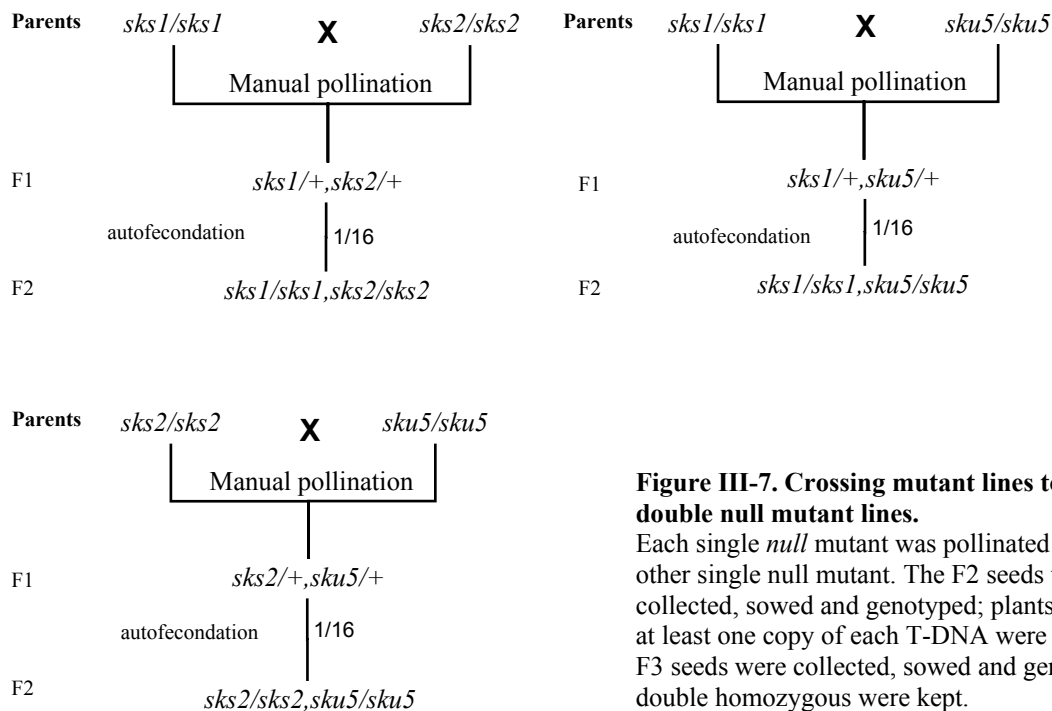


Figure III-7. Crossing mutant lines to produce double null mutant lines.

Each single *null* mutant was pollinated by the other single *null* mutant. The F2 seeds were collected, sowed and genotyped; plants exhibiting at least one copy of each T-DNA were kept. Then F3 seeds were collected, sowed and genotyped; double homozygous were kept.

After selection and genotyping of the double mutants, *sks1,sku5* and *sks2,sku5* double homozygous mutant were crossed to generate *sks1,sks2,sku5* triple mutants.

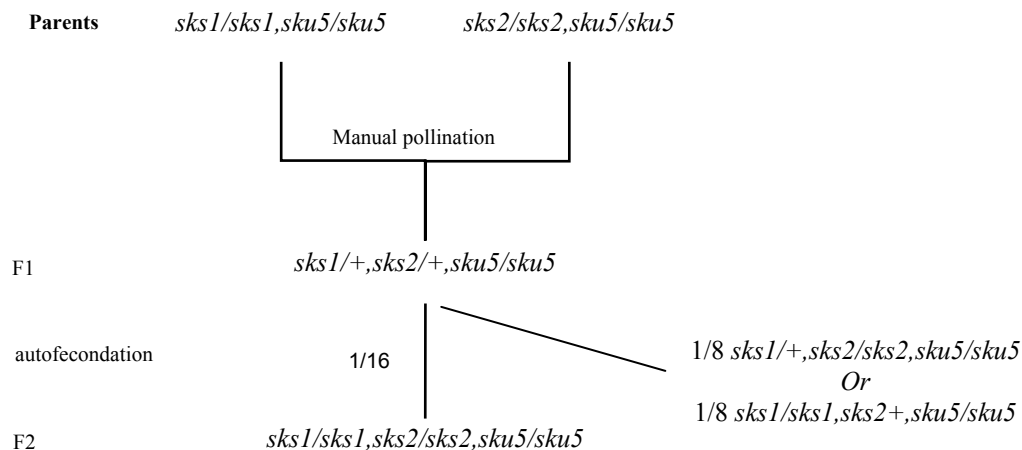


Figure III-8. Production of *sks1,sks2,sku5* triple null mutant.

sks1,sku5 and *sks2,sku5* double homozygous were crossed to produce triple mutant. After the autofecondation of F1 generation plants, seeds containing 1/16 *sks1,sks2,sku5* triple homozygous were produced.

Individual F2 plants were genotyped for the segregating insertions by PCR. Triple homozygous were selected and sesquimutants that were homozygous for 2 T-DNA insertions and heterozygous for the third one were also conserved.

III-2-3 *SKS1*, *SKS2* and *SKU5* expression in mutant plants

We previously established that the 3 *Ws* T-DNA mutants that were used to generate double and triple mutants were null for the gene disrupted by the insertion (Figure III-4). Here, we investigated whether the mutations affected the expression of the other members within the same clade. Expression of *SKS1*, *SKS2* and *SKU5* was analysed in single and double mutants by real time RT-PCR (Figure III-10).

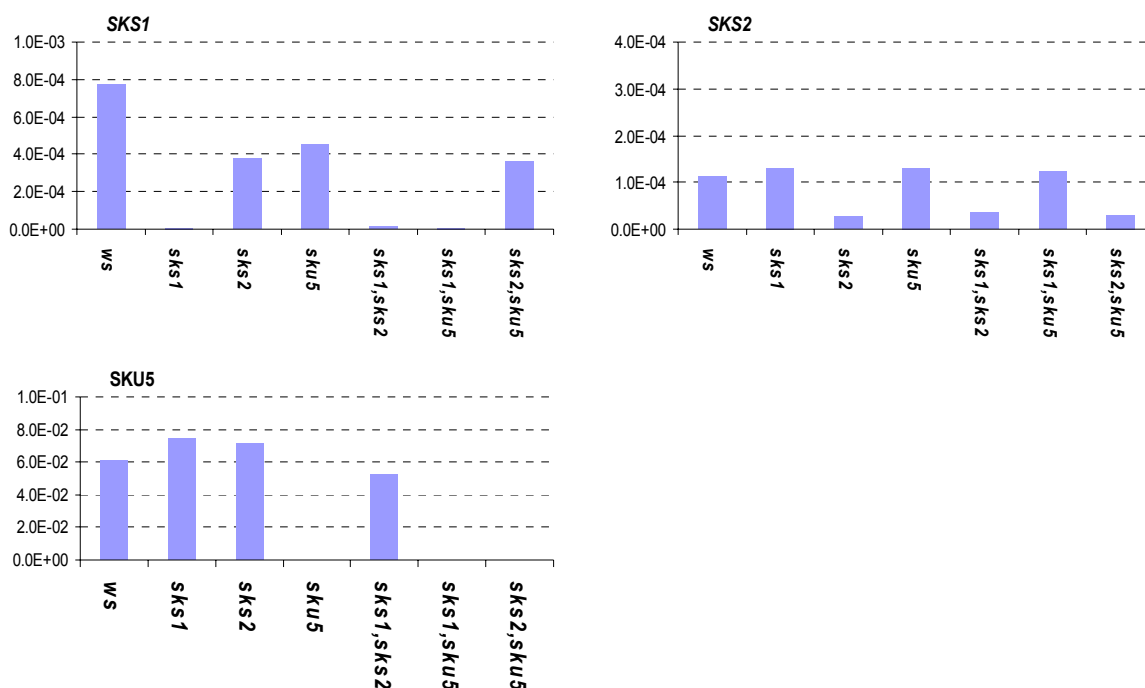


Figure III-10. Expression levels of *SKS1*, *SKS2*, *SKU5* in single and double null mutant.

Gene expression was analyzed by Real-time RT-PCR using RNA extracted from 5-day-old seedlings of different alleles.

All data were normalized with respect to *ACTIN2-8* and expressed as actin units.

For *SKU5*, no significant change in expression was observed in *sks* single mutants or in the double *sks1,sks2* double mutant. The absence of detection of *SKU5* in *sks1,sku5* and *sks2,sku5* double mutants confirmed genotyping results and the absence of *SKU5* mRNA.

SKS1 expression was consistently reduced by half in *sks2* and *sku5* single mutants and in the double *sks2,sku5* mutant. As the very low expression level of *SKS1* in seedlings, it is not possible to determine whether this two-fold change in mRNA accumulation affects the relative abundance of the SKS1 protein.

It was more difficult to evaluate the effect of *skt1* and *sku5* knock-out on *SKS2* expression as its mRNA is not detectable in seedlings even in these mutant background. But to be sure that the absence of *SKS1* and *SKU5* could not enhance the expression level of *SKS2* in seedlings, its expression was however studied. The weak signal detected with *SKS2* primers in *skt2* mutant background is not likely to result from *SKS2* amplification but to side products after a large number of cycles. (Figure III-11).

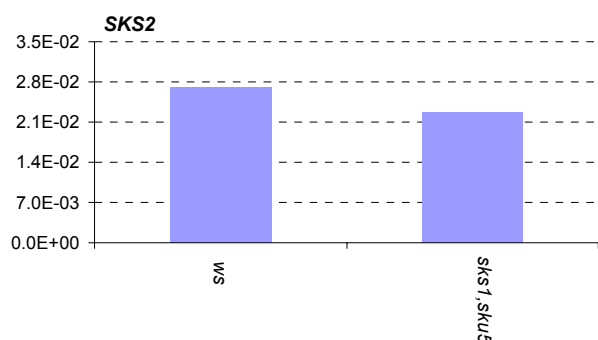


Figure III-11. Expression level of *SKS2* in flowers of *Ws* and *skt1,sku5* double null mutant. RNAs were extracted from opened flowers and analyzed by Real-time RT-PCR. All data were normalized with respect to ACTIN2-8 and expressed as actin units.

In conclusion, there is no significant effect of the mutations on the expression of the other genes of the *SKU5* clade. In particular, no compensation mechanism was observed in single or double mutant, which is a piece of important information before investigating the effect of the mutations on growth and development.

III-2-4 Analyses of *skt1*, *skt2* and *sku5* single and double mutants

As described in the original paper of *SKU5* functional analysis and the primary analyses of single mutant plants, only *sku5* null mutants exhibited twisted roots. It would be interesting to investigate the function of *SKS1* and *SKS2*, by analyzing behaviours of their null mutant growing on vertical plates. General analysis, such as root length and hypocotyl length were also performed.

SKU5 was proposed to be involved in the interaction with ABP1, experiments utilized for characterizing ABP1 conditional lines were also performed in *skt/sku5* mutants to reveal indirect evidences of a potential interaction between ABP1 and SKS/*SKU5*.

III-2-4-1 Root Phenotypes

sku5 null mutant plants were previously reported to have skewed roots and altered gravitropic response (Sedbrook et al, 2002) . The root phenotype was studied in single and double mutants of the selected *Ws* mutant, especially for *sku5* and *skt1* that were found to be expressed in roots.

III-2-4-1-1 Root Length Measurement

First, the effect of each mutation on root length was determined by comparing roots of 5-day-old seedlings grown under light conditions (ref to Method Chapter for details). Petri dishes were scanned, and the length of individual roots was measured by IMAGEJ software. Root lengths are shown in figure III-12 and the P-values appear in table III-3.

For single mutants, only *sksl* null mutant exhibits slightly shorter roots. Although *sku5* null mutant didn't exhibit shorter roots than *Ws* ecotype wild type, *sksl,sku5* double mutant exhibits significantly shorter root than wild type or any single null mutant. It implies the potential redundancy between *SKS1* and *SKU5*.

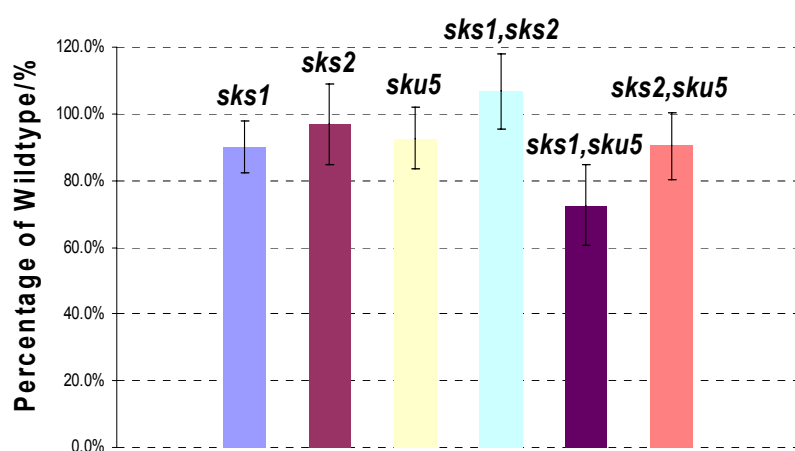


Figure III-12. Root length of single and double mutants.

20 seedlings of each single and double null mutant are vernalized at 4°C for 2 days and then grow at 22°C for 5 days under light conditions. Petri dishes were scanned, and the lengths of roots were measured by IMAGEJ software. The percentage of the root length is compared to *Ws* ecotype wild type.

Table III-3. P value of root length compared to *Ws* ecotype wild type.

	<i>sksl</i>	<i>sksl,sku5</i>	<i>sksl,sku2</i>	<i>sku5</i>	<i>sksl,sku2,sku5</i>
P value	3.88E-04	0.354	0.0126	0.454	3.45E-10

P value = student's test probability, where < 0.05 is statistically significant. The P values correspond to a comparison between wild-type *Ws* and different null mutant plants. In this case, n=20.

III.2.4.1.2 Skewed roots of single and double null mutant plants.

The analyses in root length revealed the possibility of redundancy between *SKU5* and *SKS1*, so the root twist tests were performed for further investigation. As described, only *sku5* exhibits the iconic twisted and slanting roots in all single mutant utilized for crosses (Table III-4 and Figure III-13).

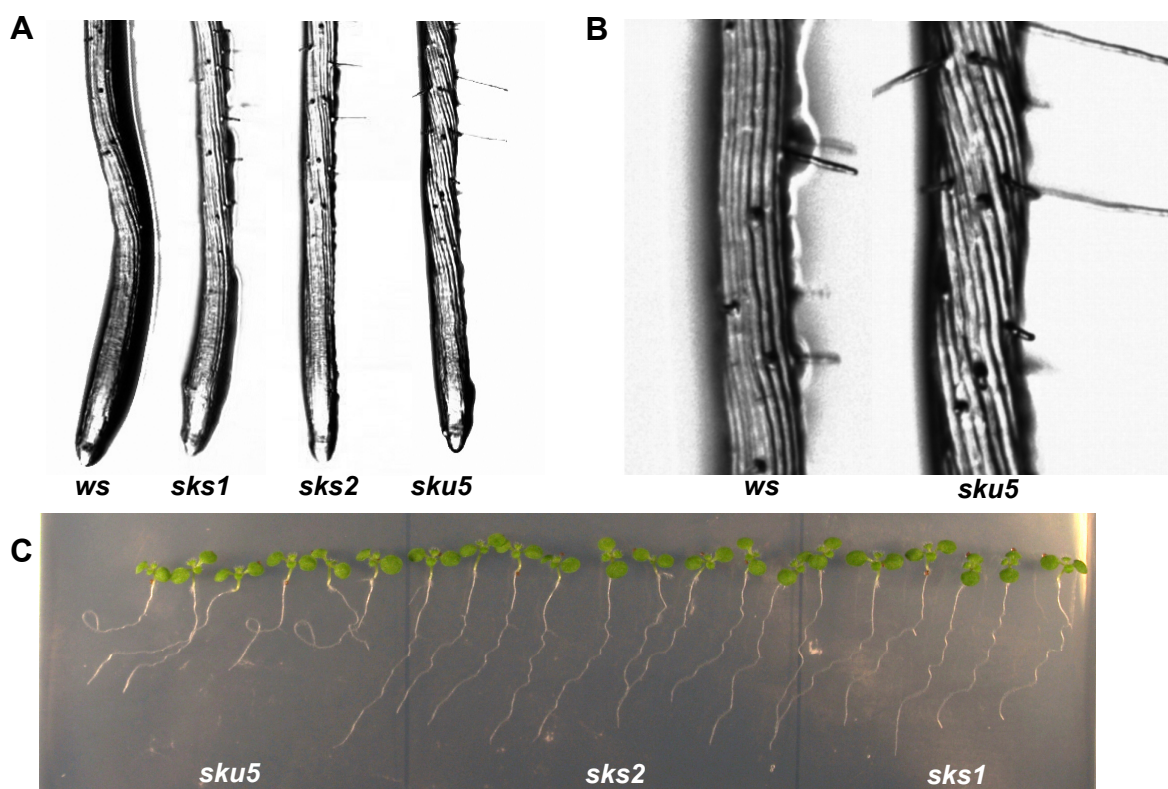


Figure III-13. Skewed roots of *sks* single null mutants.

Seeds of single mutant were sowed on ½ MS medium containing different concentration of agar for 7 days as described in Sedbrook's paper (2002).

(A) Root tips of *Ws*, *sks1-1*, *sks2* and *sku5-3* grew on ½ MS medium containing 0.8% agar for 7 days.

Only *sku5-3* null mutant have severely skewed roots. (B) Skewed roots of *sku5* and *ws*.

(C) The slanting roots of single null mutants grew on ½ MS medium containing 1.5% agar. (Grew vertically for 3 days and 45° tilted for additional 4 days)

Table III-4. Angle of roots of wild-type and different null mutant plants on titled 1.5% agar medium

	<i>Ws</i>	<i>sks1</i>	<i>sks2</i>	<i>sku5</i>
Angles	31.3 ± 6.76	26.7 ± 5.32	32.0 ± 5.11	65.0 ± 13.9
P value to WT	NA	0.27	0.08	2.36E -07

P value = student's test probability, where < 0.05 is statistically significant. The P values correspond to a comparison between wild-type *ws* and different null mutant plants. n=20.

Not surprisingly, *sks1,sks2* exhibits no phenotype in root twist because of the absence of phenotype of *sks1* single mutation and the undetectable expression of *SKS2* in roots; *sks2,sku5* exhibits the same phenotype as *sku5* single null mutant.

But dramatically, *sks1,sku5* double mutant exhibits much more severe defects compared to *sku5* or *sks1* single mutants. Roots of *sks1,sku5* were more twisted than in *sku5* single mutant, in addition the files were distorted (Figure III-14A). The close-up of *sks1,sku5* roots showed severe distortion of the cell files, which is totally different from *sks2,sku5* double mutant that exhibits an aggravated left slanting (Figure III-14B). This phenotype is intriguing as *SKS2*

was not found to be significantly expressed in roots, however we cannot exclude that *SKS2* is expressed only in specific cells. In *skl1,sku5*, the distorted root files caused the absence of left slanting on solid medium (with 1.5% agar) and the iconic left slanting on solid medium was replaced by a slightly right slanting (Figure III-14C and Table III-5).

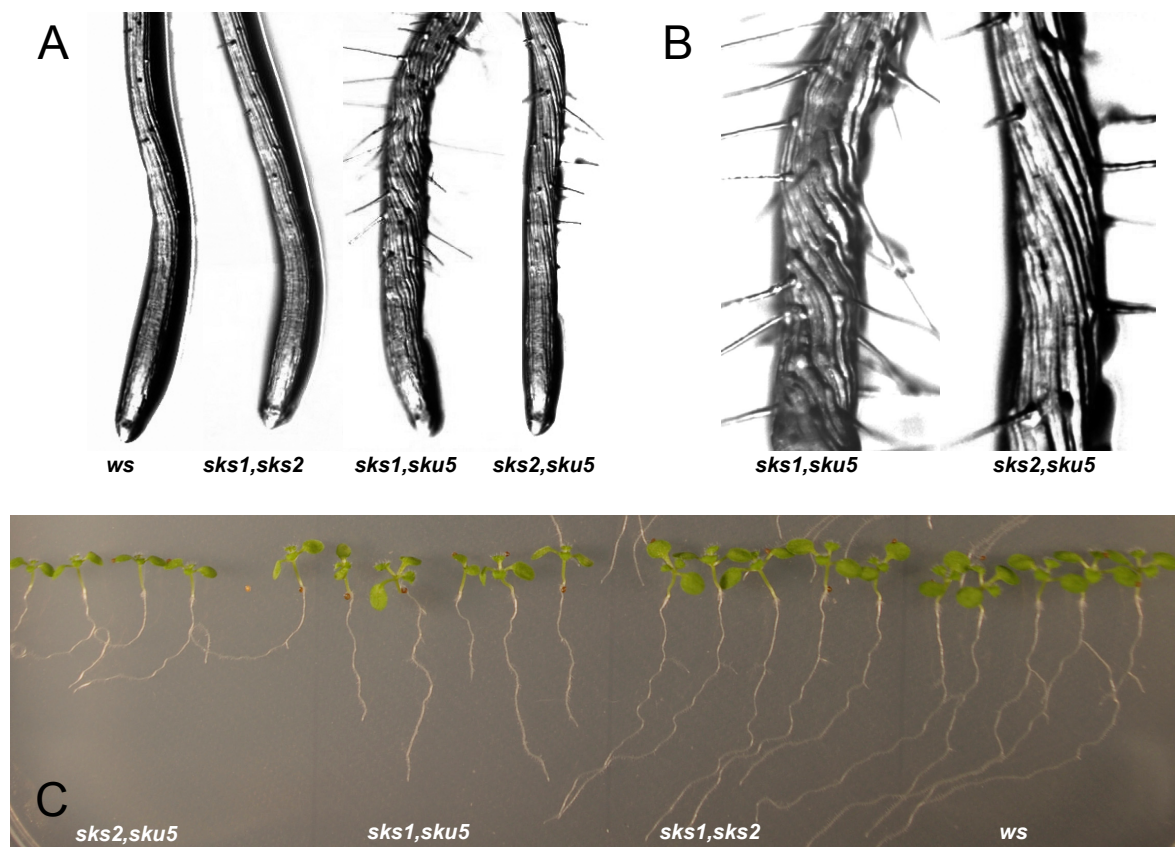


Figure III-14. Skewed roots of *skl* double null mutants.

Seeds of double mutant were sowed on ½ MS medium containing different concentration of agar for 7 days as described in Sedbrook's paper (2002).

(A) Root tips of *ws*, *skl1,skl2*; *skl1,sku5* and *skl2,sku5* double mutants grew on ½ MS medium containing 0.8% agar for 7 days. (B) Skewed roots of *skl1,sku5* and *skl2,sku5*.

(C) 7-day-old seedlings grew on 1/2MS containing 1.5% agar, (3 days vertical growth and 4 additional days' 45° title growth).

The slanting data in Table III-5 was measured, + for left slanting and – for right slanting.

Table III-5. Angle of roots of wild-type and different null mutant plants on titled 1.5% agar medium

	<i>Ws</i>	<i>skl1,skl2</i>	<i>skl1,sku5</i>	<i>skl2,sku5</i>
Angles	31.3 ± 6.76	30.8 ± 2.90	-7.42 ± 3.25	85.4 ± 12.1
P value to WT	NA	0.03	2.66E-14	4.89E-09

Measurements are averages ± SD; n= 20; positive angles mean left slanting and minus of right slanting; n=sample size; P value = student's test probability, where < 0.05 is statistically significant. The P values correspond to a comparison between wild-type *ws* and different null mutant plants.

To further investigate root distortion in *sksl,sku5* mutant, 7-day-old root tips of seedlings grown on medium containing 0.8% agar were stained by FM4-64 and observed under SP2 Confocal system (Figure III-15). The observation revealed that, the distorted files might be originated from the irregular root tips.

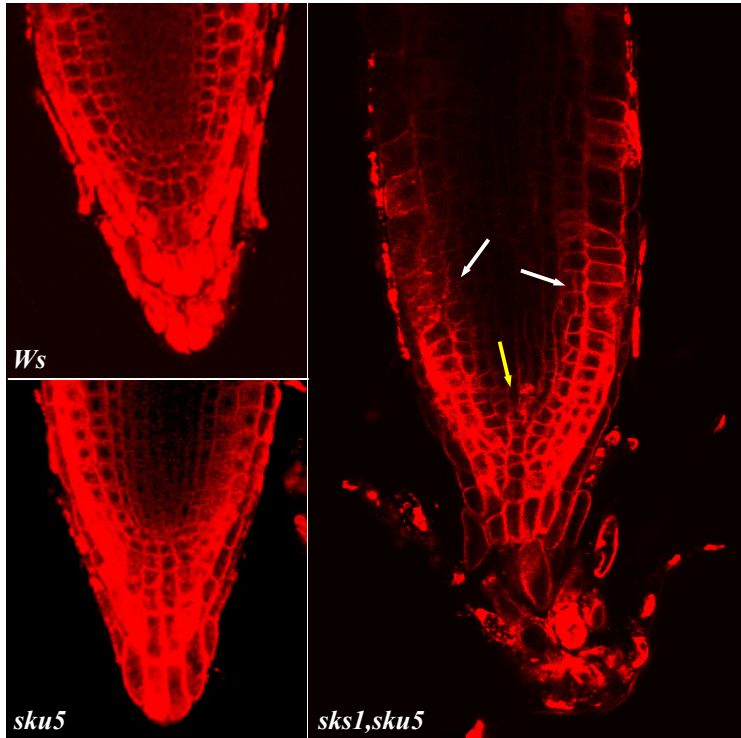


Figure III-15. Irregular root tips of *sksl,sku5* null mutant. Microscopic analysis of root tips were performed on fresh material stained with 5 μ M FM4-64 for 10 min and roots were observed using an inverted confocal microscope TCS SP2 (Leica microsystems, Heidelberg, Germany). Some aberrant division plane (white arrows) resulting in irregular cell files were observed at the root tip of *sksl,sku5* double mutant, thus before the effective twist, visible after the meristematic zone, can be observed. The organization of the stem cell niche (yellow arrow) is also potentially affected, however roots are still growing.

The dramatic root phenotypes of *sksl,sku5* strongly indicate the redundancy between *SKS1* and *SKU5*. Considering the much higher expression level of *SKU5* compared to *SKS1*, we can hypothesize that *SKS1* is functional in root growth, but in the *sksl* single mutant, *SKU5* complements the absence of *SKS1*. Only when *SKU5* is absent, the defect caused by *SKS1* mutation resulted in a detectable phenotype. Conversely the lower expression of *SKS1* cannot fully complement the absence of *SKU5*, so the root defect is exhibited in *sku5* single mutant.

III-2-4-2 Hypocotyle length analyses

SKU5 was expected to be expressed all over the plants, but the twisted files were never observed in any hypocotyls (data not shown). It suggests that the twisted phenotype was root-specific.

sksl,sku5 double mutant also exhibit shorter hypocotyls than wild-type, which means that *SKS1* and *SKU5* double mutation might cause the size reduction of plants (Figure III-16 and Table III-6).

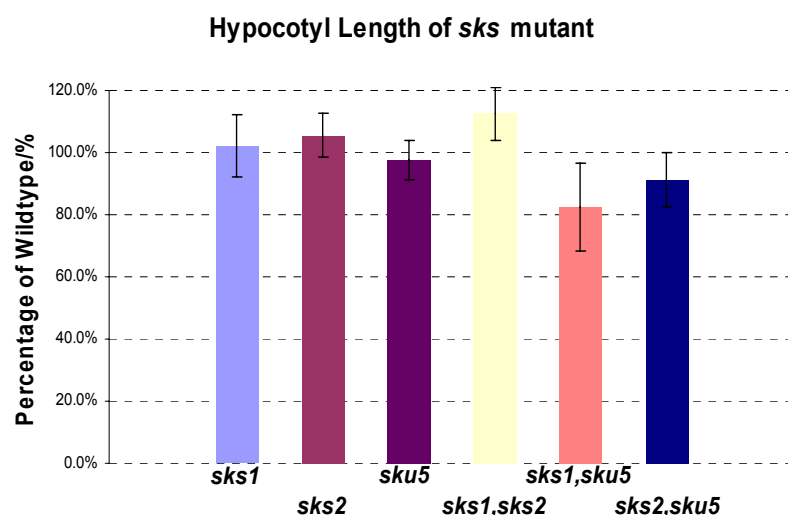


Figure III-16 . Hypocotyl length of *sks* single mutant. At least 20 Seedlings of mutants grew in dark for 5 days after 2 days vernalization. Plates were scanned and hypocotyls length was measure by ImageJ software. Different mutant lines are as indicated in figure. Data shows that most of the single and double null mutant have normal hypocotyl length except the *sks1,sku5* double mutant exhibit shorter hypocotyls.

Table III-6. P value of root length compared to *Ws* ecotype wild type

	<i>sks1</i>	<i>sks2</i>	<i>sku5</i>	<i>sks1,sku5</i>	<i>sks2,sku5</i>
P value	0.88	3.9 E-03	7.0 E-03	1.05 E-05	2.85 E-11

P value = student's test probability, where < 0.05 is statistically significant. The P values correspond to a comparison between wild-type *Ws* and different null mutant plants. n=20.

III-2-5 Analyses of *sks1,sku5* triple mutant.

SKS2 mutation was not revealed to cause any defect in root growth or seeds set. Considering the even lower expression level of *SKS2* and the redundancy between *SKS1* and *SKU5*, the absence of phenotype of *SKS2* might be because of the presence of *SKS1* and *SKU5*. It was interesting to investigate the function of *SKS2* in triple null mutant.

sks1,sku5 triple null mutants were produced as described in Figure III-8. They were then genotyped by checking each T-DNA insertion (Figure III-17).

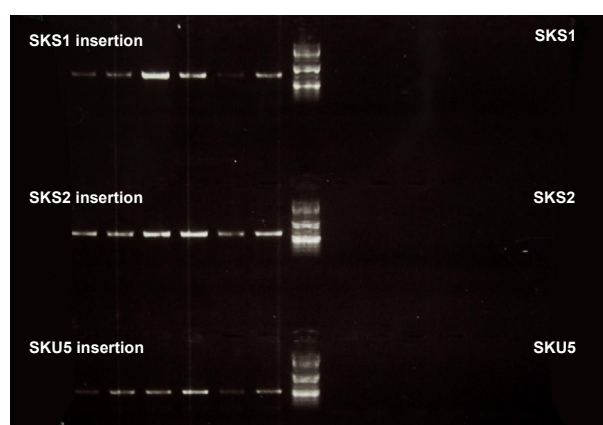


Figure III-17 Genotyping of *sks1,sku5* triple null mutant.

Crude DNAs were extracted from seedlings of *sks1,sku5* triple null mutants (method was described in Method chapter). No amplification product is observed with P2-P3 primers for each gene, whereas amplification products are obtained using P1 and P2, P1 being on the T-DNA.

Dramatically, *sks1,sku5* triple null mutant plants produce very few seeds (about 100-300 seeds per plants), which will be described later (see Chapter IV).

To determine whether *sks1,sku5* triple mutant were infertile or if the only seeds produced were because of the contamination by pollens from other plants, 48 plants from one

triple mutant plant were germinated and genotyped. Results showed that all of them were *sks1,sks2,sku5* homozygous (Data not shown). It proved that the large reduction of seeds was because of the triple mutation itself.

III-2-5-1 Root phenotype

SKS2 was not or very weakly expressed in roots, however an aggravated root slanting was observed for *sks2,sku5*. In normal growth conditions the double mutant did not exhibit significant root phenotype; the *sks1,sks2,sku5* triple mutant was then supposed to exhibit the same root phenotype as *sks1,sku5* double mutant but root phenotypes were much more complicated than for the *sks1,sku5* double mutant. All seeds from three individual triple null mutant plants were carefully collected and were grown *in vitro* for phenotype analysis.

A large range of distinct phenotypes was observed as illustrated Figure III-18. The seedlings were classified according to the root length into three classes: Ungerminated, Rootless, and Rooted; each proportion was indicated in Table III-7.



Figure III-18. Roots of triple null mutant have different root phenotypes in a large range.
Triple null mutant and *Ws* wild-type seedlings as indicated in the figure.

Table III-7 Classified seedlings of triple mutant.

	Ungerminated	Rootless	Rooted	n=
Total	7.40%	9.75%	82.85%	513

Seeds were from 3 individual triple mutant plants and grown *in vitro* under continuous light for 7 days.

The root length of germinated seedlings from one individual triple mutant was measured, and a continuous profile of root length was found after ordering them by increasing values (Figure III-19A). As previously mentioned about 10% is rootless, root length of others are quite broadly distributed from very short roots to nearly wild-type roots. The average of the root length is then about half the length of *wild-type* with a large standard deviation (SD) of 3.53 times the one of the control (Figure III-19B).

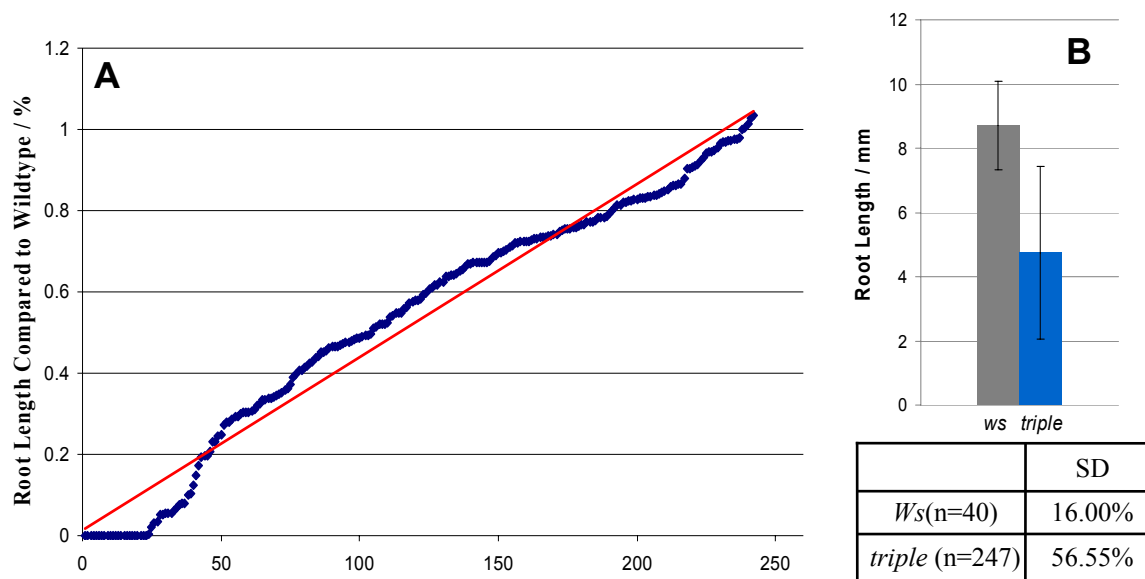


Figure III-19. The uneven root length of *triple null mutant* Seedlings.

All seeds from one triple null mutant plant were carefully collected and germinated at the same condition as described for analyzing *single* and *double null mutant*.

(A). Putting the root length of the triple mutant in order and drew the chart, the root length is more or less continuous.

(B). Average root length of triple mutant and SD.

The large range of *sksl,skss2,sku5* triple mutant phenotypes indicated that, the root phenotype is strongly affected by the combined absence of the three genes. Again even if SKS2 is very weakly expressed in roots, its knockdown in the *sksl,sku5* background generates very severe root phenotype. To determine whether the effect is initiated in embryogenesis or during root elongation, root phenotype of the different classes of mutants was studied carefully.

The root development of the triple mutant was severely disturbed for a subset of seedlings. In Figure III-20A, the elongation of hypocotyl and root stopped even after 11 days of *in vitro* culture. In rootless seedlings, the primary root failed to be formed (Figure III-20 B-D). The hypocotyl ends with small aggregation of non photosynthetic cells that can potentially develop root hairs.

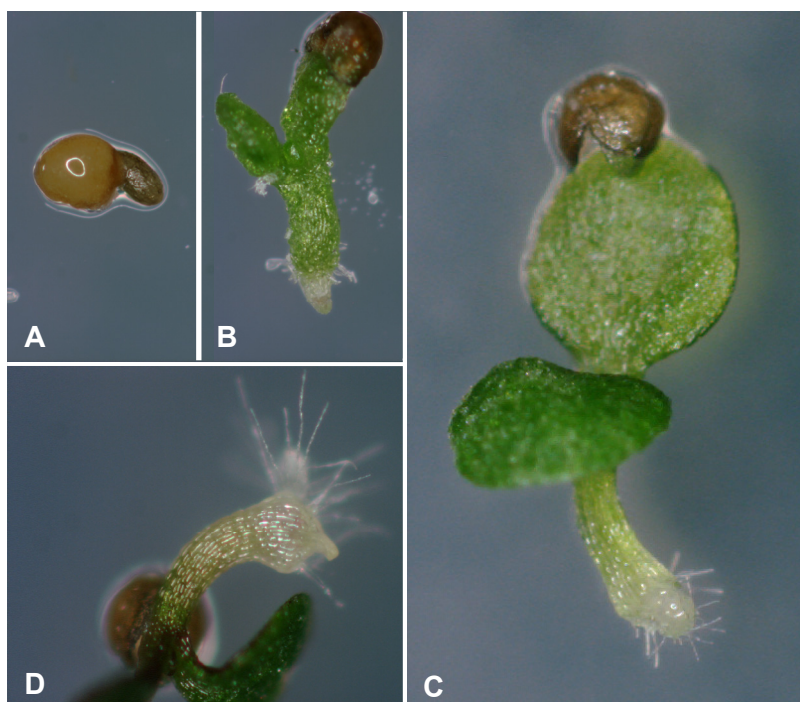


Figure III-20 . The rootless seedlings of *sks1,sks2,sku5* triple mutant.

Seeds of triple mutant plants grew *in vitro* under continuous light for 7 days.

(A). Ungerminated seeds. An hypocotyl like structure elongated a little after seed imbibition but cannot develop further.

(B-D) Rootless seedlings of the triple mutant.

The root primordia is missing, few cells develop root hairs at the basis of the hypocotyl.

Few rootless seedlings were able to survive after development of adventitious roots that overcome the defect of the primary root (Figure III-21). Figure III-21B shows a close-up of such adventitious root developed at the basis of the hypocotyl (Figure III-21A), the aborted primary root can also be observed. After clearing, no typical root pattern is observed in the aborted primary root confirming an early defect in primary root formation during embryogenesis (Figure III-21C) . After transfer on soil such seedling is able to survive and to give rise to seeds. The different classes of *sks1,sks2,sku5* triple mutant were found in the progeny as for seedlings that exhibited a much less altered phenotype.



Figure III-21. Triple mutant seedlings with aborted primary roots and development of adventitious roots.

Some *sks1,sks2,sku5* triple null mutant exhibit severe defects in root formation. Seedlings grown for 11 days at 22°C under constant light.

(A). seedlings with an aborted primary root and a well growing adventitious root.

(B). close-up of A

(C). aborted primary root.

Even for seedlings exhibiting an embryonic primary root, further growth alterations can still occur. After germination, root growth can be arrested which compromises further development of the seedling. Observation of the root revealed a severe alteration of the root tip or the root cap, which was either shrank or disorganized (Figure III-22).



Figure III-22. Abnormal root tips of triple mutant seedlings.

Some seedlings of triple mutant stopped developing. The roots are very short even after 11 days germination *in vitro*. The already formed primary root of triple mutant seedlings exhibit shrank or disorganized root tips (**A and B**); or the differential cells were totally disordered and stick to root tips (**C and D**). (**D**) FM4-64 stained primary root exhibited in (**C**).

But seedlings with similar root length compared to *sksl,sku5* double mutant exhibit twisted and distorted roots, which were the same as *sksl,sku5* double mutant (Figure III-23, Table III-8). The angle of the twist was quantified but surprisingly it was often less severe in the triple mutant than in the *sksl,sku5* double mutant as can be seen on the close-up figure III-23 B.

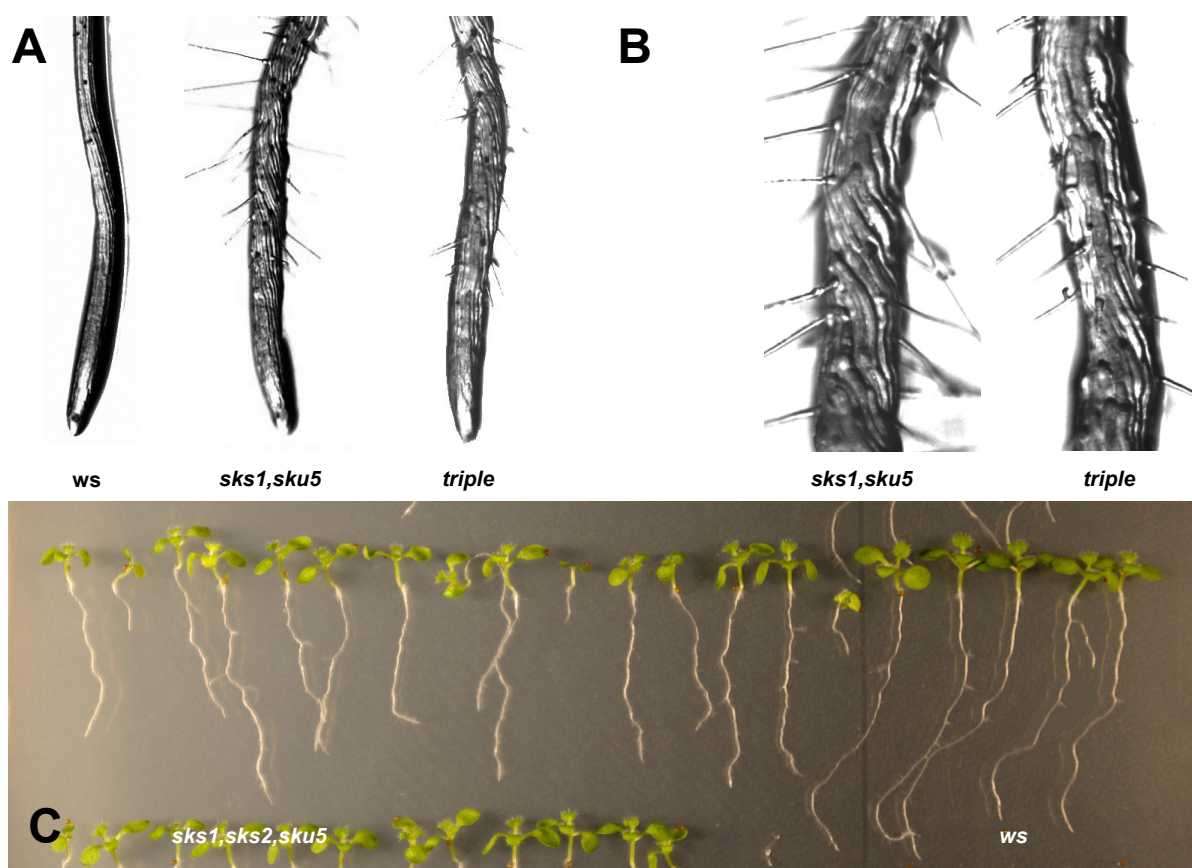


Figure III-23. Root twist of *sks1,sku2,sku5* triple null mutant.

(A) and (B) 7-day-old seedlings grew on 1/2MS containing 0.8% agar.

(C) 7-day-old seedlings grew on 1/2MS containing 1.5% agar, (3 days vertical growth and 4 additional days' 45° title growth).

The slanting data in Table x was measured, + for left slanting and – for right slanting.

Table III-8. Angle of roots of wild-type and different null mutant plants on titled 1.5% agar medium

	<i>Ws</i> (n=29)	<i>sks1,sku2,sku5</i> (n=54)
Angle	31.3 ± 6.76	-6.55 ± 12.8
P value	NA	4.06E-11

Measurements are averages ± SD; n=sample size ; P value = student's test probability, where < 0.05 is statistically significant. The P values correspond to a comparison between wild-type *ws* and different null mutant plants.

Root tips of different classes were also visualized by 5 minutes treatment of FM4-64 under confocal microscope (Figure III-24) some mutants exhibit similar defects as those observed in the *sks1,sku5* double mutant. In mutants developing a very short root, the pattern of the root tip is altered and cell file organisation is partially disturbed. It was not possible to recognize the quiescent center due to alterations of cell shape. The lateral root cap is very short and the meristem is reduced to few cells.

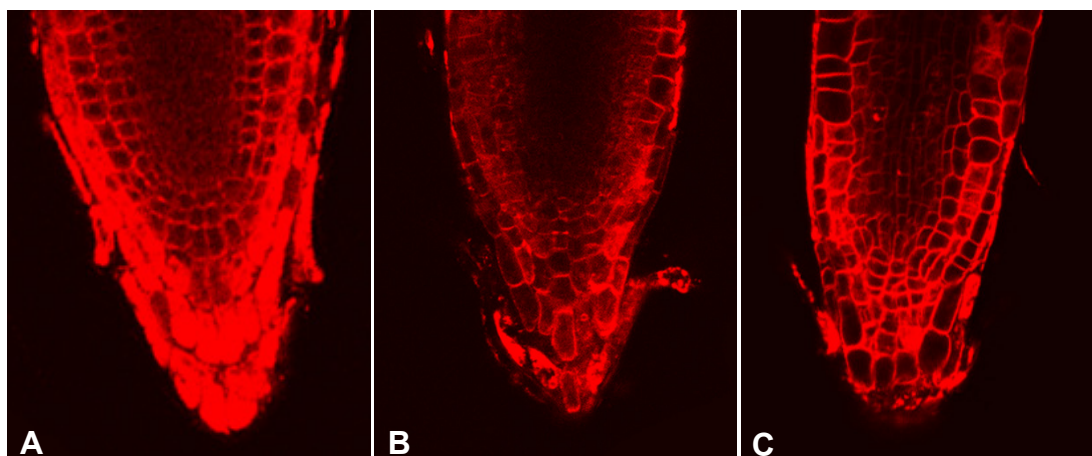


Figure III-24 . Root tips of triple mutant.

(A) Ws, (B) *sks1,sks2,sku5* triple mutant with longer roots similar as *sks1,sku5* double mutant, (C) *sks1,sks2,sku5* triple mutant with extremely short roots which is shown in Figure III-22.

III.2.5.2. Hypocotyl length.

The hypocotyl length of *sks1,sks2,sku5* are shorter than Ws wild-type, but is not significantly different from the *sks1,sku5* double mutant (Figure III-x).

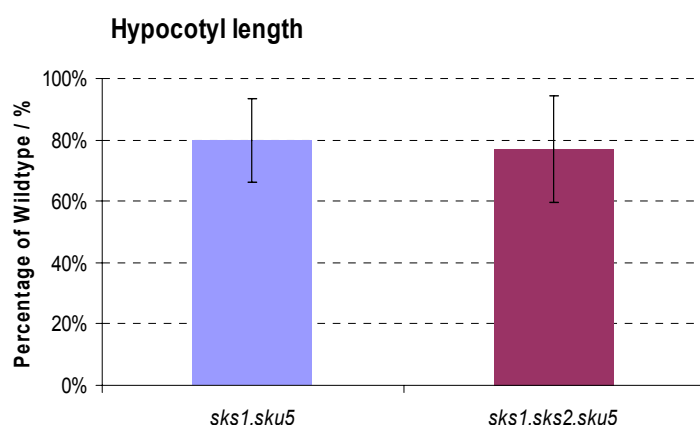


Figure III-25. Hypocotyls length of triple mutant.

All seeds from on individual triple mutant plants grew *in vitro* under dark condition for 5 days. The average length of hypocotyls was normalized with Ws and compared to *sks1,sku5* double mutant .

The above data on *sks1,sks2,sku5* roots revealed that much more severe phenotypes were observed for the triple mutant compared to double mutants, including the *sks1,sku5* double mutant. Part of these defects result from embryogenesis alterations, especially from the formation of the primary root pole during embryogenesis. Interestingly, formation of the primary root was reported to be strongly regulated by auxin. Well studied mutants as *monopteros/arf5 (mp)* loss of function and *bodenlos/iaa12 (bdl)* gain of function are rootless mutants and are altered in auxin signalling

III-3 Functions of *SKU5*, *SKS1* and *SKS2* in auxin responses and cell cycle.

All experimental data suggest that ABP1 is only functional when it is located at the outer surface of plasma membrane. It was hypothesized that GPI-anchored SKU5/SKS would be the candidates contributing to ABP1 targeting to the plasma membrane from the ER and/or to be the interactor of ABP1 at the membrane as part of a co-receptor complex. Alteration of primary root formation during embryogenesis for a subset of triple mutants was an additional argument supporting a role of SKU5/SKS GPI-anchored proteins in auxin signalling. The panel of *sksl,skss2,sku5* triple mutant phenotypes is however distinct from the phenotype of ABP1 loss of function plants (Chen et al., 2007; Braun et al., 2008; Tromas et al., 2009). ABP1 knockdown were found to affect the expression of auxin response genes and cell cycle response genes. The expression level of auxin response genes and cell cycle response genes in all GPI-anchored SKS knock-out plants was then interesting to explore.

III-3-1 Expression of early auxin response genes in the single, double and triple null mutant seedlings.

Auxin response genes to be analyzed were selected mainly within the Aux/IAA gene family, as genes that are expressed in seedlings and that are sensitive to subtle changes to auxin signaling like IAA5 and IAA6 or to be involved in lateral root initiation (SLR/IAA14, ref). The common feature of these genes is that they were all shown to be differentially expressed in seedlings inactivated for ABP1 (Braun et al., 2008; Tromas et al., 2009). Braun (2008) described that functional inactivation of ABP1 caused the decrease of auxin response genes IAA1, IAA5, and IAA19 in seedlings, which were not observed in any single or double *sku5/sks* null mutants (Figure III-26).

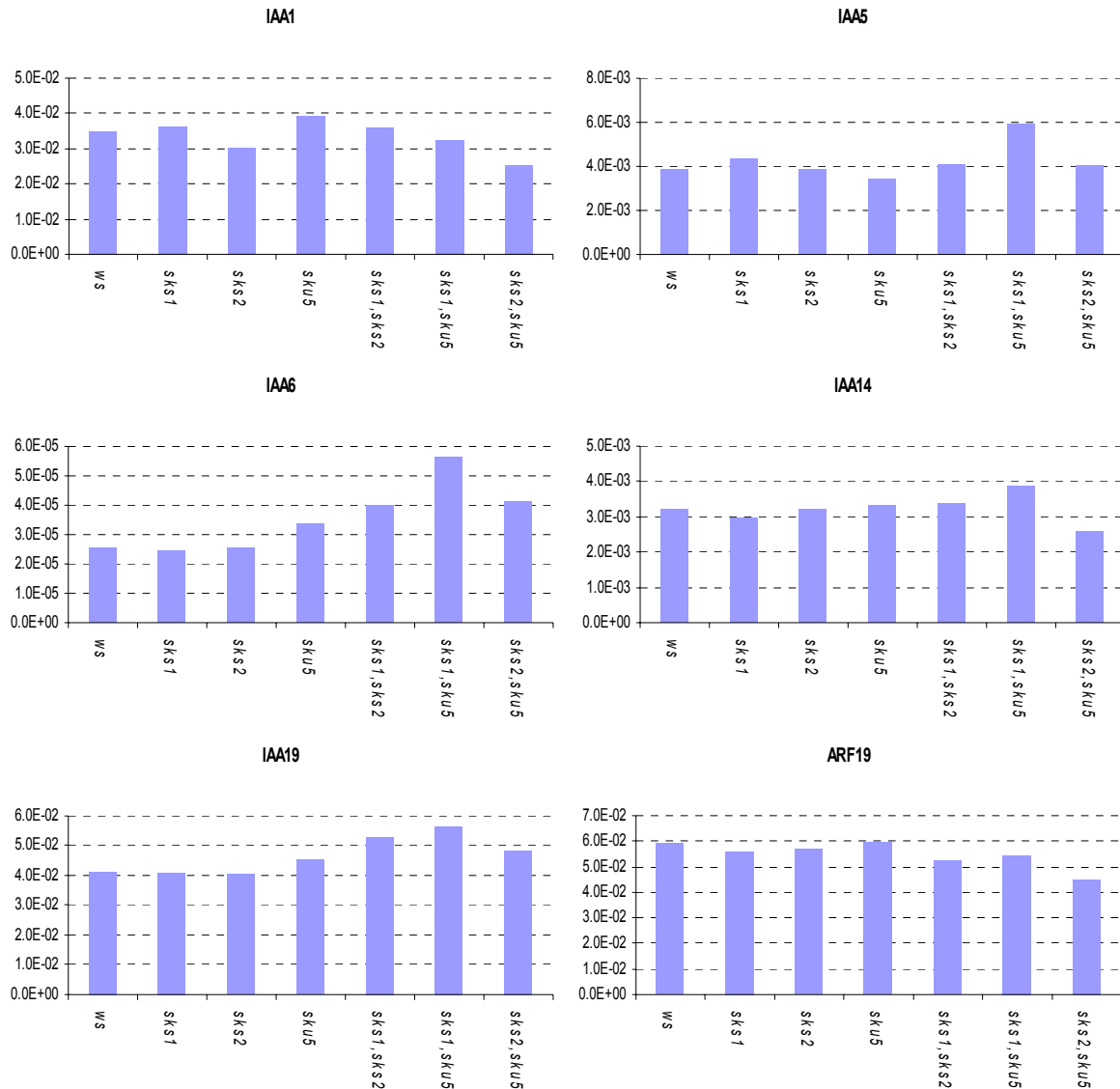
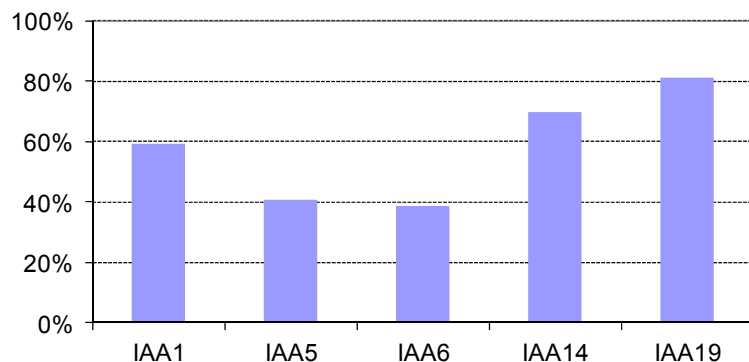


Figure III-26. Auxin response genes in single and double null mutant seedlings.

RNA were extracted from roots 5-day-old seedlings and utilized for real time RT-PCR.

Data was normalized with *ACTIN2-8*.

These auxin response gene expression levels were also tested in seedlings of the triple mutant (Figure III-27). A slight decrease of the steady state expression of the selected genes was observed in the triple mutant compared to the wild-type seedlings, with a maximal difference of two times. This experiment was only performed once and would merit being repeated using biological replicates to determine whether these changes are significant.



Figur III-27. Expression level of auxin response genes in triple mutant.

RNAs were extracted from 5-day-old seedlings of triple mutant and real time RT-PCR was performed. The data were normalized with ACTIN2-8 and expression level in *Ws*.

To further explore whether SKU5/SKS GPI-anchored proteins interfere somehow with genomic responses to auxin, the expression of the selection of auxin response genes was also studied after auxin treatment.

5-day-old *skt1,skt2,sku5* seedlings were chosen (the mix seedlings with longer or shorter roots). They were treated with 1 μ M IAA for 0min, 30mins, 60mins and 120mins. Seedlings treated for different times were collected and used for RNA extraction. Real time RT-PCRs were performed.

Amongst the selected Aux/IAA genes, all were induced by the exogenous auxin treatment except *IAA14* that was not differentially expressed over time. The responsiveness to auxin was increased in the triple mutant compared to wild-type seedlings treated in the same conditions. However, this experiment was done only once, due to the reduced availability of triple mutant seedlings.

An increased responsiveness to auxin was also reported for these genes for ABP1 loss of function seedlings. However, to the difference of what is observed for the triple mutant, this increased responsiveness was correlated with a strong reduction of their expression in the absence of auxin (Braun et al., 2008). It is not the case for the *skt1,skt2,sku5* triple mutant, which makes a great difference with ABP1 knockdown.

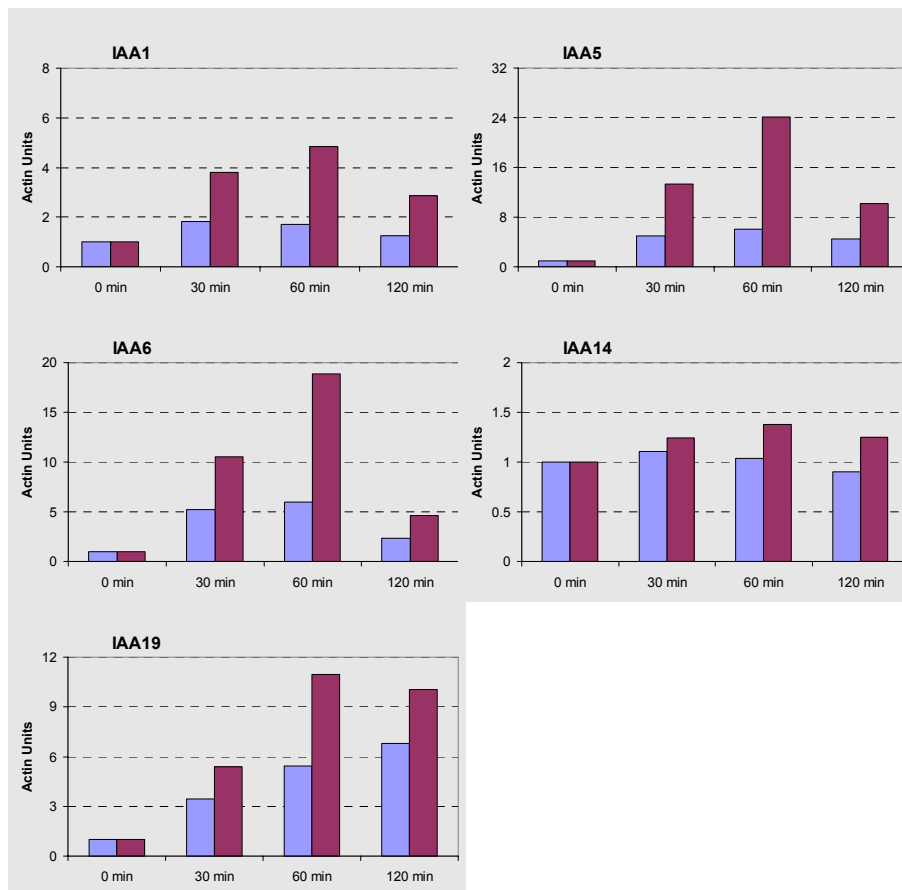


Figure III-28. Auxin response genes expression after 1 μ M IAA treatment.

5-day-old *sks1, sks2, sku5* triple null mutant seedlings mix were treated by 1 μ M IAA for different minutes.

Data were normalized with ACTIN2-8 then to the expression level at time zero of auxin application.

Ws is in blue and *sks1, sks2, sku5* in red

III.2.6.4 Cell cycle response gene in *sks1, sks2, sku5* triple mutant plants

ABP1 knockdown were also found to affect the expression of core cell cycle related genes in seedlings (Braun et al., 2008). But in *sks1, sks2, sku5* triple null mutant seedlings, none of these gene exhibit a significant difference of expression compared to wild-type.

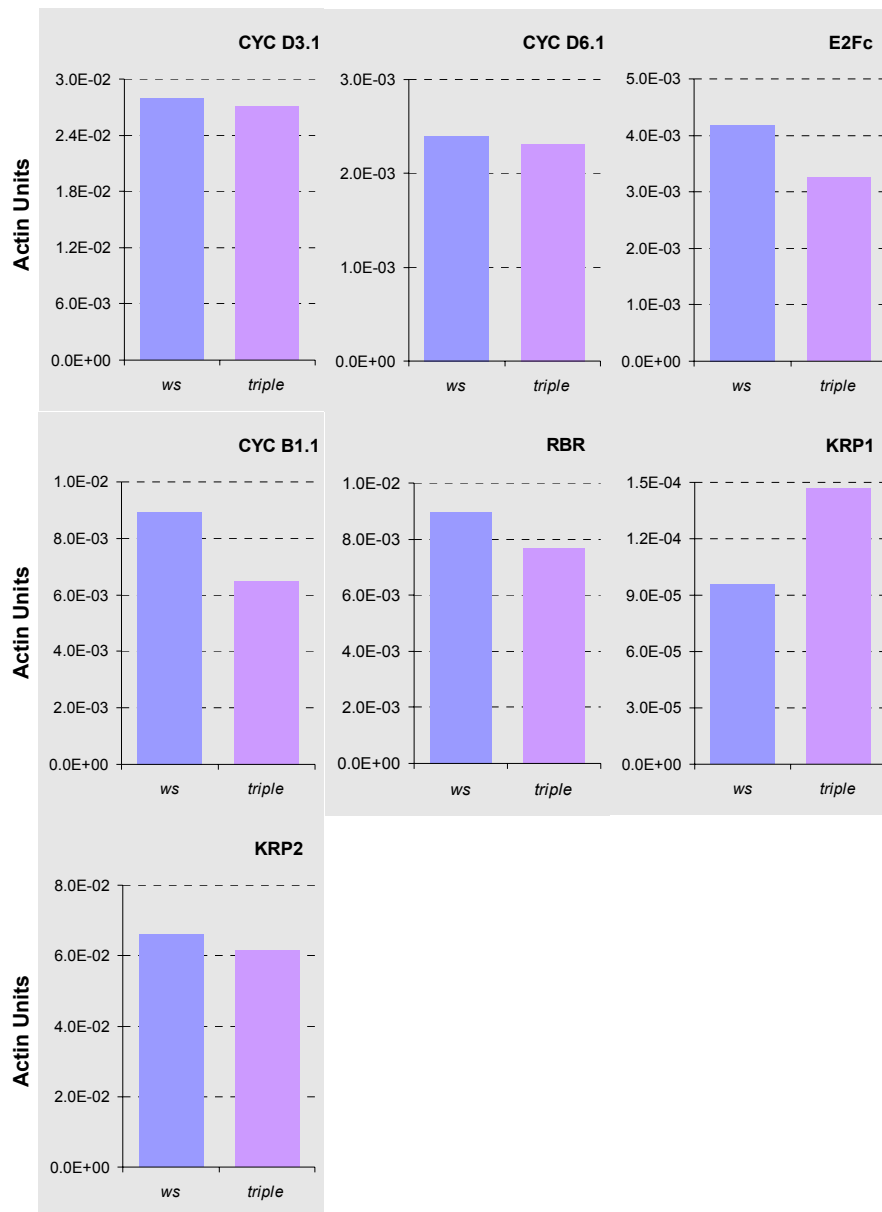


Figure III-29. Cell cycles relative genes expression levels in triple mutant.

RNAs from 5-day-old seedlings of *Ws* and *Triple* mutant were extracted and Real-time RT-PCR was performed. Data was normalized with ACTIN2-8

ABP1 knockdown exhibited short roots resulting from cell cycle arrest of meristematic cells, and small epinastic cotyledons (Braun et al., 2008; Tromas et al., 2009). In the triple mutant, there is a large range of root length; and no epinasty of the cotyledons was found in any seedlings whatever their root length (Data not shown).

As SKU5, SKS1, SKS2 were supposed to be the candidates for binding or docking protein of ABP1, null mutant plants of them could logically exhibit the relative phenotypes as ABP1 loss of function. But in fact, besides few changes in the responsiveness to auxin of Aux/IAA genes, there is no more evidence supporting such hypothesis.

Conclusion and Discussion

1. The redundancy of *SKS1*, *SKS2* and *SKU5* genes:

The additional *sksl* mutation in *sku5* single mutant exhibits additional phenotype which was not found in *sksl* single mutant; the additional *SKS2* mutation in *sksl,sku5* double mutant exhibits phenotype which was not found in *sksl* mutant. These data strongly suggest the redundancy between these three genes.

In roots, *SKU5* was expressed much higher than *SKS1*, and *SKS1* was expressed much higher than *SKS2*. If the redundancy does exist, then the *SKU5* gene can compensate the *sksl* and *sksl* mutation, *SKS1* can only compensate the mutation of *SKS2*. It could perfectly explain why the *sku5* single mutation exhibits defect in root grow, *sksl* mutation only exhibits defect underlie by the *sku5* mutation, and *sksl* mutation only exhibits defect underlie by *sksl,sku5* double mutation.

In reproduction organs, these three genes were highly expressed with not so much difference. If the redundancy does exist, the defects would be exhibited only when the triple mutation occurred. The dramatically reduced seed production that was only found in *sksl,sksl,sku5* triple mutant could be explained by their strong co-expression in reproductive organs.

2. The functions of *SKS1*, *SKS2* and *SKU5* genes:

As explained in (1), the phenotype caused by each *sksl*, *sksl* and *sku5* mutation could be revealed by the single, double and triple mutations. *sksl* knock-out caused distorted root files; *sku5* knock-out caused twisted root files; *sksl* mutation doesn't confer any defect in root or hypocotyl growth where the gene is not or very weakly expressed. *sksl,sksl,sku5* triple mutant analyses however revealed an important contribution of *SKS2*, together with the two other member of the family in root formation during embryogenesis. The function in embryogenesis would be discussed in chapter IV.

To investigate the exact function of *SKS2*, the expression pattern of *SKS2* should be studied in more details, which is not included in my thesis.

3. Indirect evidence for ABP1 binding.

Compared to the conditional ABP1 knockdown, no matter seedling shapes, auxin response, or core cell cycle response gene expression, there is no evidence to confirm the linkage between ABP1 and SKS/SKU5.

Chapter IV: *SKS1*, *SKS2* and *SKU5* are required for fertilization and embryogenesis

As described in chapter III, the *sks1,sks2,sku5* triple mutants exhibited a severe defect in seed production and root formation. That prompted us to explore why. Before presenting the experimental data, it appeared necessary to introduce some general background on reproduction in Arabidopsis.

IV-1 Introduction to fertilization, pollen tube guidance and embryogenesis

IV-1-1 Male and female gametophytes

Mature male gametophyte, or pollen grain, is a three-celled organism and consists of two smaller sperm cells and one bigger vegetative cell. The pollen grain originates from pollen mother cell. The pollen mother cells are covered by nutritive cell layer, which is called the tapetum. Undergoing meiosis, each pollen mother cell divides into a tetrad, which is enclosed by a thick callose wall. Callase from tapetum digests it and frees the microspores. After asymmetric mitosis, microspores divide into a smaller generative cell and a larger vegetative cell. The vegetative cell will not divide but form pollen tube eventually, and the generative cell will divide into two sperm cells after mitosis. When the pollen grain arrives at the pistil, it germinates and the elongated pollen tubes transport the two sperm cells inside the pistil and fertilize the female gametophyte (Figure IV-1).

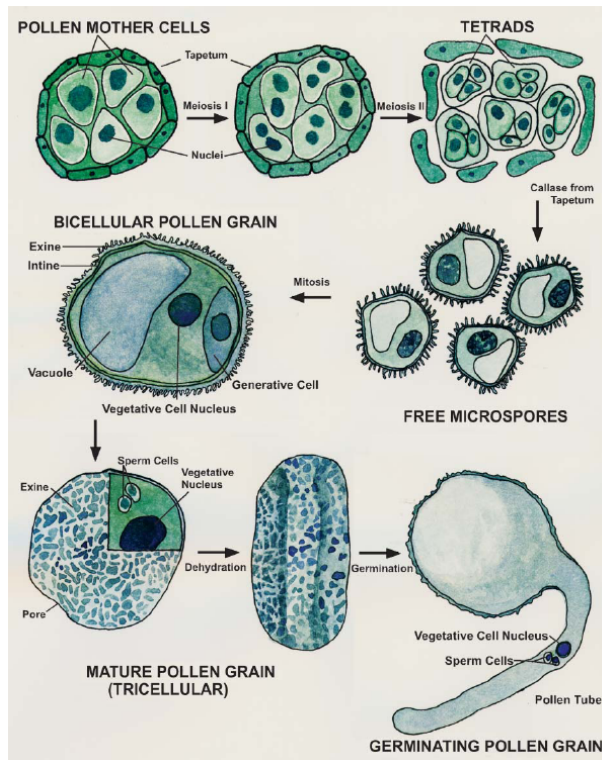


Figure IV-1. Male gametophyte development.

The pollen mother cells are covered by nutritive cell layer, which is called tapetum. Undergoing meiosis, each pollen mother cell divides into a tetrad, which is enclosed by a thick callose wall. Callase from tapetum digests it and frees the microspores. After asymmetric mitosis, microspores divide into a smaller generative cell and a larger vegetative cell. The vegetative cell will not divide but form pollen tube eventually, and the generative cell will divide into two sperm cells after mitosis (from (McCormick, 2004))

For female gametophyte, the situation is much more complicated. At least 15 different patterns of female gametophyte development have been described, including polygonum, alisma, drusa and so on. Some of different patterns were shown in Figure IV-2.

	MEGASPOROGENESIS				MEGAGAMETOGENESIS			
	MMC	Meiosis 1	Meiosis 2	Functional Megaspore	Mitosis 1	Mitosis 2	Mitosis 3	Mature FG
Monosporic (Polygonum)								
Bisporic (Alisma)								
Tetrasporic (Drusa)								

FigureIV- 2. Patterns of Female Gametophyte Development Exhibited by Angiosperms. (Yadegari and Drews, 2004)

More than 70% flowering plants exhibit a polygonum pattern, including Arabidopsis (Figure IV-2.) (Yadegari and Drews, 2004).

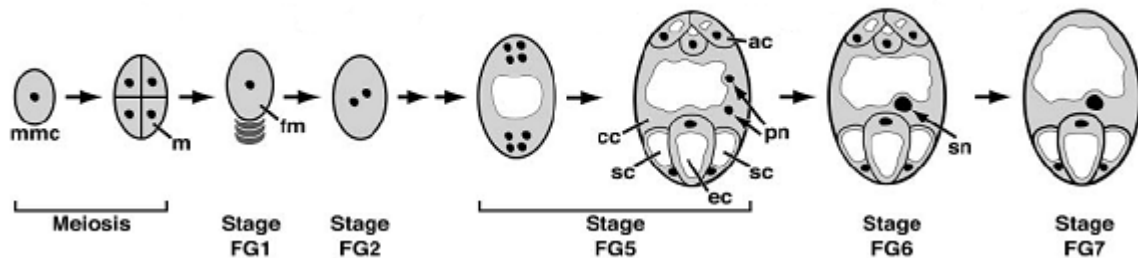


Figure IV-3. Female Gametophyte Development in Arabidopsis

The gray areas represent cytoplasm, the white areas represent vacuoles, and the black areas represent nuclei. In this figure, the chalazal end of the female gametophyte is up and the micropylar end is down. ac, antipodal cells; cc, central cell; ec, egg cell; fm, functional megaspore; m, megaspore; mmc, megaspore mother cell; pn, polar nuclei; sc, synergid cell; sn, secondary nucleus (Yadegari and Drews, 2004).

Undergoing meiosis, mother megaspore cell (mmc) divides into 4 megaspores, in which three of them enter in apoptosis. The left megaspore divide into 8 nuclei. With the fusion of two polar nucleus, the mature female gametophyte is formed (Figure VI-3). It consists of seven cells of four different types: three antipodal cells, two synergid cells surrounding one egg cell and one large central cell (Figure IV-4).

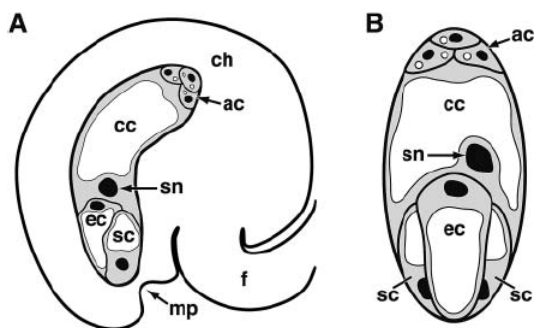


Figure IV-4. Female Gametophyte of Arabidopsis.

(A) Ovule of Arabidopsis.

(B) Female gametophyte.

The view in (B) is perpendicular to that in (A). The gray areas represent cytoplasm, the white areas represent vacuoles, and the black areas represent nuclei.

ac, antipodal cells; cc, central cell; ch, chalazal region of the ovule; ec, egg cell; f, funiculus; mp, micropyle; sc, synergid cell; sn, secondary nucleus. (Yadegari and Drews, 2004)

IV-1-2 Pollen tube guidance

Synergid cells are proved to be essential for pollen tube attraction. After laser ablation of central cell, synergid cells or egg cell, only the ovules without synergid cells lose the ability to attract pollen tube (PT), which suggest that pollen tubes are attracted by signals provided by synergid cells (Higashiyama et al., 2001) (Figure IV-4). Other research revealed that *ccg* (*central cell guidance*) mutant, which abolishes micropylar pollen tube guidance, can be rescued by central cell-expressing nuclear protein CCG; which suggests that central cell is also involved in pollen tube guidance (Chen et al., 2007).

But the exact mechanism of pollen tube guidance is not clear. Several membrane proteins seem to be involved in PT guidance. *POD1*, which was identified from the *pod1* (*pollen defective in guidance1*) mutant, localizes at the ER lumen and interacts with pollen grain and pollen tube specific protein CRT3 that is a Ca^{2+} binding ER chaperone CALRETICULIN involved in the folding of membrane receptors. Loss-of-function causes micropylar pollen tube guidance and early embryo developmental defects (Li et al., 2011). *GEX3*, which encodes a plasma membrane localized protein of unknown function, is expressed in both male gametophyte and egg cell. Down-regulation of *GEX3* blocks fertilization due to micropylar pollen tube guidance defects. Over-expression of *GEX3* affects pollen tube guidance and generates few non-viable embryos (Alandete-Saez et al., 2008). Egg Apparatus 1 of maize (*ZmEA1*), which is exclusively expressed in maize egg apparatus, encodes a small transmembrane protein of 94 amino acids; this protein is a signalling molecule in maize short-range pollen tube guidance (Marton et al., 2005). Expression of *ZmEA1* in ovules of *Arabidopsis* can overcome the hybridization barriers to attract maize pollen tube *in vivo* (Marton et al., 2012).

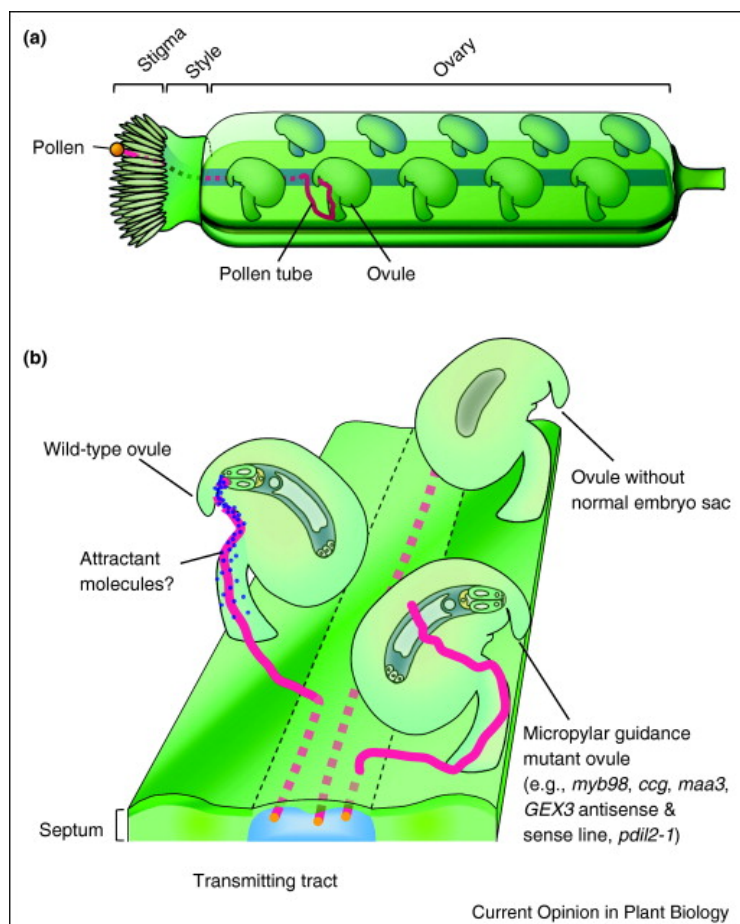


Figure IV-5: Schematic representations of pollen tube guidance in the pistil of *Arabidopsis*.

(A) Guidance from the stigma to the ovule and **(B)** close-up from the transmitting tract to the embryo sac. (A) A pollen tube (red solid and dashed line) germinated from a pollen grain penetrates the stigma cell and the style, and enters the transmitting tract (shown as blue region) within the ovary. The pollen tube emerges from the transmitting tract and grows to the ovule. (B) Ovules on the septum (parietal placentas) and pollen tubes. Pollen tubes grow straight into the transmitting tract. A pollen tube emerges on the surface of the septum, targets a wild-type ovule, and consequently reaches the synergid cell without deviation, probably related to a predicted attractant molecule(s). Another pollen tube also targets a micropylar guidance mutant ovule, but does not enter the micropyle and wanders on the surface of the ovule despite arriving at the funiculus. No pollen tube grows to an ovule without a normal embryo sac. (Takeuchi and Higashiyama, 2011)

Besides the trans-membrane proteins, several small peptides are also involved in pollen tube guidance. In *Torenia fournieri*, two of a series of defensin-like secreted cysteine-rich polypeptides (CRPs), which are called LURE1(TfCRP1) and LURE2(TfCRP3) respectively, that are produced by synergid cells show abilities to attract pollen tubes of their own species *in vitro* (Okuda et al., 2009). Defensin-like protein ZmES4 (*Zea Maise Embryo sac 4*) opens the inward rectifying potassium channel KZM1 and induces rapid pollen tube burst in less than a minute *in vitro* with species preferences (Amien et al., 2010).

The GPI-anchored protein LORELEI was also identified to function in pollen tube guidance. Loss-of-function causes ovule to attract more than one pollen tube or additional growth of pollen tube after entering the micropyle (Tsukamoto and Palanivelu, 2010; Tsukamoto et al., 2010).

IV-1-3 Double fertilization of flowering plants

Unlike the fertilization in other living organisms, flowering plants have developed their own fertilization mechanism, which is called double fertilization. In this mechanism, two immotile sperm cells fertilize two different female gametophytes. Two sperm cells in mature pollen grain are taken inside female gametophyte by pollen tube, and fuse with each target; one fertilizes the egg cell, and the other fuses with the central cell (Figure IV-5.). Egg cell fused with a sperm cell develops to embryo, and central cell fused with the other sperm cell develops to endosperm (Hamamura et al., 2012).

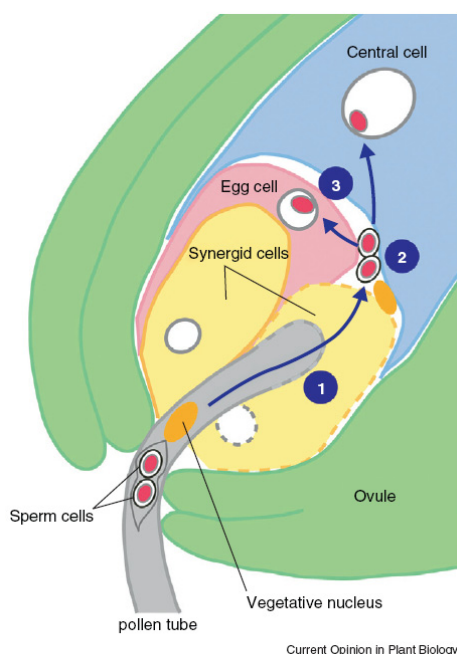
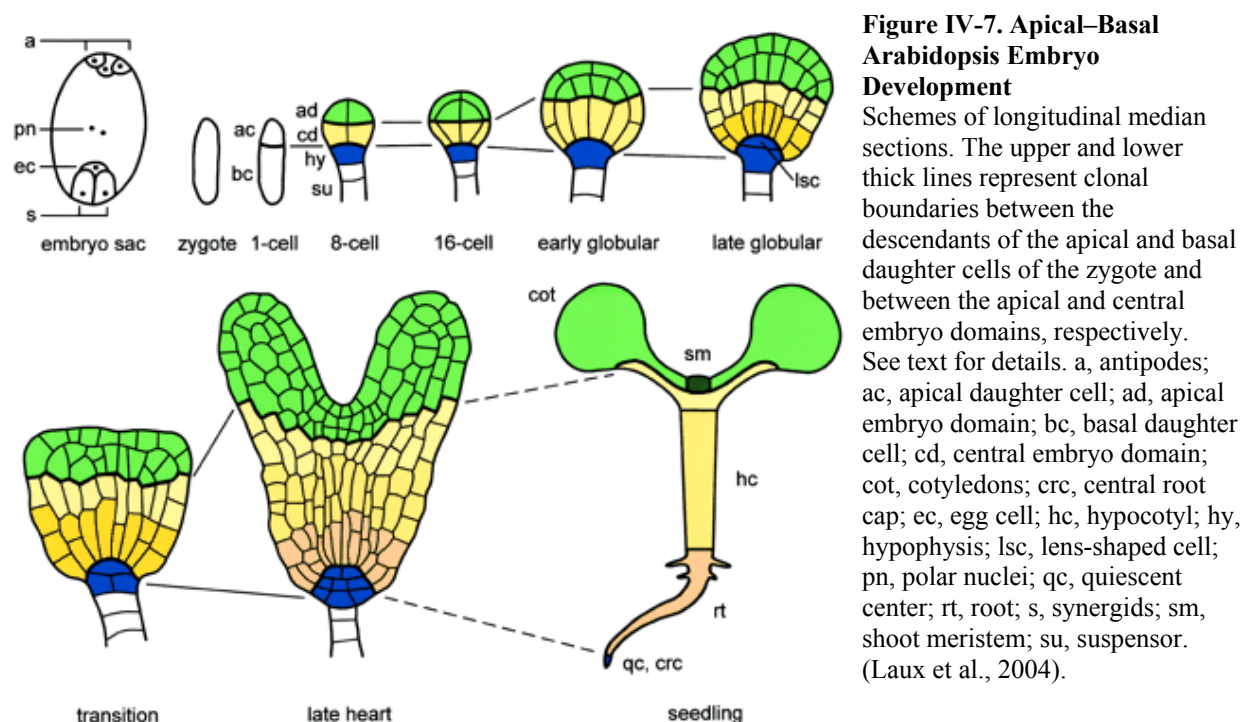


Figure IV-6. Double fertilization of flowering plants
Two sperm cells are transferred inside ovule by pollen tube and start the fertilization.

Step 1: two sperm cells delivered into female gametophyte (pollen tube discharge phase).
 Step 2: sperm cells remain at the boundary region between egg cell and central cell (immobility phase).
 Step 3: sperm cells fuse with each target; one to central cell, and the other to egg cell (double fertilization phase). (Hamamura et al., 2012)

IV-1-4 Arabidopsis embryogenesis

Followed by the fertilization, the embryogenesis occurred. Embryogenesis in Arabidopsis consists in two major phases, morphogenesis and maturation. Morphogenesis involves the establishment of the embryo's body plan, and maturation involves cell expansion, seed desiccation allowing further germination and early seedling growth (Park and Harada, 2008). The embryogenesis of Arabidopsis is briefly described in Figure IV-6 (Laux et al., 2004).



The morphogenesis phase starts from zygote, which is formed by sperm-fused egg cell. The first important event is the acquisition of polarity. Polarized egg cell has its nucleus localized to the chalazal/apical end and the larger vacuole to the micropylar/basal end. After fusion with the sperm cell, the zygote is polarized again with the nucleus localized to the chalazal/apical end and the larger vacuole to the micropylar/basal end (Ueda et al., 2011). Then an asymmetric division happens and the zygote divides into a smaller embryonic apical cell and a larger basal cell that will give rise to the suspensor. The *WUSCHEL RELATED HOMEODOMAIN (WOX)* genes *WOX2*, *WOX8* and *WOX9* encode essential regulators in this progress (Breuninger et al., 2008; Ueda et al., 2011).

After the first asymmetric division, the apical embryonic cell divides and daughter cells are formed following a series of symmetric or asymmetric divisions resulting in a specific pattern. Intermediate stages of 2-cells, 8-cells, 16-cells, early globular, late globular, transition, and late heart stages have been identified (Laux et al., 2004). The cotyledons are formed from the apical cells of the embryo, the hypocotyl from the medium and basal cells and the root

primordia results from an asymmetric division of a big cell named hypophysis at the junction between the embryo and the suspensor.

IV-1-5 seed maturation and dessication

As the morphogenesis is completed, the seed maturation follows. It includes accumulation of storage products, suppression of precocious germination, acquisition of desiccation tolerance, water loss and often the induction of dormancy (Wobus and Weber, 1999). In *Arabidopsis thaliana*, four transcription factors, *ABSCISIC ACID INSENSITIVE 3 (ABI3)*, *FUSCA3 (FUS3)*, *LEAFY COTYLEDON1 (LEC1)*, and *LEC2* control most aspects of seeds maturation (To et al., 2006). The transcript levels of these four major regulators are abundant during late embryogenesis, decrease during germination and are expressed at low level in vegetative organs (Chiu et al., 2012).

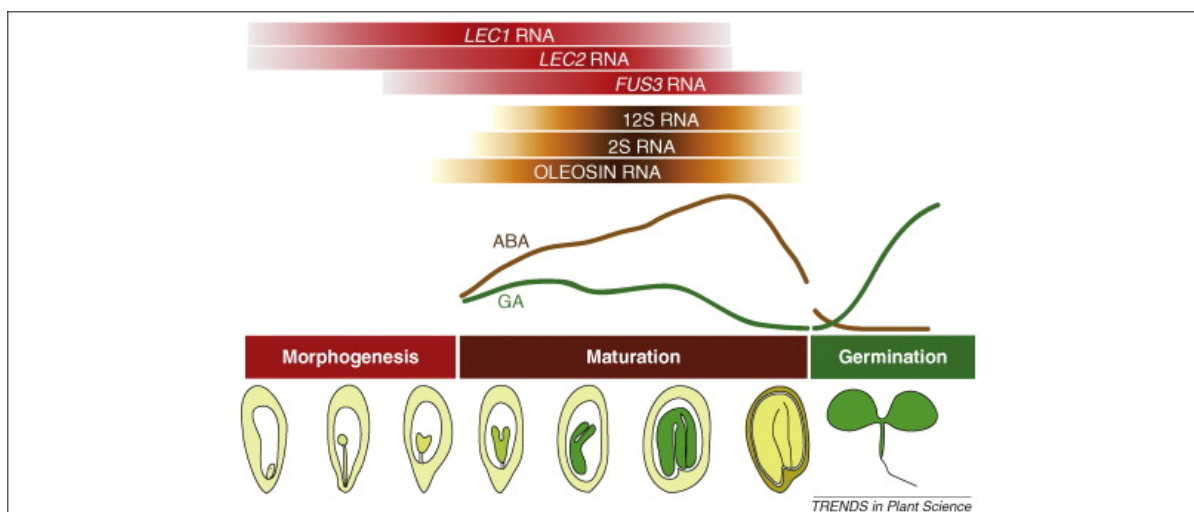


Figure IV-8 Embryo development in seed plants.

Embryo development consists of two phases, morphogenesis and maturation. During the morphogenesis phase, different morphological domains of the embryo are specified and the embryonic tissue and organ systems are formed. During the maturation phase, the embryo expands by accumulating storage macromolecules (represented by brown/orange bars at the top of the figure), including 2S and 12S storage proteins, fatty acids and the major oil body protein oleosin, and starch. The embryo also acquires the ability to withstand desiccation during the maturation phase. LEC TFs are master regulators of embryo development whose RNAs (represented by red/pink bars at the top of the figure) primarily accumulate during embryogenesis in both the morphogenesis and maturation phases of development. Maturation-phase seeds also possess a high ratio of ABA to GA that influences physiological processes. At the end of maturation, embryos are arrested developmentally and metabolically quiescent. Upon favorable environmental conditions, the embryo will recommence growth and seeds will germinate, as marked by radicle emergence. The ratio of ABA to GA becomes low during germination. The break in lines depicting ABA and GA levels represents the metabolically quiescent mature seed. (Braybrook and Harada, 2008)

LEC1 is expressed in developing siliques. *LEC1* overexpressors could induce embryo development in vegetative cells (Lotan et al., 1998). *LEC1* is also a key regulator of fatty acid biosynthesis in *Arabidopsis*. The overexpression of *LEC1* gene causes globally an increased

expression of fatty acid biosynthetic genes; it results in higher level of various fatty acids around 10-15d after germination (Mu et al., 2008).

LEC2 overexpression leads to the accumulation of storage oil and seed specific mRNA in leaves (Santos Mendoza et al., 2005).

FUS3 was only found to be expressed in siliques (Luerßen et al., 1998) and the expression level is influenced by auxin (Gazzarrini et al., 2004). In *fus3* mutant, the ABA cannot be accumulated to the peak concentration as in wildtype at 10 DAF and transcript levels of two key steps in GA3 biosynthesis were decreased. Interestingly, ABA stabilizes FUS3 protein whether GA decreases its stability indicating that relative abundance of the protein results from the combined ABA/GA action (Gazzarrini et al., 2004).

abi3 mutant results in green seeds failing to establish desiccation tolerance and precocious germination; the immature seeds could germinate at up to 10 DAF (Nambara et al., 1995).

Studies in yeast and plants revealed the mechanisms by which *FUS3*, *LEC2* and *ABI3* regulate seed maturation: FUS3 and LEC2 proteins can bind to each other and activate the transcription of downstream genes as of the model storage protein gene At2S3 (Kroj et al., 2003).

IV-2 Absence of *SKS1*, *SKS2* and *SKU5* affect fertilization and embryogenesis.

As briefly mentioned in “chapter III”, the siliques of *skt1 skt2,sku5* triple null mutants are extremely short. These siliques are mostly empty or with very few seeds inside (normally 100-300 per individual plant). Further investigation revealed that the *skt1,sku5* double mutation also cause a seeds reduction, however the reduction is not as significant as triple mutant.

To investigate what happened in these siliques, the mature siliques of *Ws*, *skt1,sku5* and *skt1,skt2,sku5* triple mutant were collected and dissected; the numbers of unfertilized ovules, which are in white and very small, were counted (Figure IV-9 and Table IV-1). Data shows that, in the triple mutant, more than 85% of the ovules were unfertilized; but up to 40% ovules of *skt1,sku5* were unfertilized, which is significant higher than in *Ws* wild-type but lower than in the triple mutant.

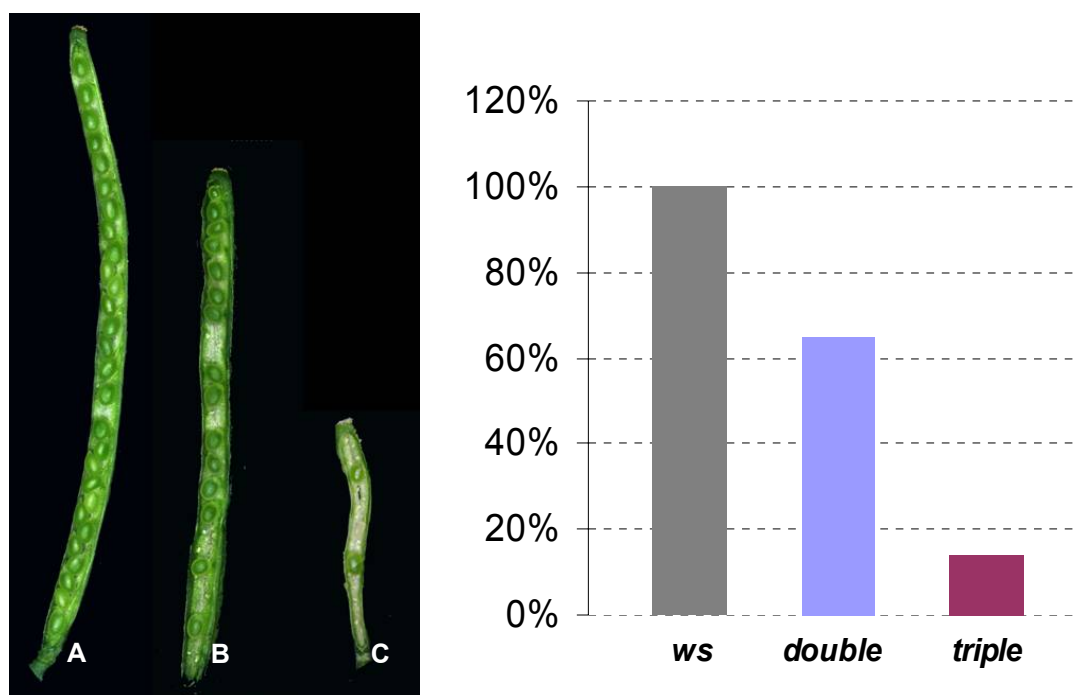


Figure IV-9. Fertilization rate of *WS*, *skt1,sku5* and *skt1,skt2,sku5*.

Mature siliques were dissected and taken pictures. Mature seeds are in green, unfertilized ovules were very small and in white.

(A) *Ws* (B) *skt1,sku5* (C) *skt1,skt2,sku5* siliques were dissected and observed under macroscope.

The percentage of seeds set was indicated in the chart and Table IV-1

Table IV-1 Fertilization rate of siliques of *Ws*, *sksl,sku5* and *sksl,sksl,sku5*

<i>Ws</i>	<i>sksl,sku5</i>	<i>sksl,sksl,sku5</i>
98.7% (n=157)	64.7%(n=624)	14.1 %(n=440)

n= total number of ovules, including fertilized and unfertilized.

To further investigate the mechanism of the seeds reduction, more siliques were dissected. We found that, although the fertilization rate of double and triple mutant are both lower than *Ws*, the mechanism is not the same. A large proportion of these fertilized ovules from the *sksl,sksl,sku5* mutant were aborted, which is rarely found in double mutant and *wild-type* (Figure IV-10 and Table IV-2).

**Figure IV-10 Aborted seeds in the triple *sku5,sksl,sksl* mutant.**

The aborted ovules were in brown and smaller size; unfertilized ovules were very small and in white; the mature seeds were in green and bigger size. The proportion of aborted ovules was indicated in Table IV-2.

Table IV-2 Aborted seeds / all fertilized seeds %

<i>Ws</i>	<i>sksl,sku5</i>	<i>sksl,sksl,sku5</i>
0 (n=157)	3.35% (n=418)	37.1% (n=62)

These data indicate that with the double mutation of *SKS1* and *SKU5*, the fertilization rate is slightly decreased. With the triple mutation of *SKS1*, *SKS2* and *SKU5*, the fertilization rate is much more severely decreased and a large proportion of ovule/seed abortion was observed. It suggests that, with the additional null mutation for *SKS2* in *sksl,sku5* double mutant background, the alterations are dramatically enhanced. *SKS2* was found to be mainly expressed in flowers and is likely to be required for fertilization and seed development. However no seed production defect was noticed in the single mutant *sksl2* or in the double mutants *sksl,sksl2* or *sksl2,sku5* but *sksl2* null mutation aggravates the seed production defect of the double mutant *sksl,sku5*. It is indicative of gene redundancy between these three genes with more or less efficient compensation mechanisms occurring when only two of them are mutated.

Seed abortions at early stages of development suggest that lethal alterations occur during embryogenesis. In addition to these abortions, a large proportion of seeds from the triple mutant suffered from abnormal shapes and behaviours. Abnormalities were detected at

various stages of seed development within the siliques of the triple mutant. A variety of more or less well shaped structures were emerging from the seeds, sometimes resembling to cotyledons sometimes more to undifferentiated callus (Figure IV-11). In some cases, it looks like whether the seed content would have been pushed out but differentiated structures were not possible to be identified (Figure IV-11D). The proportion of abnormal seeds is indicated in Table IV-3.

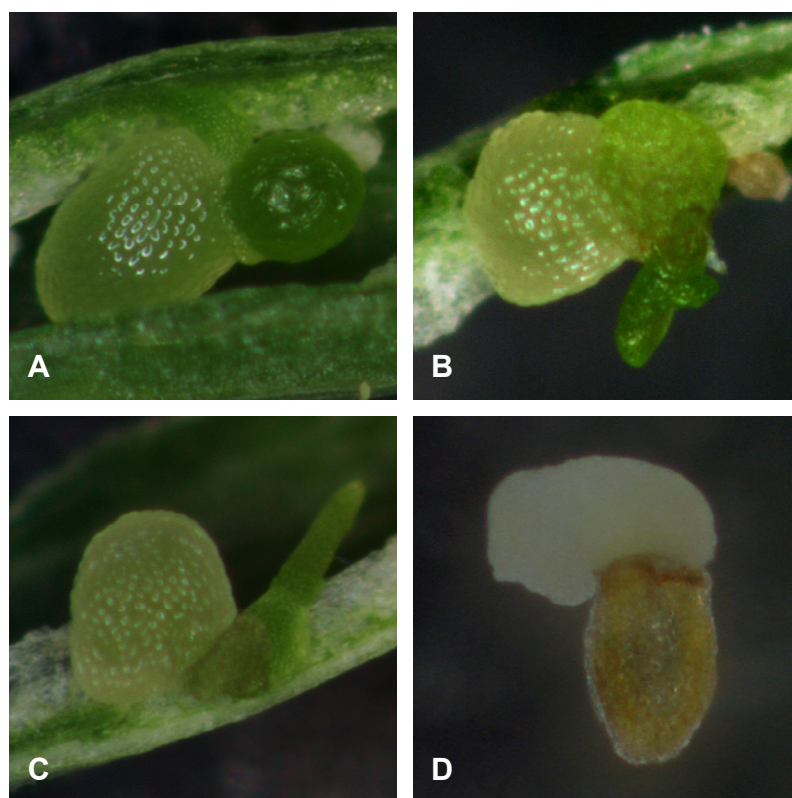


Figure IV-11 Abnormal seeds of triple mutant.

(A-C) observations performed within the siliques (A) Unknown structure was pulled out from the immature seed, (B) cotyledon-like material was pulled out from the seed, (C) hypocotyl-like material was pulled out from the seed, (D) dry aborted seeds with unshaped tissues emerging from the seed.

Table IV-3 Proportion of abnormal seeds amongst developing seeds

<i>Ws</i>	<i>sksl,sku5</i>	<i>sksl,sksl2,sku5</i>
0% (n=200)	0% (n=106)	40.32% (n=62)

Siliques around 10 DAP were dissected and the numbers of abnormal seeds were counted in regards to the total number

Then the dried siliques were collected and dissected. Not surprisingly, after failure of fertilization, abortion and abnormal development, only very few mature seeds were produced by *sksl,sksl2,sku5* mutant plants, the rest corresponded to abnormal seeds, shrivelled testa and early abortion ovules (Figure IV-12 C and D).

In consequence the number of seeds of the triple mutant following apparently the whole developmental program drops down to an average of less than one seed per silique. This was an important constraint for further work and characterization of the triple mutant.



Figure IV-12. Seeds shape of *Ws*, *sks1,sku5* and *sks1,sku2,sku5*.

(A) *Ws*, (B) *sks1,sku5*, (C) and (D) *sks1,sku2,sku5*.

Sks1,sku5 produced seeds were not as full as in *Ws*, and included few aborted seeds.

Sks1,sku2,sku5 produced shriveled and small seeds, and included a large proportion of aborted (pointed by “*”) and abnormal seeds.

The abnormal seeds have irregular shapes (pointed by red arrow), abnormal hypocotyl elongation (white arrow), or unknown material pulled out (cyan arrow).

The dramatic decrease in seed production occurred only when *SKS1*, *SKS2*, *SKU5* were knocked-out together. It strongly indicates the redundancy between these genes.

These phenotypes seems to be resulted from cumulated defects along the reproduction processes, we then tried to identify the most limiting steps.

IV-2-1 *SKS1*, *SKS2*, *SKU5* in fertilization

As the fertilization rate was low in *sks1,sku5* and *sks1,sku2,sku5*, several aspects known to affect the fertilization rate were investigated, including flower shapes, pollen viability, female gamophyte and pollen tube guidance.

IV-2-1-1 Flower shapes of *sks1,sku5* and *sks1,sku2, sku5* mutants

Arabidopsis is autogamous and failure of fertilization might start with alteration of flower development, including mechanical or physical constraint impairing deposition of the pollen to the stigma. We observed the shape of the flowers and elongation of stamens of *sks1,sku5* and *sks1,sku2,sku5* mutants. Flowers of *sks1,sku2,sku5* triple mutant were smaller than control plants but no significant alteration of shape and floral organs was observed (Figure IV -13A), Stigma observation in different stages also indicated that pollen grains could stick to the stigma. All these evidences suggest that no morphological defect and resulting physical constraint can explain the lack of fertilization.

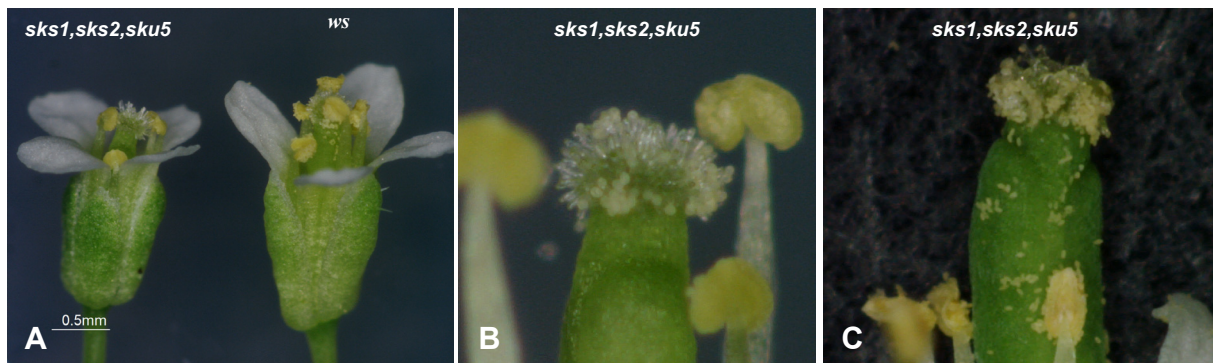


Figure IV-13. Flowers of *Ws* and *sks1,sks2,sku5* triple mutant were observed.

(A) Flower shape observation of *Ws* and *sks1,sks2,sku5* triple mutant, **(B, C)** close-up stigmas of *sks1,sks2,sku5* in different stages.

IV-2-1-2 Pollen viability analyses.

To investigate whether the vitality of the pollen grains was affected, pollens from *Ws* and the *sks1,sks2,sku5* triple mutant were collected and stained by Alexander's staining and their capacity to germination *in vitro* were also investigated.

By Alexander's staining, the aborted pollen grains would be stained in blue and living pollen in red. Pollen grains from *sks1,sks2,sku5* didn't exhibited significantly different viability compared to wild-type (Figure IV-14 A and B).

For *in vitro* germination assay, pollen grains from *Ws* and *sks1,sks2,sku5* germinated normally (Figure IV-14 C and D).

These results showed that pollen grains of *sks1,sks2,sku5* triple mutant are viable and can germinate normally. The elongation of pollen tube was not analysed *in vitro*.

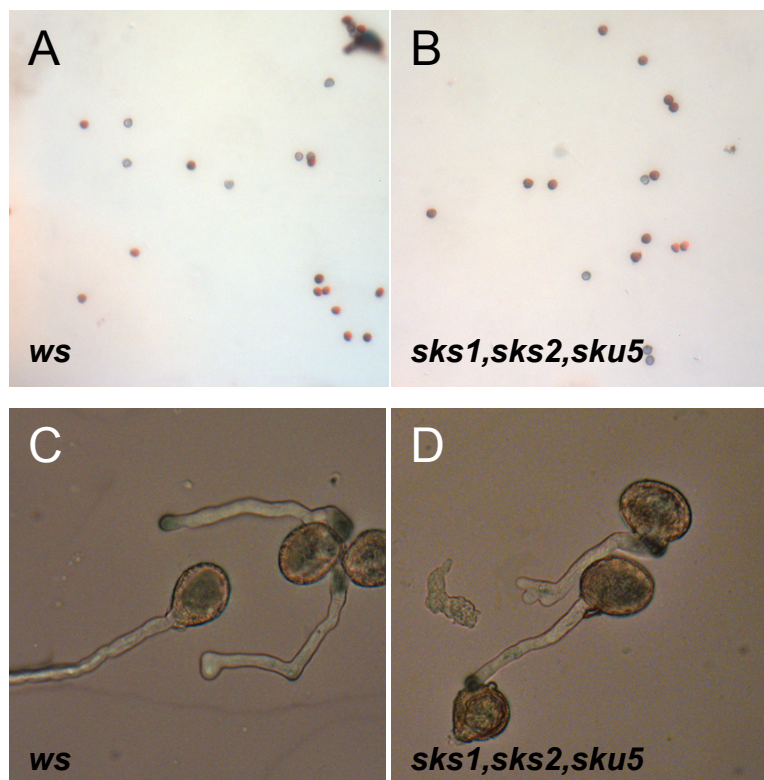


Figure IV-14. *In vitro* pollen analysis.

(A) and (B) Pollens from wild-type and triple mutant are treated by Alexander's staining
(C) and (D) Pollen germination on the pollen germination medium.

The ratio of vital pollens and germination rate are calculated and shown in Table IV-4.

Table IV-4 Pollen viability in vitro

	<i>Ws</i>	<i>sks1,sks2,sku5</i>
Pollen viability	73.8% (n=172)	73% (n=118)
Germination rate	58.9% (n=141)	61.8% (n=55)

Based on the performed assays, it is likely that the fertilization defects observed in *sks1,sku5* and *sks1,sks2,sku5* mutants do not result from deficiency of male gametophytes. In consequence, SKS1, SKS2 and SKU5 do not seem to be required for male gametophytic formation and viability. .

IV-2-1-3 Manual pollination between *Ws* and *sks1,sks2,sku5*

To identify whether the male or female gametophyte is responsible for the largely reduced fertilization rate, we performed the manual pollination between *Ws* and the triple mutant in reciprocal combinations.

1 day before flowering, the flowers were castrated and manually pollinated. 7 days after manual pollination, siliques were collected and seeds produced were counted. Interestingly, *Ws* mother plant pollinated with *sks1,sks2,sku5* pollen produced a reasonable amount of seeds albeit 3 times lower than using *Ws* pollen instead. Conversely, we failed to obtain mature

seeds for the reciprocal cross of *Ws* pollen on *sksl,sksk2sku5* mother plant. Collected siliques are shown in Figure IV-15 and the seed production is shown in Table IV-5.

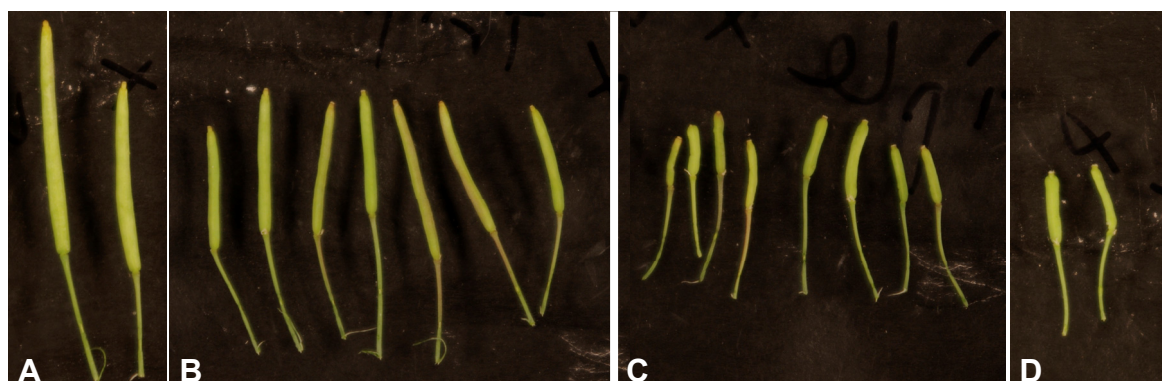


Figure IV-15 . Manual-pollination of *Ws* and *sksl,sksk2sku5*.

Stamens were removed 1 day before flowering and pistils were pollinated by pollens from *Ws* and triple null mutants. 7 days after pollination, siliques were collected.

(A) *Ws*♀ x *Ws*♂, (B) *Ws*♀ x *sksl,sksk2sku5*♂, (C) *sksl,sksk2sku5*♀ x *Ws*♂, (D) *triple*♀ x *triple*♂.

Table IV-5. Seeds production of *Ws* and Triple Cross siliques

Female	Male	Pollination Mode	Seeds production*
ws	ws	auto	98.7% (157)
triple	triple	auto	14.1 % (440)
ws	ws	manual	61.97% (142)
triple	triple	manual	0% (86)
ws	triple	manual	21.38% (304)
triple	ws	manual	0% (398)

* The numbers of ovules are indicated in ().

We previously showed that there was no difference of viability and germination between wild-type and *sksl,sksk2sku5* pollens. These data suggest however that both pollens and ovules might affect the efficiency of fertilization but a more severe defect seems to result from the female.

IV-2-1-4 Female gametophyte analyses *in vitro*

As no significant defect was found in male gametophyte, we investigated whether the female gametophyte was responsible for the low fertilization in *sksl,sksk2sku5* triple mutant plants.

Pistils were collected on flowers to be fixed and cleared by Chloral Hydrate before being observed under differential interference contrast (DIC) microscopy.

Some of the *sksl,sksk2sku5* female gametophyte exhibit misorganized synergid cells and egg cell (Figure IV-16). The relative position of synergid cells and egg cell was inverted with the synergid cells appearing between the central cell and the egg cell. In such pattern, the egg cell is at the basal pole. In addition, the micropyle seems to be exaggeratedly opened in

sks1,sks2,sku5 compared to the tiny aperture that is observed in wild-type. It is however difficult to know whether this change in micropyle opening is a defect on its own or if it results from the misorientation of the female gametophyte. These data suggest that the *SKS1*, *SKS2* and *SKU5* genes are collectively required for proper female gametophyte organisation.

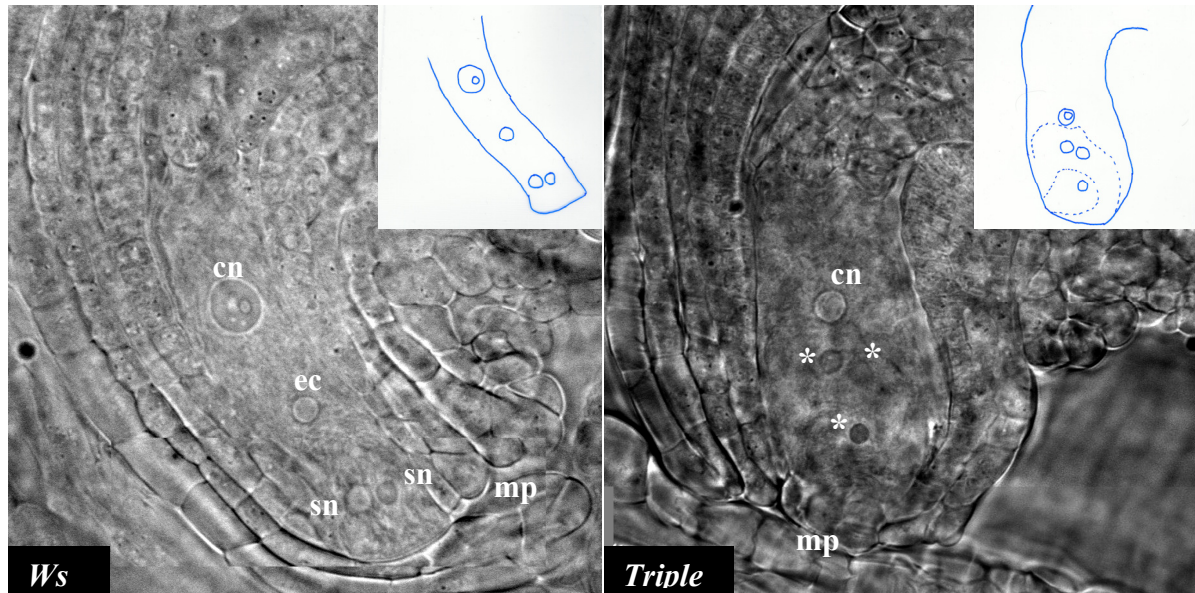


Figure IV-16. Female gametophyte of *Ws* and *sks1,sks2,sku5* triple mutant.

The pistils of *Ws* and *sks1,sks2,sku5* triple mutant plants were collected and cleared by Choral Hydrate, then observed under microscope. The schematic diagrams were shown above each picture.

The female gametophyte of triple mutant looks misorganized. The two synergid cells and one egg cell which are labeled by *, however no significant evidence to distinguish them, were at the wrong position. It suggests that *sks1,sks2,sku5* mutation cause defect on female gametophyte polarity.

Compared to *Ws*, the micropyle of triple mutant was extended. The irregularly swollen synergid cells and egg cell were dotted lines in schematic diagrams.

cn: central nuclei; ec: egg cell; sn: synergid cell; mp: micropylar.

Interestingly, synergid cells and central cell were identified to be involved in pollen tube guidance (Higashiyama et al., 2001; Chen et al., 2007). With the observed misorganized female gametophyte we can anticipate that the triple mutant might also be affected in pollen tube guidance.

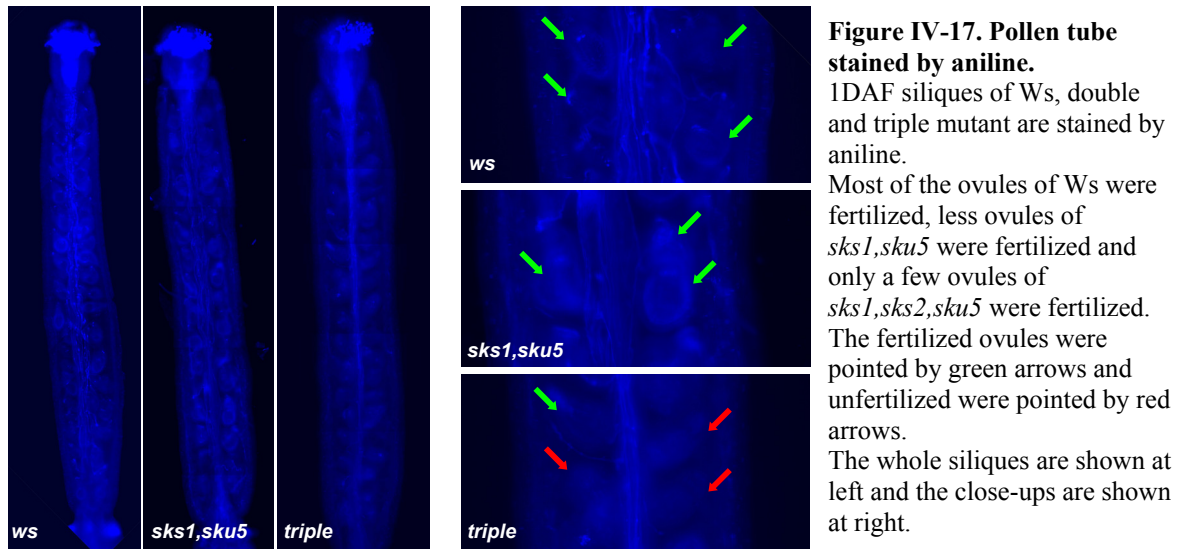
IV-2-1-5 Pollen tube guidance analysis in *sks1,sks2,sku5* triple mutant.

According to the data of manual pollination, both male and female gametophytes seem to be affected by the triple mutation, but the female gametophyte appears to be more severely affected. Together with the disorganized female gametophyte we hypothesized that pollen tube guidance might be affected in the triple mutant.

The pollen tube growth within the pistil to the ovules can be visualized by aniline blue staining under UV light. This method was used to investigate whether a defect in pollen tube guidance is partly responsible for the defect in fecondation.

Pistils of opened flowers from *Ws*, *sks1,sku5* double and *sks1,sks2,sku5* triple mutant were collected and stained by aniline blue. Pollens germinated on all pistils and pollen tube elongated inside the pistils. Considering previous observation on pollen viability with *in vitro* analysis, the observation confirms that pollens of double and triple mutant were viable and that germination is efficient also *in vivo*.

For all genotypes, pollen tubes elongate till they reach the ovules. However whereas ovules from *Ws* were mostly fertilized, less ovules from *sks1,sku5* were fertilized, and no or only very few ovules from the triple mutant plants were found to be fertilized (Figure IV-17).



The failure of fertilization in the triple mutant was apparently caused by a low efficiency of pollen tubes entering through the micropyle to fertilize the female gametophyte. Various configurations are illustrated Figure IV-18. In several cases, the pollen tube could not find the micropyle, which indicates the defect in pollen tube attraction (Figure IV-18C), or pollen tube twisted but cannot enter the micropyle, which indicates the defect in pollen tube entry (Figure IV-18D).

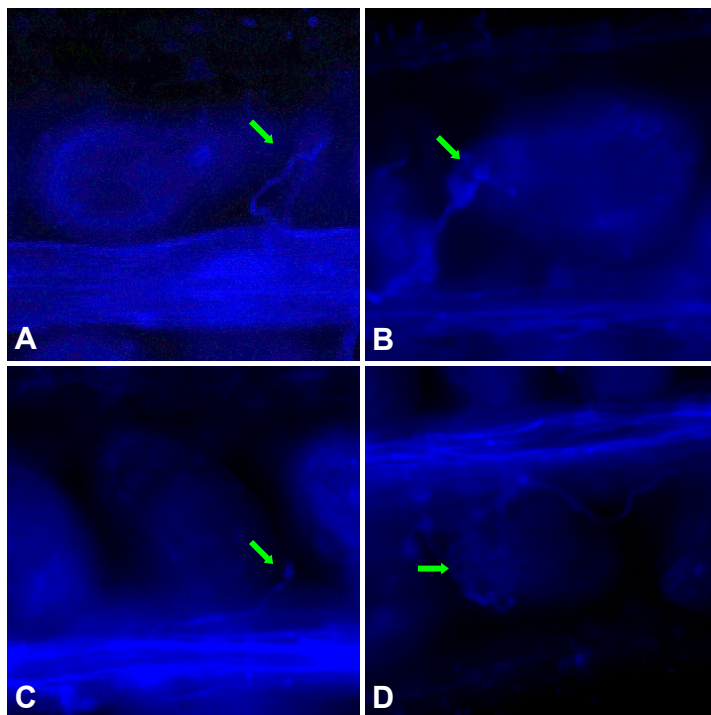


Figure IV-18. Pollen tube attraction in the triple mutant.

1DAF siliques of triple mutant were stained with aniline blue and observed by DMI6000 microscope system under UV light.

(A) *Ws* fertilized ovule, (B) *sks1,sks2,sku5* fertilized ovule, (C) ovule of *sks1,sks2,sku5* with no PT attraction, (D) ovule of *sks1,sks2,sku5* attracted the pollen tube, but the pollen tube was twisted at the micropyle.

The pollen tube was stained in blue and pointed by the green arrows.

On the basis of these observations, it is likely that pollen tube guidance is affected in the *sks1,sks2,sku5* triple mutant. This is in accordance with a defect coming from the female gametophyte. It indicates that SKS1, SKS2 and SKU5 are required for this process. It is reminiscent to the reported involvement of LORELEI, another class of GPI-anchored proteins (Tsukamoto and Palanivelu, 2010; Tsukamoto et al., 2010).

These efforts on male, female gametophytes and fertilization revealed that, the *SKS1*, *SKS2* and *SKU5* mutation strongly affected the fertilization rate. Considering that the synergid cells, as well as the central cell, are involved in pollen tube guidance, and that the triple mutations alter the female gametophyte, it is possible that the pollen tube guidance defect is because of the misorientation defect of the female gametophyte.

Besides the attraction and entry of pollen tube, the pollen tube elongation could also affect the fertilization. Although we haven't checked the elongation of pollen tube in vitro yet, the fact that fertilized seeds of *sks1,sku5* and *sks1,sks2,sku5* were more localized at the upper part of the siliques that required less elongation might give us some information that the elongation might be affected by the double or triple mutation.

IV-2-2 SKS1, SKS2 and SKU5 in embryogenesis.

IV-2-2-1 SKS1, SKS2 and SKU5 in embryonic development.

The large proportion of abortion and abnormality of seeds in *sksl,skss2,sku5* prompted us to investigate the embryogenesis in the triple mutant to reveal the function of GPI-anchored SKS members in embryogenesis.

Seed abortion is often caused by developmental arrest of the embryos. Siliques of *sksl,skss2,sku5* were collected and observed under DIC microscopy. Embryo arrest was observed in some cases (Figure IV-18). Some embryos of *sksl,skss2,sku5* mutant plants were observed to form zygote (C), and then 2,4-cell stage, but they were arrested at very early stage (8-cell stage), and later start some dessication or apoptosis processes (Figure IV-18F).

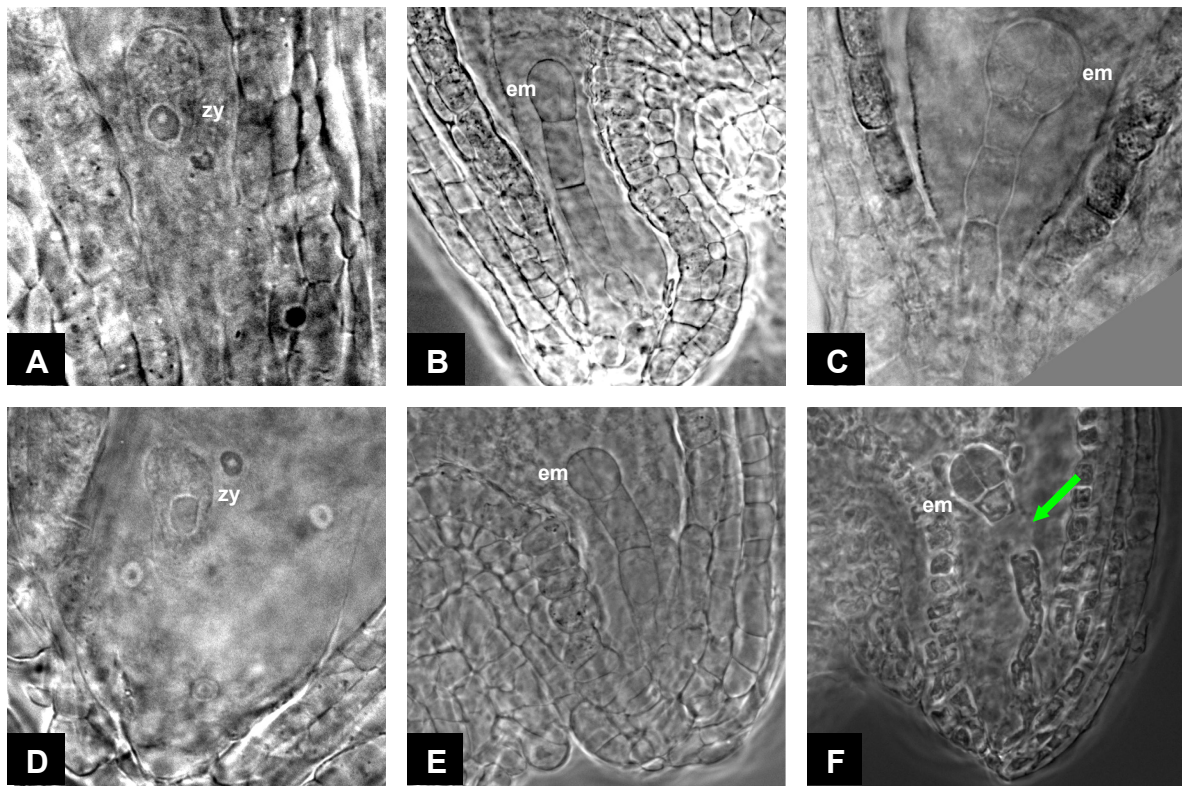


Figure IV-18 Embryos were arrest in *sksl,skss2,sku5* triple mutant.

Different stages of embryogenesis were observed. (A-C) are in *Ws* and (D-E) are in *sksl,skss2,sku5*. Zygote could be formed in some *sksl,skss2,sku5* ovules (D). They could develop normally to 4-cell stage (E), but they might be arrested at 8-cells (F). The arrested embryo start dessication (pointed by green arrow).

zy: zygote; em: embryo.

It suggests that the *SKS1*, *SKS2* and *SKU5* are very important for the embryogenesis. With the absence of these genes, the embryo can be arrested at an early stage. It can partly explain seeds abortion.

As there are seeds produced in the *sksl,skss2,sku5* triple mutant, although very few, some embryos can overcome this lethality. Further observation of these embryos revealed that some of them suffer from severe defect where the lens-shaped cell was absent (Figure IV-18B). In this case, the lens-shaped cell was totally missing. As mentioned in introduction of this chapter, this cell results from the asymmetric division of the big cell positioned at the basis of the embryo, at the junction with the suspensor. This cell is going to develop into the primary root. The defect in the formation of this cell explains the rootless phenotype found in a subset of *sksl,skss2,sku5* triple mutant seedlings (described in Chapter III).

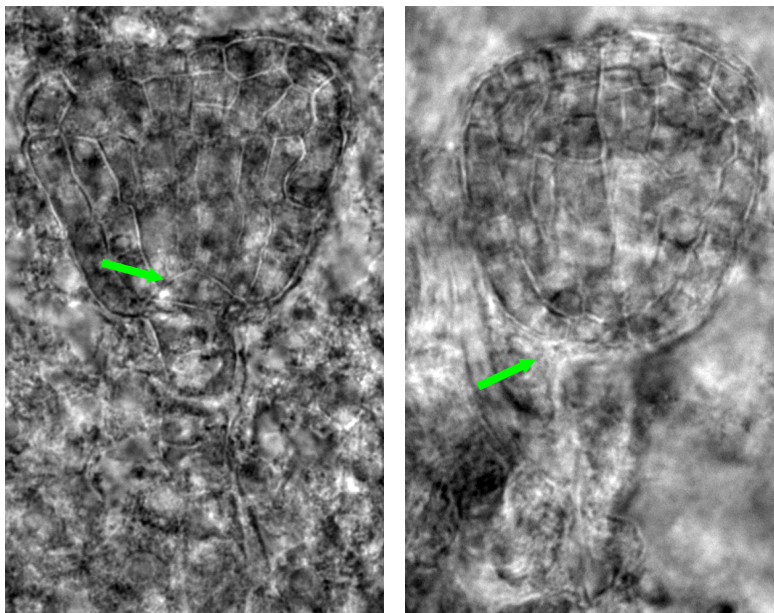


Figure IV-19. The abnormal embryo in late globular stage of *sksl,skss2,sku5* triple mutant. (A) embryo of Ws, (B) embryo of *sksl,skss2,sku5*.

In triple mutant, the lens-shaped cell, which has its destiny to be the primary root, was missed (pointed by green arrow).

At a later stage, various abnormalities can be observed as illustrated in Figure IV-20. Even within the siliques protruding structure resembling can emerge from immature seeds. In most cases the corresponding embryos are lacking a differentiated primary root primordia. Cotyledons and hypocotyls are usually formed but the shape of the embryo is altered. These defects can result from early alteration during embryo formation as shown Figure IV-19.

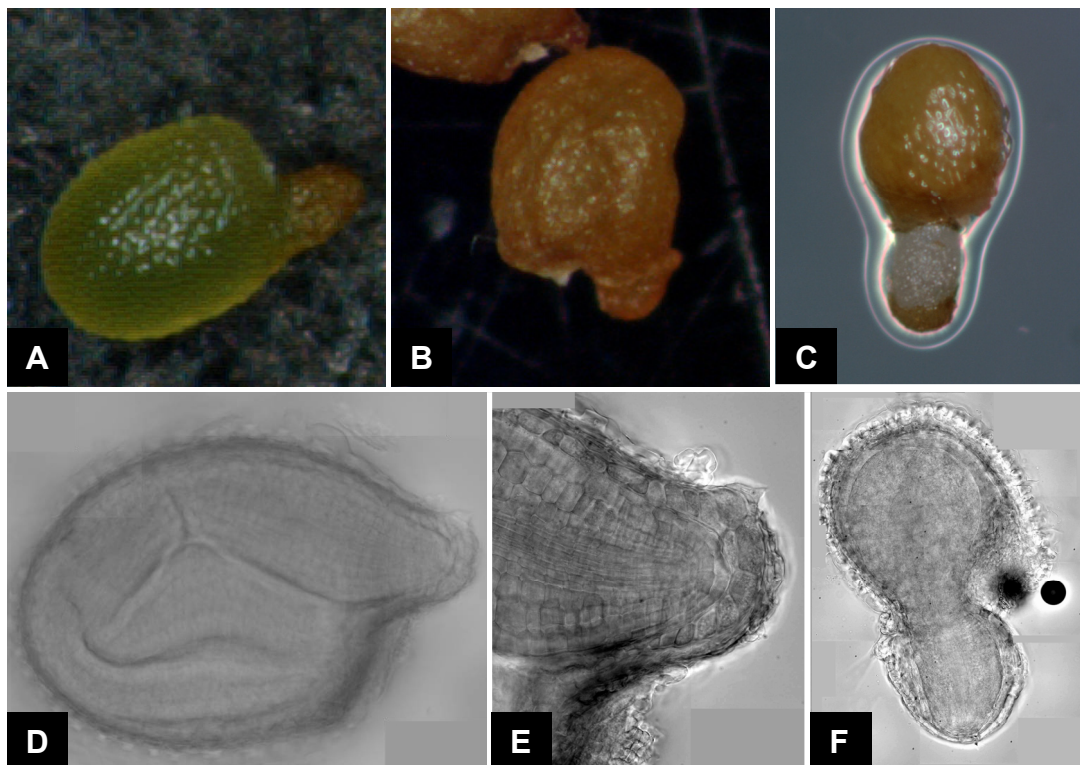


Figure IV-20 Abnormal embryo development in the triple mutant found in green siliques (A) immature seeds exhibiting abnormal shape. an hypocotyl-like structure is emerging from the immature seed. (B) dried seed with abnormal shape, (C) dried seed germinated on $\frac{1}{2}$ MS medium and showing emergence of the hypocotyl, this seedling missing the root. (D) Embryo with an altered morphology, the primary root is potentially missing (E) magnification of the hypocotyl/root tip from (D) (F) germinating seedling without root

These defects in embryogenesis reveal that SKS1, SKS2 and SKU5 are required for embryogenesis even if a small proportion of embryos bypass the deficiencies and develop normal embryo.

VI-2-2-2 SKS1, SKS2 and SKU5 in embryo orientation.

As more and more embryos were observed, we found that the root pole defects were not the sole alteration responsible for seed abortion and abnormality. More fertilized female gametophytes were observed to exhibit severe defect in orientation (Figure IV-21). These female gametophytes were swollen and appeared to be up side down facing the micropyle. Most of them failed to form an embryo (Figure IV-21B). A few of them succeed to form an embryo-like structure but with the wrong orientation (Figure IV-21C). These embryo-like structures can also be observed when opening green siliques. Seeds with cotyledon-like structure pushed out from the teguments are seen (Figure IV-21 D-F).

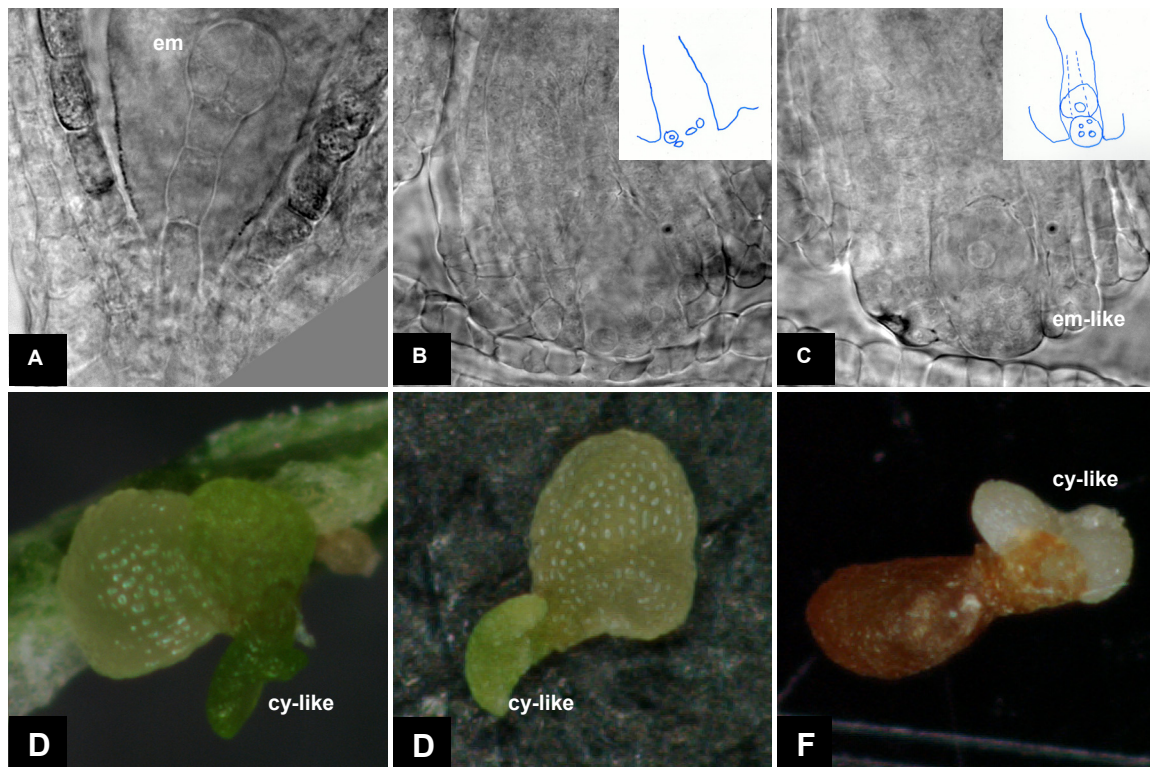


Figure IV-21 Embryo-like structure grow out of ovules.

(A) *Ws*, (B) female gametophyte with defect in polarity cannot form an embryo, (C) female gametophyte with wrong polarity and formed an embryo-like structure, (D-F) cotyledon-like structures grow out of seed coats in different stages. The cotyledon-like structures probably grew out through the micropyles. em: embryo; em-like: embryo-like structure; cy-like: cotyledon-like structure.

Sometimes, almost the whole embryos were outside of the seed coat, and only part of the cotyledon stay inside (Figure IV-22). It looks like that the embryo with wrong orientation developed through the micropyle. The schematic diagrams are shown in Figure IV-22D and E.

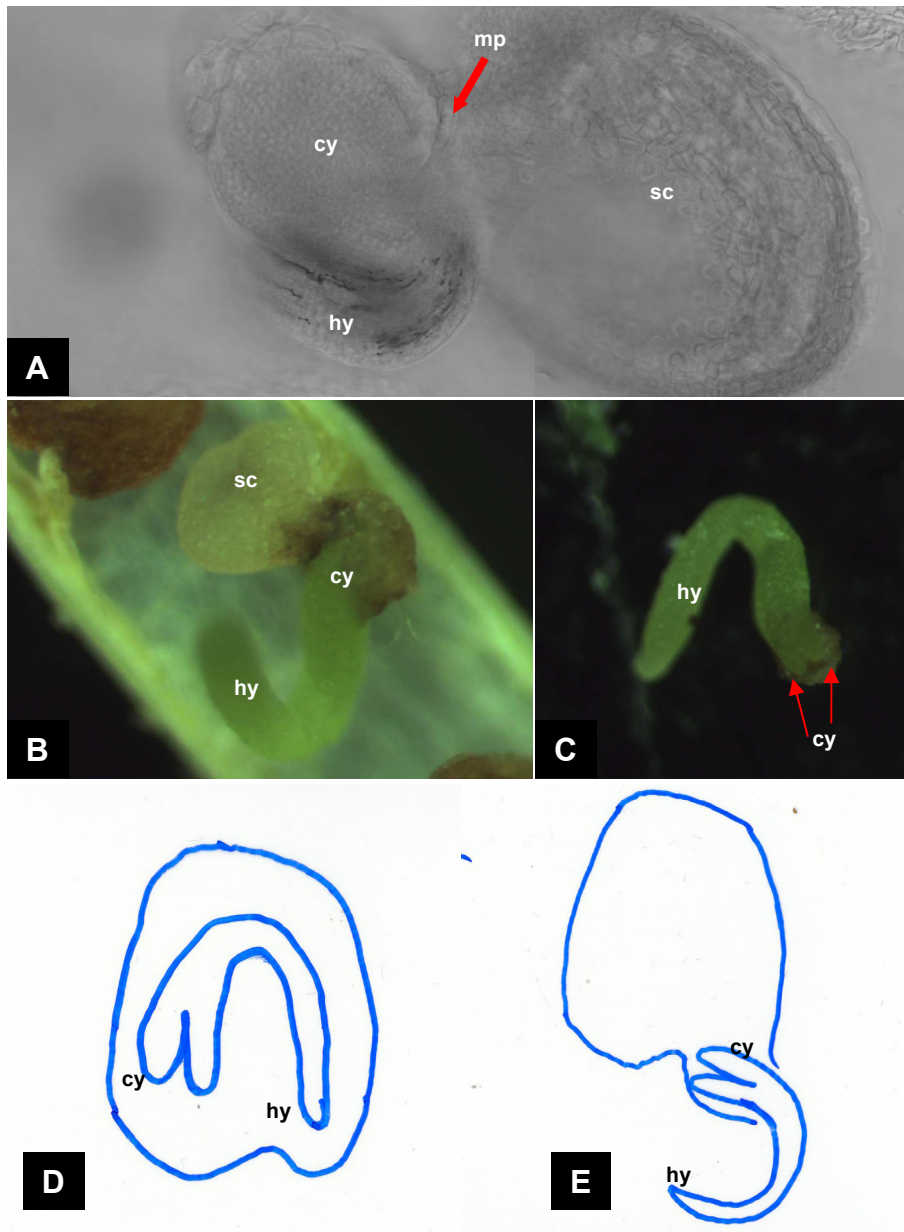


Figure IV-21. The whole embryos were almost developed outside the seed coat.

(A) Seed from *sks1, sks2, sku5* was cleared by Chloral Hydrate and observed under microscope; (B) seed of *sks1, sks2, sku5* in dissected siliques; (C) embryo in (B) was departed from seed coat, and the two cotyledons were pointed by red arrows; (D) *Ws* and (E) *sks1, sks2, sku5* the schematic diagrams of embryo development inside siliques.

sc: seed coat; hy: hypocotyl; cy: cotyledon; mp: micropyles.

These orientation defects explained why in siliques there are seeds exhibiting structures pushed out of seed coat. This appears to be different from an anticipated germination as reported for viviparous mutants.

Conclusion and Discussion

Surprisingly, nearly all the phenotypes we found in reproductive processes of *sksl,skss2,sku5* triple mutant resulted from alterations of orientation, both at cellular and embryo levels. It is worth notice that SKU5 was originally characterized as a GPI-anchored protein involved in directional root growth (Sedbrook et al., 2002)

1. In fertilization.

Male and female gametophytes were both expected to be involved in fertilization.

In Arabidopsis, to date, various work indicated that the female gametophyte, especially the synergid cells, are essential for pollen tube guidance. The misorganized female gametophyte in the triple mutant is potentially related alterations of the pollen tube guidance and pollen tube entry through the micropyle. The apparent variety of phenotypes of the *sksl,skss2,sku5* triple mutant suggests that there is not a single defined step or target that is affected during the reproductive process. Fertilization occurs, with a low efficient but some ovules can be fecundated indicating that pollen tube attraction by the female gametophyte happened. Similarly few embryos successfully develop to give rise to nearly normal seedlings. These data suggest rather random defects that become limiting enough with a rather high probability to impair or to block the fertilization or the embryogenesis. However not all the attracted pollen tubes can enter the female gametophytes through the micropyles even if they were attracted adequately. Twisted pollen tubes were found outside the micropyles, turning around but not entering, potentially because these micropyles were stocked by misorganized gametophyte cells.

Although the elongation of pollen tube *in vitro* was not measured, more seeds near the stigmas were produced indicating that the elongation of pollen tubes was reduced by the triple mutation. That could explain why the male gametophytes of *sksl,skss2,sku5* could fertilize the female gametophyte of *Ws* but with significantly low rate compared to *Ws* manual self-pollination.

2. In embryogenesis.

Obviously, the misorganized female gametophytes could affect the embryogenesis. And in this part, I just discuss the fertilized female gametophyte.

The egg cells or embryos might be displaced out of the seed coat through opened micropyles as they were growing when they were mis-oriented and localized at the bottom of the female gametophyte. Such alteration resulted in seed abortion.

Even though the egg cells or embryos were not displaced out of the seed coat, their orientation could be changed by the pressure of other misorganized gametophyte cells, like the central cell or synergid cells. That makes the embryos, or embryo-like structures grew out of seed coat through micropyles. Such abnormal behaviors were observed and explained that in some seeds, cotyledon-like structures grew out without resembling an anticipated germination within the silique.

In some cases, the misorientated embryo was stocked in the position of micropyle. It kept growing and the hypocotyl grew out of the seed coat through micropyle, then only the cotyledons were left inside. Interestingly, the cotyledon inside developed to a nearly normal shape, which is distinguished from the cotyledon-like structures outside of ovules.

These situations are described in Figure IV-23.

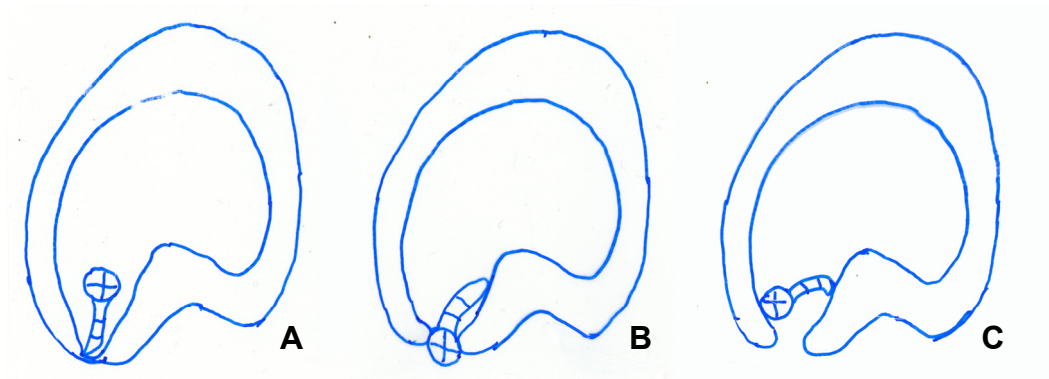


Figure IV-23. Embryo orientation of *sks1,sks2,sku5* mutant.

(A) normal embryo orientation, (B) embryo grow out of seed through micropyle, (C) embryo was stocked at the position of micropyle

Even coincidentally, the female gametophyte cells were at the right position and they could be fertilized properly, the formed embryos might also abort. A group of embryos were observed to be arrested in early stages. They exhibited normal divisions before arrest and closed micropyles. But the embryos were going to be arrested in very early stage, basically 8, or 16-cells stage.

Even though the embryos overcome the arrest in early stage, they might also exhibit abnormality with the absence of the lens-shaped cell thus without differentiated primary root primordia. This causes the rootless phenotype that was observed on a small proportion of germinated seeds.

Chapter V. Functions of GPI-anchored SKS and the roles of GPI anchors by overexpression analyses

Besides the reverse genetic tools, overexpression analyses are of importance for functional investigation. GPI-anchored SKS genes were introduced and overexpressed in wild type to explore the effect of an increased production of the proteins, so to learn more about their function.

To date, the role GPI anchor for the function of GPI-anchored protein in plant was not deeply studied. In our research, GPI-anchored *SKS* genes were modified and the sequence coding the hydrophobic C-terminal domain allowing further replacement by the GPI-anchor was cleaved. These modified genes were introduced and overexpressed also in wild type. Sub-cellular localization of the truncated SKS1, SKS2, SKU5 proteins was also interesting. So the constructs containing the truncated SKS sequences were fused to a fluorescent protein and used for transient assay.

The other member of *SKS* gene family, *SKS9*, which is far away from the clade of *SKU5/SKS1/2*, was also utilized to investigate the function of GPI anchor through addition of the omega domain sequence from SKU5 at C-terminus, and to explore the functional divergence between two distant members of the same family.

V-1 Tools for transient assay and *SKS* overexpression

V-1-1 *SKS9* was cloned from Arabidopsis

SKS1, *SKS2* and *SKU5* genes were cloned from the Arabidopsis when performing the protein interaction studies by Yeast two hybrid system, but not *SKS9*. Here, full length of *SKS9* was amplified from the cDNAs produced in Chapter II, and the primers are indicated in Table V-1.

Table V-1 Primers for amplifying *SKS9* from cDNA

GENES	Primers	cDNA Resource	Product length
<i>SKS9</i>	TGTCAAAGCGAGTATGTGCTG GTCTGAGTAGAGTCATTAAGGAGTG	Arabidopsis seedlings	1678 bp

Following the same protocol as described in Chapter II, the *SKS9* gene was cloned in pCR2.1® vector and then sequenced.

V-1-2 SKS genes modifications

Proper gene modifications were firstly performed on *SKS1*, *SKS2*, *SKU5* and *SKS9*, and then they were introduced in binary vector with strong promoter and fluorescent label. These modified genes were used for producing overexpressors in plants.

Because GatewayTM technology was utilized for building constructs, modification was performed at BP reaction by adapter PCR protocol (BP reaction and adapter PCR protocol were described in chapter II).

V-1-2-1 Modifications of *SKS1*, *SKS2* and *SKU5*

Two kinds of cloning were performed for these genes: 1, Full length cDNAs with signal peptide at the N-terminus and omega domain at the C-terminus followed by a STOP codon ; 2, Genes with signal peptide at the N-terminus and without omega domain and STOP codon at C-terminus in order to be fused with the fluorescent gene localized in binary vector and ended by a STOP codon.

In Chapter “*in silico analyses*”, the C-terminal hydrophobic domains and cleavage sites of *SKS1*, *SKS2* and *SKU5* were indicated. When the C-terminal hydrophobic domain was absent, the GPI anchor was not supposed to be synthesized in mature protein as the process of modification is impaired.

Then proper primers with attB1/2 adapters for the first amplification of BP reactions were designed (Table V-2) and the amplifications were performed as indicated in Figure V-1. The sequence correspondence to adapters is in red and for genes is in black. The STOP codons are in bold.

Table V-2 Primers for *SKS1*, *SKS2* and *SKU5* modification

Modified Genes	Primes	Templates
<i>SP:SKS1</i>	5'- AAAAAGCAGGCT TCATGGCGGCGACTTGT-3' 5'- AGAAAGCTGGGT TCAGCAAAATCTGAAC-3'	pCR2.1- <i>SKS1</i>
<i>SP:SKS1Δω</i>	5'- AAAAAGCAGGCT TCATGGCGGCGACTTGT-3' 5'- AGAAAGCTGGGT GGTGATGTTGTTTCCTT-3'	
<i>SP:SKS2</i>	5'- AAAAAGCAGGCT TCATGGCGGCTACTGAT-3' 5'- AGAAAGCTGGGT GTCAGCAAAAGGACGA-3'	pCR2.1- <i>SKS2</i>
<i>SP:SKS2Δω</i>	5'- AAAAAGCAGGCT TCATGGCGGCTACTGAT-3' 5'- AGAAAGCTGGGT GGTGATGTTGTTTCCTT-3'	
<i>SP:SKU5</i>	5'- AAAAAGCAGGCT TCATGGATTTGTTCAAG-3' 5'- AGAAAGCTGGGT TCAATGCTGAAGCATC-3'	pCR2.1- <i>SKU5</i>
<i>SP:SKU5Δω</i>	5'- AAAAAGCAGGCT TCATGGATTTGTTCAAG-3' 5'- AGAAAGCTGGGT GTGAAACCTTCTGTGG-3'	



Figure V-1 SKS1, SKS2, SKU5 gene modifications.

The backbone of the genes were separated into different colors depending on the regions they encoded. From left to right, there is N-terminal signal peptide (blue), mature protein (dark blue), the hydrophobic region (olive) coding sequence, and stop codon (black) respectively. The site between mature protein and hydrophobic region coding sequence is the cleavage site as GPI-anchor was synthesized. The primers were indicated as red arrows with additional attB adapter in green, which utilized for gateway technology. Amplified by P1 and P2, the fragment would encode full length SKS protein with GPI anchor at C-terminus. Because of the presence of stop codon, these genes would not fuse with the fluorescence protein genes included in destination vectors. Amplified by P1 and P3, the fragment would encode mature SKS protein with signal peptide at N-terminus, but without GPI anchor at C-terminus. Because of the absence of stop codon, these fragments would fuse with the fluorescence protein genes which are included in destination vectors.

V-1-2-2 Modification of *SKS9*

In our research, *SKS9* that do not include a C-terminal hydrophobic domain and is not predicted to be modified with a GPI-anchor was cloned in fusion with the fluorescent protein. In addition the omega domain coding sequence of *SKU5* was fused at C-terminus of *SKS9* coding sequence in order to analyse whether the Pm localization of the protein would affect the function.

The modification is indicated in Figure V-2 (A-C) and the primers designed are shown in Table V-3. Sequence correspondence to adapter is in red, to genes is in black and STOP codon in bold.

Table V-3 Primers for fusing omega domain coding sequence from *SKU5* with *SKS9*

attB1-P1	5'- AAAAAGCAGGCT TTCATGTGCTGGTGGCTA-3'
attB2-P2	5'- AGAAAGCTGGGT TCAATGCTGAAGCATC-3'
P3	5'-AACACACCACTCCTTCGTCGGCATCGAA-3'

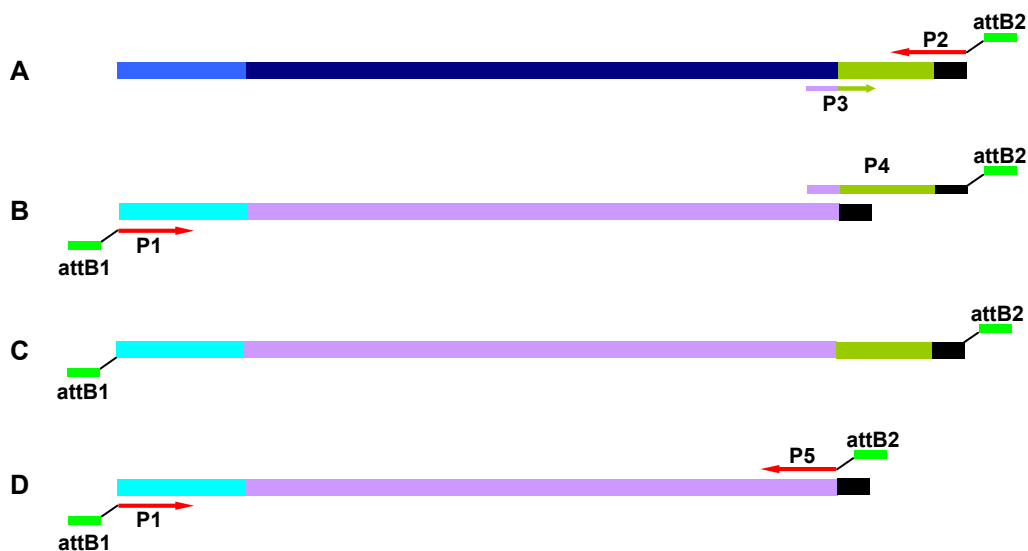


Figure V-2 *SKS9* gene modification.

(A) Omega domain coding sequence was amplified from *SKU5*, (B) *SKS9* gene and P3-P2 amplification product from *SKU5* (C) modified *SKS9* gene with omega domain coding sequence from *SKU5*, (D) modified *SKS9* gene without omega domain coding sequence. Coding sequence of signal peptide (light blue), mature protein (*SKU5* in dark blue, *SKS9* in purple), hydrophobic region (olive) and stop codon (black) were indicated in different colours. Sequences of primers were indicated in Table V-3 and V-4.

To fuse *SKS9* with fluorescent genes within binary vector, *SKS9* was modified as described in Figure V-2D, where the STOP codon was removed. Primers designed were in Table V-4. Sequence correspondence to adapter is in red, to genes is in black.

Table V-4 Primers for fusing *SKS9* with fluorescent genes

attB1-P1	5'- AAAAAGCAGGCT TCATGTGCTGGTGGCTA-3'
attB1-P5	5'- AGAAAGCTGGGT GAGGAGTGGTGTGTTT-3'

SKS9 without STOP codon for C-terminal fusion with a fluorescent protein were generated.

To confirm the GPI modification, the amino acid sequence of *SKS9* fused with omega domain from *SKU5* was analyzed by GPI predictors (PredGPI). Data shows that this fused protein would be modified to become a GPI-anchored protein.

V-1-3 Vectors for SKS overexpressors

BP reaction of Gateway® technology was utilized to build the constructs, and pDONR207, which has gentamycin resistance, was chosen as shuttle vector. After the second amplification was performed by adapter primers, the modified *SKS* fragments were cloned in pDONR207 by BP reaction and introduced in *E.coli*, the constructs were sequenced to verify that they did not contain mutations and that the recombination sites were as designed.

The constructs with the right fragments were cloned in pEARLEY102 by LR reaction in *E.coli*. Considering the *sksl,sku5* mutant has also Basta resistance, which is the same as pEARLEY102 exhibits in plants, pMDC83 vector with hygromycin resistance was chosen for transforming mutant plants.

The maps of vectors utilized are shown in Figure V-3.

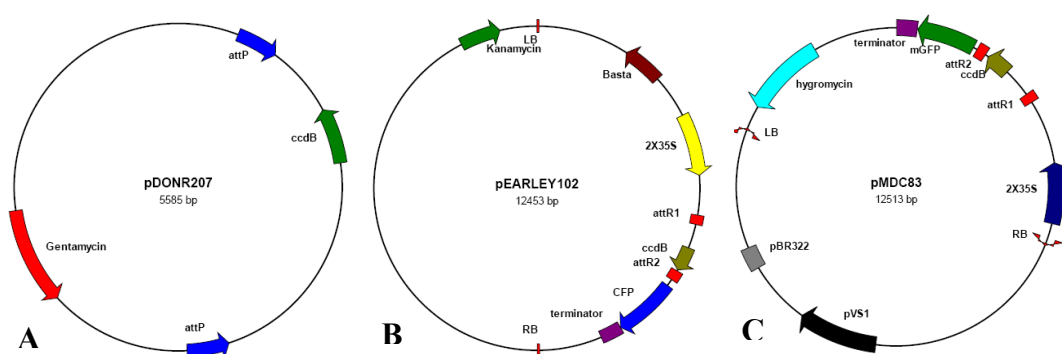


Figure V-3 Vectors with gateway technology utilized for SKS overexpression.

(A) pDONR207, (B) pEARLEY102 with Cyan fluorescent protein fusion, (C) pMDC83 with Green fluorescent protein fusion.

The genes for the fluorescent proteins CFP and GFP were present at the 3'-terminus of the insertion site in pEARLEY102 and pMDC83. In both cases the expression is under the control of a double *35S::CaMV* promoter that allows a strong and rather broad expression. As described in Figure V-1 and Figure V-2, the C-terminal translation fusions with the genes of the fluorescent protein were achieved for the truncated versions of SKS1, SKS2 and SKU5 missing the hydrophobic domain, and for *SKS9* without the stop codon. These constructs were named *SKU5* or *SKSΔω:CFP/GFP*. On the contrary, fragments with the omega domain still have their stop codon. Despite the interest to have reporters also for the full length proteins, no fluorescent or tagged version was produced as it was not possible to use straight forward N-ter or C-ter fusions due to the leader peptide and hydrophobic C-terminus, respectively. However, a line expressing SKU5-GFP with the GFP inserted between the leader peptide and the N-terminus of the mature protein was obtained from J. Sedbrook (Sedbrook et al., 2002) and used in comparison with the truncated protein.

After all the constructs were introduced into binary vectors pMDC83 or pEARLEY102, the plasmids of each construct were prepared following the same protocol described in ‘chapter II’. Then the plasmids were introduced in *Agrobacterium* line *Agl-0* (described in ‘Method’).

Transformed *Agrobacteries* were selected on plates containing proper antibiotics and resistant colonies were chosen and amplified.

1µl culture was lysated by boiling for 5 minutes and PCR amplified with the primers provided in Table V-5 for confirming the insertions. The positive colonies were conserved utilized for the further investigation.

Table V-5 Primers for confirming insertions

Genes	Primers	Length of Products (bp)
<i>SKS1</i>	5'-GGGATGCCAGATGGAGTCCTCA-3' 5'-TGTGGCGTCTTGGTCCATGGTT-3'	288
<i>SKS2</i>	5'-ACTTGGGATGCCCCGATGGAGT-3' 5'-GGGAGGTGTAGCGACCCTCAGT-3'	215
<i>SKU5</i>	5'-ACCACACGGCTTTGAGGAAGGC-3' 5'-CAACCCGAGCACTCGCGACA-3'	369
<i>SKS9</i>	5'-TCACCATGGACCAGCCTGACCA-3' 5'-CCTTGGCCCAGACGCGTTA-3'	224

V-2 GPI-anchors for localization by transient assay

Before transformation in *Arabidopsis*, the construct *SKU5ΔωCFP/GFP* with fluorescent gene fusions were introduced in tobacco leaves by transient infiltration (See 'method') to check the constructs and also investigate the subcellular localization of SKU5 without GPI anchor.

In original paper of *SKU5*, the GPI anchored SKU5GFP was localized at the plasma membrane and partly in the cell wall (Sedbrook et al., 2002). In our research, SKU5 without GPI anchor was observed with an irregular distribution in the cytosol that underlines the shape of the epidermis cells as it is present as a thin layer between the plasma membrane along the cell wall and the vacuole. In addition, some cytosolic bundles are occasionally observed across the cells. The *SKU5ΔωGFP* still has the leader peptide at the N-terminus and should enter the ER (Figure V-4A). The plasmolysis after 0.8M mannitol treatment revealed that most SKU5ΔωGFP protein stay inside the cell (Figure V-4B).

This localization is distinct from the one reported for GFP fused only with a signal peptide, that is found in the extracellular space, the ER and around the nucleus (Fan et al., 2001). It suggests that without the GPI-anchor, SKU5 doesn't exhibit the same behaviour as the GPI-anchored protein and not also as a normal secreted protein (as GFP). The GPI anchor seems to be required for plasma membrane localization of SKU5.

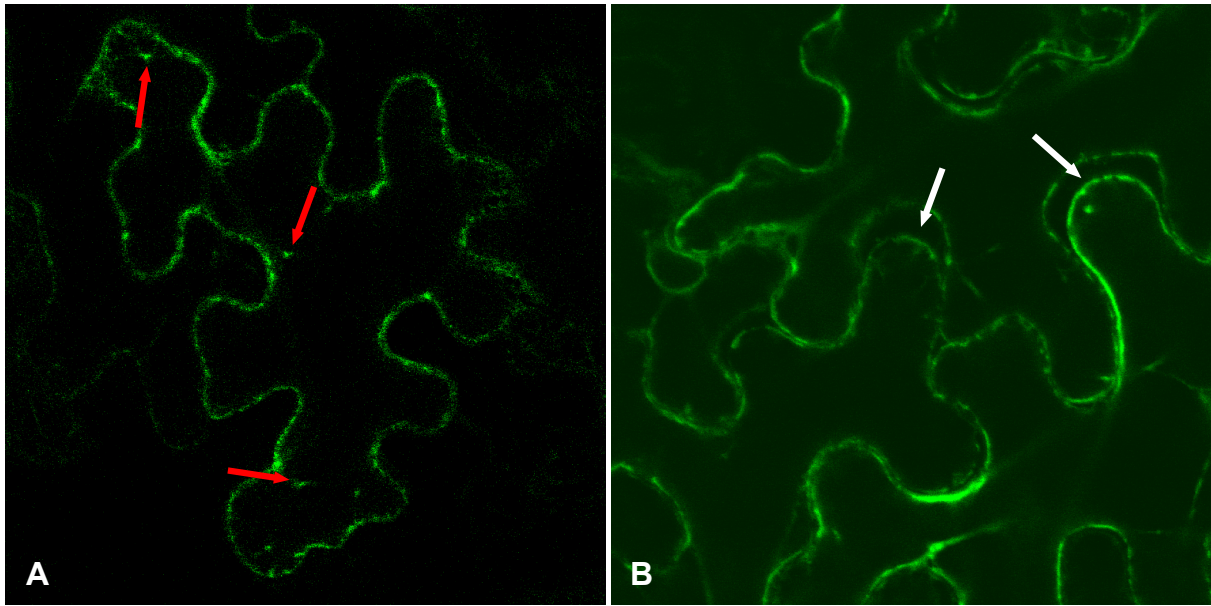


Figure V-4 localization and transport of SKU5Δω in tobacco leaves.

pMDC83:35S:SKU5Δω::GFP was introduced into tobacco leaves by infiltration for transient expression.

(A) Observation under SP2 Cofocal System, (B) observation under DMI-6000 microscope system with 0.8M Mannitol treatment.

SKU5Δω::GFP is mainly detected in the ER. The spots pointed by red arrows highlight intracellular bundles of cytosol containing dots of SKU5Δω::GFP protein.

With 0.8M mannitol treatment, the plasmolysis happened, which are pointed by white arrows.

ABP1GFP and *SKU5/SKS1/SKS2* were co-transformed into tobacco leaves together by transient assay. Their localizations were observed under fluorescent microscope. But the relevance between ABP1 localizations and *SKU5/SKS1/SKS2* overexpression was never found. In Figure V-5B, *SKU5* was transiently co-overexpressed with ABP1:GFP.

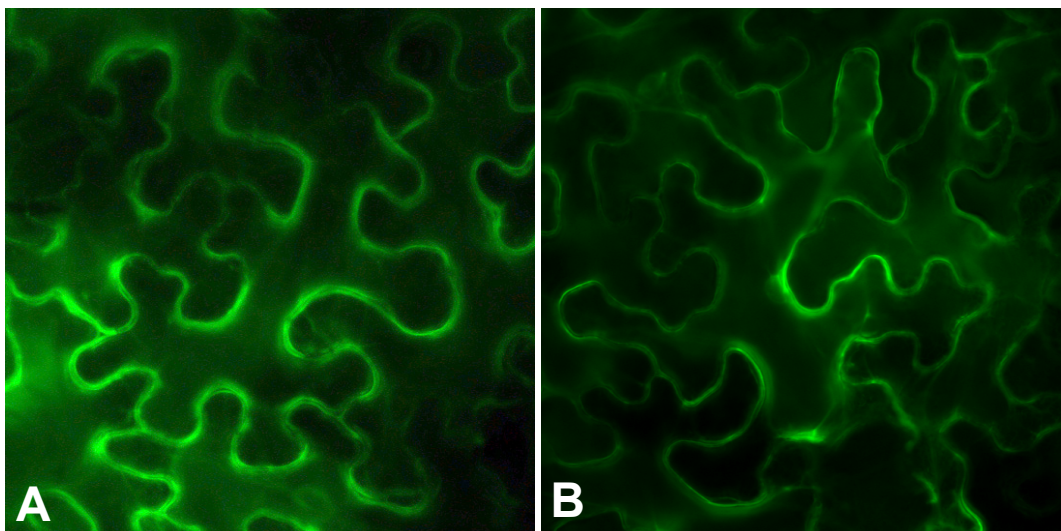


Figure V-5 Co-transformed ABP1GFP and SKU5 in tobacco leaves by transient infiltration assay.

(A) ABP1GFP was introduced in tobacco leaves by transient assay. **(B)** ABP1GFP and SKU5 were co-introduced in tobacco leaves by transient assay.

V-3 Overexpressors in *Ws* background acquisition and analyses.

As all the mutants were all analyzed within *Ws* background, we introduced the constructs with full length or truncated sequences for overexpression into *Ws* ecotype.

V-3-1 Overexpressors acquisition.

Agrobacterium containing constructs within pEARLEY102 binary vectors were utilized and floral dip transformation assay was performed for *Ws* ecotype plants transformation (Harrison et al., 2006).

T1 seeds were collected and selected on plates containing 7.5mg/L Basta. Resistant seedlings were transferred into soil and T2 seeds were collected and sowed on medium containing Basta. After growing and flowering in soil, the progeny was again selected on Basta selective medium to identify homozygous lines (Figure V-6).

In total, 3 lines of *SKS1*, 2 lines of *SKS1ΔωCFP*, 6 lines of *SKS2*, 8 lines of *SKS2ΔωCFP*, 4 lines of *SKU5*, 4 lines of *SKU5ΔωCFP*, 7 lines of *SKS9+ω*, and 4 lines of *SKS9CFP* independent resistant homozygous were obtained.

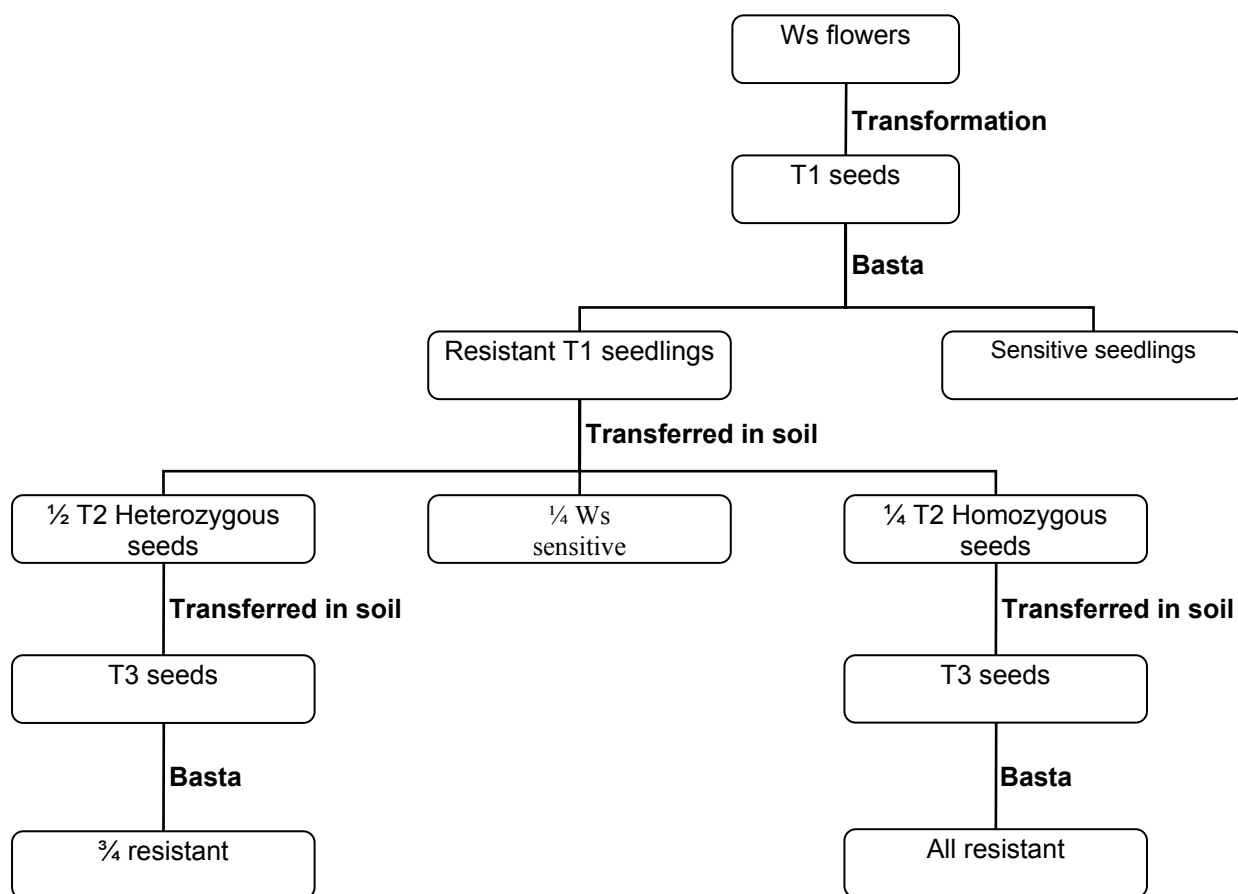


Figure V-6. To obtain homozygous of *SKS* overexpressor in *Ws*.

V-3-2 Expression levels of *SKS* Overexpressors in *Ws* background.

Although resistant homozygous plants were acquired, to confirm that these resistant plants were truly overexpressing the corresponding *SKS* constructs in plants, RNAs were extracted from 5-day-old seedlings for 2 to 3 homozygous transformants of each and the expression analysis was performed by real time RT-PCR. Primers utilized were indicated in Table V-6.

Table V-6 Primers for RT PCR in overexpressors

Genes	Primers	Length of Products
<i>SKS1</i>	5'-CGGATCACAAACCCCGAGGAGGAT-3'	171 bp
	5'-CACCGAGGCGAGCAACACCATTAG-3'	

<i>SKS2</i>	5'-ACCCTGAGGAAAACGGAAGTACGG-3' 5'-TGTGGCCGAGCTGTGATGTTGTTC-3'	104 bp
<i>SKU5</i>	5'-AAGGTCTCTTAGGGAAATCAAGC-3' 5'-CAACGCTTAATGGCATATCGT-3'	105 bp
<i>SKS9</i>	5'-TCACCATGGACCAGCCTGACCA-3' 5'-CCTTGGCCCAGACGCGGTTA-3'	224 bp
<i>CFP/GFP</i>	5'-AGGGCTATGTGCAGGAGAGA-3' 5'-CTTGTGGCCGAGAATGTTTC-3'	152 bp

Expression levels are shown in Figure V-7. For translational fusions with a fluorescent protein, specific gene primers or CFP/GFP primers were used to detect the transgene. Primers utilized were indicated above each chart, and lines were indicated at the x-axis.

Amongst the lines that were checked, most of them exhibited a significant increase in the expression of the gene that was introduced by construct with the exception of *SKS1ΔωCFP*. No matter primers for *SKS1* or *GFP*, no significant gene expression was found (Figure V-8). Although the transformations were performed twice, no *SKS1ΔωCFP* overexpressor plants were validated.

The others could be considered as overexpressors, however with various degrees of expression.

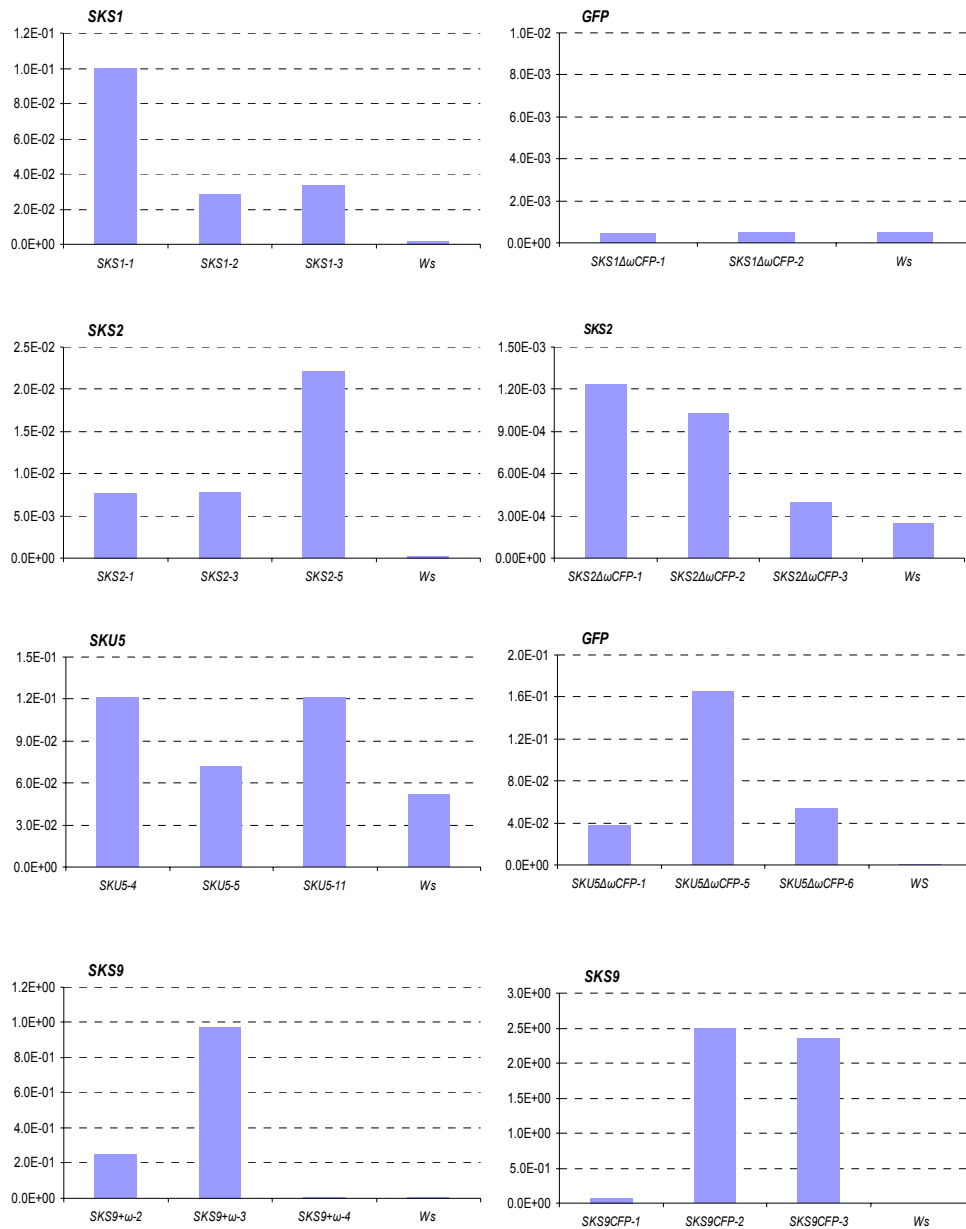


Figure V-7 Expression levels of SKS overexpressors within *Ws* background.

RNAs were extracted from 5-day-old seedlings of 3 alleles per constructs. Then real-time RT-PCRs were performed. The data was normalized by ACTIN2-8.

Genes detected were indicated at the tops of each chart. X-axis: Overexpressors Alleles, Y-axis: Actin Units.

V-3-3 Phenotype analyses of overexpressors.

Data extracted from null mutant analyses suggest that *SKS1* and *SKU5* genes were mostly functional in orientation of root cells, whereas *SKS1*, *SKS2* and *SKU5* were collectively important for pollen tube guidance and embryogenesis. Single *sku5* mutant exhibited twisted root and root left slanting; *sksl*, *sku5* double mutant exhibited increased twisted root but no slanting, and lower fertilization rate; the triple mutant exhibited defects in fertility and embryogenesis besides that were exhibited in *sksl*, *sku5* double mutant.

Although all of the transformants were grown on plates and in green house until seeds were collected, no significant phenotype was found. 2 transformants of each construct with different expression levels were picked out for further investigation.

The primary data should be root length measurement. Root lengths of 5-day-old seedlings grown under constant light were measured.

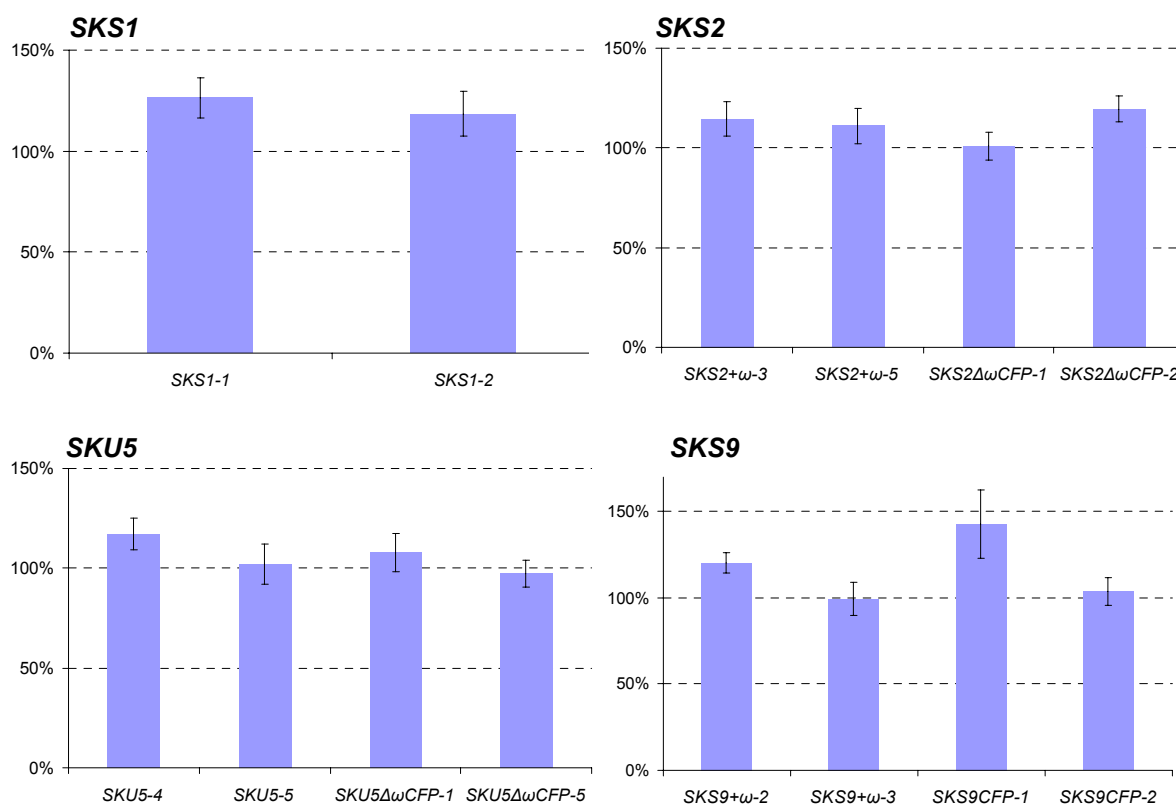


Figure V-6. Root length of *SKS* overexpressors (with and without GPI anchors)

20 seeds were sowed on 0.5MS medium and grew under constant light for 5 days after 2 days of stratification.

x-axis: Overexpressor lines; y-axis: root length of overexpressors alleles/*Ws* %.

Most of the lines didn't exhibit significant differences compared to wild type that can be correlated with the expression of the transgene. Although some of the overexpressors exhibit slightly longer roots than Ws, no phenotype relative to orientation, such as root twist, was found. The seed production was also normal.

The absence of obvious alterations of overexpressor lines made us very difficult to extract useful information helping further understanding of SKS1, SKS2 and SKU5 function.

V-4 Overexpressors in *skl1,sku5* background acquisition.

skl1, sku5 double mutants cause severe defects in both roots and seed production, which phenotypes were easy to be observed. We tried to introduce the different constructs in pMDC83 vectors into *skl1,sku5* mutant to determine which of these constructs would be able to complement the defects of the double mutant. The objective was also to better discriminate between the function of proteins exhibiting or not the GPI-anchor and to investigate whether the more distant SKS9 gene would be able to complement the double mutant when the SKU5 omega domain was added. The transformation was achieved and the transformed mutants are under selection but it has not been yet possible to characterize these plants.

Conclusion and Discussion

1. GPI in localization

By transient overexpression, we introduced and made the SKS Δ GFP protein visible in tobacco leaves. Most of the fluorescence was found to be present as a thin layer in cytosol along the PM. But according to the SKU5 original paper, SKU5GFP with GPI anchor was mostly found at the PM and cell wall.

The distinguished localization suggests that, the PM-localization of GPI-anchored protein is dependent on the GPI-anchor.

Interestingly, the SKS without GPI anchor was not mostly secreted out of cells as other secreted proteins but stay in cytosol. It suggests an unclear signal or pathway to maintain these proteins inside of the cell.

2. Co-localization of ABP1 and SKU5/SKS

Co-localization of fluorescent ABP1 and SKU5 by transiently expressed in tobacco leaves didn't provide any evidence for the potential interaction between them.

To extract more information, the localization of fluorescent ABP1 by transient overexpression in *skt1,skt2,sku5* triple mutant seedlings should be analysed.

3. Functional analyses by SKS overexpression

As no phenotype was found in *SKU5GFP* overexpressor, it's not very surprising that no phenotype was found within any SKU5/SKS overexpressors.

It's very difficult to conclude only by these data.

4. Functional analysis of GPI-anchors

We had expected to introduce SKU5/SKS Δ GPI in *skt1,sku5* background, and find out whether these GPI absent protein could complement the defect. But unfortunately, I didn't have enough time to finish this.

Chapter VI Discussion and Perspectives

In the ‘introduction’, we discussed that ABP1 was localized at the outer surface of the PM indirectly, and that a GPI-anchored protein named CBP1 was supposed to interact with ABP1 and possibly to dock the protein at the PM in maize. It was hypothesized that CBP1 could act as a carrier helping ABP1 to reach and be positioned at the outer surface of the plasma membrane or to be directly part of an auxin receptor complex (Shimomura, 2006; Tromas et al., 2010).

By ‘*in silico* analyses’, we know that *SKU5* and *SKS* genes are homologous genes of *CBP1* in Arabidopsis. They belong to a rather ancient gene family containing 19 members. And they encode proteins with conserved amino acid sequences and domains but including mutations impairing copper-binding and oxidase activity. *SKU5*, *SKS1*, *SKS2* and *SKS3* encode proteins with the highest similarities with CBP1. Despite the relatively high homology between the members, *SKU5*, *SKS1*, *SKS2* are the only three members predicted to be modified at their C-terminus by substitution of the hydrophobic domain by a GPI anchor as CBP1, in which *SKS1* and *SKU5* were confirmed by proteomic and genomic analysis (Borner et al., 2003).

The other members are unlikely to get this post-translational modification, but according to recent proteomic data that were kindly provided to us by Wojciech Majeran (ISV, protein maturation, cell fate and therapeutics team), not only *SKS1*, *SKS2*, *SKU5*, but also *SKS3* and possibly *SKS16* were found in PM enriched fractions despite the absence of C-terminus hydrophobic domain that could be replaced by GPI anchor (Figure 1).

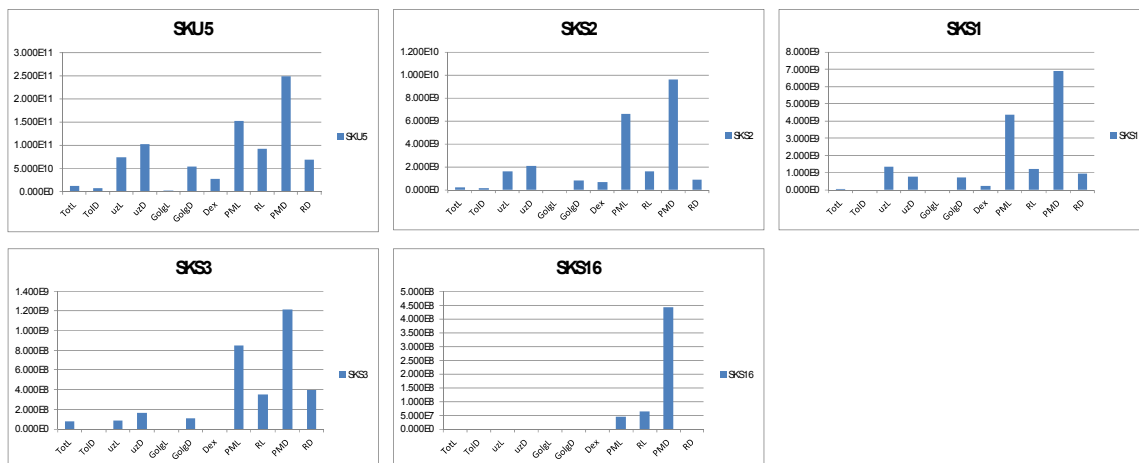


Figure 1. SKS protein in Arabidopsis cell cultures [provided to us by Wojciech Majeran (ISV, protein maturation, cell fate and therapeutics team)].

L: light grown; D: dark grown; Tot: total fraction; μz: microsomal fraction Golgi + part of ER

Dex: dextran partitioning PM enriched; R: raft

These proteomic analyses were performed using Arabidopsis cell cultures where a large number of the SKS family are co-expressed. Importantly, the PM localization of *SKU5*, *SKS1* was confirmed as previously reported in proteomic approaches (Borner et al., 2003) and *SKS2*, that is also expressed, is clearly associated to PM fractions. In these cells the expression of *SKS16* is extremely low thus making the partitioning more uncertain. Interestingly, *SKS3* behaves to the same subfamily as *SKU5*, *SKS1* and *SKS2*. As for the mutants of these two latter genes, *sk3* mutant plants did not exhibit any significant phenotype. If it is confirmed, *SKS3* is associated to the PM while no GPI anchor was predicted for this protein. Either the prediction program failed to predict such modification or *SKS3* interact with the membrane through another mechanism that would be very interesting to explore. It can also be hypothesized that *SKS3* without its own GPI anchor forms a dimer with one of the other member of the subfamily. Yeast two hybrid was not successful to demonstrate ABP1-CBP1 interaction but weak interaction was found between CBP1 subunits. Heterodimers with close relative of *SKU5* might be formed. This hypothesis can be checked by Y2H. An alternative approach would be to develop BiFC approach in Arabidopsis cells or in tobacco leaves.

The same large scale proteomic approach also revealed the partitioning of other SKS members in two categories. *SKS5*, *SKS7*, *SKS8*, *SKS12*, *SKS17* are not associated to membrane fraction at all whereas *SKS4*, *SKS9*, *SKS10* and *SKS6* are associated to endomembranes, potentially golgi and/or ER. These data suggest that there are at least three distinct subcellular localizations for SKS members, thus reinforcing divergences within the family and suggesting distinct functions.

1. Interaction between ABP1 and GPI-anchored SKS/CBP1.

GPI-anchored SKS proteins exhibit some probabilities to interact with ABP1, but none of direct or indirect conclusive evidence was found from neither yeast two hybrid or *sk3* mutation analysis, respectively.

The negative results extracted from yeast two hybrid system indicated several possibilities:

- a. There is no direct interaction between ABP1 and GPI-anchored SKS/CBP1.

Considering the CBP2, which was also identified with the same ability to bind C-terminus synthesized peptide of ZmABP1 (Shimomura, 2006), but was not supposed to be the ABP1 binding protein because of its cytosolic localisation, there is a risk that CBP1 is not the true ABP1 binding protein and the reported interaction was an artefact.

- b. The modification of GPI anchor affects the interaction.

As described in the ‘introduction’, the GPI anchors might affect conformation of the whole protein and function of these proteins. In yeast two hybrid system, the GPI anchor had to be cleaved, which might affect the folding of the protein and potential its ability for binding ABP1.

c. The production or conformation of ABP1 might affect the interaction.

The conformation of ABP1 is changeable, which depends on auxin-binding, pH or redox conditions (David et al., 2001; Woo et al., 2002; Bertosa et al., 2008) . In yeast nucleus where the potential interaction happened, the environment must be different from the ER or from the outer surface of plant cells where the interaction with ABP1 should happen. Especially the redox conditions are often evoked as responsible for alteration of protein folding in yeast and we failed to detect ABP1 dimerization in Y2H.

d. The interactions need the presentation of a third component.

Very recently, the identification of a series of 4 leucine-rich repeat receptor-like kinase proteins as interactors of ABP1 at the plasma membrane was reported in a commentary following the last auxin meeting in December 2012 (Strader and Nemhauser, 2013). ABP1 and LRR-RLK might form the function receptor unit at the plasma membrane. This does not exclude a contribution of CBP1/SKU5/SKS1 but involves at least a third component in the interaction.

But interestingly, the dimers of SKU5 and CBP1 were found in yeast two hybrid system.

The indirect evidence extracted from the study of *skt1,sku5* and *skt1,skt2,sku5* mutants, where the expression patterns of auxin response genes and critical cell cycle relative genes were different from alterations in ABP1 conditional loss of function, also cannot support the hypothetical interaction between ABP1 and these GPI-anchored proteins.

To investigate a possible effect of ABP1 interaction with members of the SKU5/SKS family, *skt1,sku5* or *skt1,skt2,sku5* mutants might be nice tools to observe the localization of ABP1 by transient assay or overexpression. As the *skt1,skt2,sku5* is mainly sterility, *skt1,sku5* should be utilized for stable overexpression. An ABP1 translational fusion might be used for such analyses. A line overexpressing an ABP1-GFP fusion can be crossed with the double mutant. An ABP1-Eos construct was also built during the thesis in this perspective, however the recombinant protein failed to be photoconvertible, potentially because Eos was inserted within the ABP1 sequence, in a flexible loop similarly to the ABP1-GFP construct (Robert et al., 2010). Another constraint is that to detect ABP1-GFP fusion, it was driven by a 35S

CaMV promoter otherwise it is too weakly expressed to be detected. Such overexpression might have an effect on ABP1 sub-localization.

2. The redundancy of *SKS1*, *SKS2* and *SKU5* genes:

Nearly all the results obtained by mutant crossing strongly suggest the redundancy of these three GPI-anchored *SKS* genes.

The additional *SKS1* mutation to *SKU5* mutation aggravates root phenotypes of *sku5* single mutant whereas no significant phenotype was not found in *sksl* single mutant; the additional *SKS2* mutation in *sksl,sku5* double mutant exhibits phenotypes which were neither found in the single *sksl* mutant nor in double mutants *sksl,sksl* or *sksl,sku5*.

In roots, *SKU5* was expressed at a much higher level than *SKS1*, and *SKS1* was itself expressed much higher than *SKS2*. It is likely that the *SKU5* gene can compensate the absence of functional *SKS1* and *SKS2* genes, and *SKS1* can only compensate the mutation of *SKS2*. In reproductive organs, these three genes were highly expressed with not so much difference. Defects in fertilization and seed development were exhibited only when the triple mutation occurred, suggesting that each gene is equally important, can replace each other and are redundant. The dramatic reduction in seed production that was only found in the *sksl,sksl,sku5* triple mutant could be explained by their strong co-expression and functional redundancy in reproductive organs.

However, with a low efficient it was possible to obtain triple mutant homozygous seedlings that were viable and exhibited a phenotype resembling the one of the double *sksl,sku5* mutant. Taking into account that at least a fourth member of the family, *SKS3*, can be found at the plasma membrane, it is possible that the expression and function of this protein can occasionally bypass the absence of the three others. Unfortunately the PM localization of this protein was not known at the beginning of this work and the *sksl* mutant was not included in the genetic approach. However, *sksl* mutants were only available in Columbia ecotype, thus complicating the analyses of plant phenotypes if combined with Ws mutants.

sksl,sksl,sku5 triple mutant is mostly sterile, and is very difficult to be used for crossing or transformation. To investigate a possible functional redundancy with non-GPI-anchored members, complementary analyses in *sksl,sku5* mutant should be performed by overexpressing non-GPI-anchored proteins exhibiting an additional C-terminal hydrophobic domain conducting to modification and addition of a GPI anchor. Such experiment was initiated, notably with *SKS9* and addition of the *SKU5* omega domain but unfortunately few

primary transformants were obtained and time was missing to select and characterize these plants.

3. *SKS1*, *SKS2* and *SKU5* genes were mostly involved in orientation:

All the phenotypes caused by *SKS1*, *SKS2*, *SKU5* mutations strongly suggest that they are involved in orientation at the cellular or organ levels.

- a. *sku5* mutation caused the root twist and root slanting (Sedbrook et al., 2002).
- b. *sksl,sku5* mutation caused root files misorientation aggravating the root twist caused by *SKU5* mutation.
- c. *sksl,sksl,sku5* mutation caused the misorientation of female gametophyte, which might effect the pollen tube guidance and embryo development.

But how the misorientation occurs is still unclear. The alteration of cytoskeleton should be studied by visualizing cytoskeleton-relative proteins.

Considering this orientation defect, it would be also interesting to investigate whether the loss of function of *SKU5*, *SKS1* and *SKS2* would affect the localization of polarly localized proteins, like the efflux carriers PIN proteins. These proteins are involved in the orientation of the flux of auxin, and play essential role in the orientation at the cellular level. In collaboration with the group of J. Friml (Vienna), fluorescent PIN reporters were introduced in *sksl,sku5* and the localization of PIN proteins is in progress by immunolabelling in the triple *sksl,sksl,sku5* mutant. Primary data suggest that the loss of function of *SKS1*, *SKS2* and *SKU5* affects at various degrees the polar localization or the turn-over of PIN proteins at the PM. If an effect on endocytosis would be confirmed, it would provide an interesting and unexpected link with an ABP1 and auxin dependent mechanism. More experiments will be required to determine whether this effect is confirmed.

The expression pattern of *SKU5*, *SKS1*, *SKS2* should be interesting to be determined at the cellular resolution in various organs, especially for *SKS2* during female gametophyte formation and embryonic development. It could be achieved by promoter investigation with transcriptional reporter or translational fusion.

4. The functions of the other members and GPI anchors

Nothing is known on other members of the SKS family and it would be interesting to develop a systematic analyses of each member. Considering the potential redundancy between

members, the functional analyses of the other members should be performed clade by clade (at phylogenetic tree). Instead of studying knock-down mutants, it would be interesting to knock-down several members of the family together using an RNAi or miRNA strategy.

No obvious phenotype alteration was found in *sks3* null mutant and *SKS9* overexpressors, no matter with or without additional GPI anchor. Nothing could be concluded by this.

For investigating importance of GPI anchor in these members, overexpressing *SKU5*, *SKS1* or *SKS2* without GPI anchor in *sks1,sku5* double mutant and observing whether they could complement the defect caused by *SKS1* and *SKU5* double mutation was also initiated.

Characterization of these plants will have to be performed to evaluate the relative importance of the GPI-anchor and also to determine the consequence of the absence of GPI-anchor on protein localization.

- Alandete-Saez, M., Ron, M., and McCormick, S.** (2008). GEX3, expressed in the male gametophyte and in the egg cell of *Arabidopsis thaliana*, is essential for micropylar pollen tube guidance and plays a role during early embryogenesis. *Mol Plant* **1**, 586-598.
- Altschul, S.F., Madden, T.L., Schaffer, A.A., Zhang, J., Zhang, Z., Miller, W., and Lipman, D.J.** (1997). Gapped BLAST and PSI-BLAST: a new generation of protein database search programs. *Nucleic Acids Res* **25**, 3389-3402.
- Altschul, S.F., Wootton, J.C., Gertz, E.M., Agarwala, R., Morgulis, A., Schaffer, A.A., and Yu, Y.K.** (2005). Protein database searches using compositionally adjusted substitution matrices. *Febs J* **272**, 5101-5109.
- Amien, S., Kliwer, I., Marton, M.L., Debener, T., Geiger, D., Becker, D., and Dresselhaus, T.** (2010). Defensin-like ZmES4 mediates pollen tube burst in maize via opening of the potassium channel KZM1. *PLoS Biol* **8**, e1000388.
- Barbez, E., Kubes, M., Rolcik, J., Beziat, C., Pencik, A., Wang, B., Rosquete, M.R., Zhu, J., Dobrev, P.I., Lee, Y., Zazimalova, E., Petrasek, J., Geisler, M., Friml, J., and Kleine-Vehn, J.** (2012). A novel putative auxin carrier family regulates intracellular auxin homeostasis in plants. *Nature* **485**, 119-122.
- Bertosa, B., Kojic-Prodic, B., Wade, R.C., and Tomic, S.** (2008). Mechanism of auxin interaction with Auxin Binding Protein (ABP1): a molecular dynamics simulation study. *Biophys J* **94**, 27-37.
- Borner, G.H., Lilley, K.S., Stevens, T.J., and Dupree, P.** (2003). Identification of glycosylphosphatidylinositol-anchored proteins in *Arabidopsis*. A proteomic and genomic analysis. *Plant Physiol* **132**, 568-577.
- Borner, G.H., Sherrier, D.J., Stevens, T.J., Arkin, I.T., and Dupree, P.** (2002). Prediction of glycosylphosphatidylinositol-anchored proteins in *Arabidopsis*. A genomic analysis. *Plant Physiol* **129**, 486-499.
- Braun, N., Wyrzykowska, J., Muller, P., David, K., Couch, D., Perrot-Rechenmann, C., and Fleming, A.J.** (2008). Conditional repression of AUXIN BINDING PROTEIN1 reveals that it coordinates cell division and cell expansion during postembryonic shoot development in *Arabidopsis* and tobacco. *Plant Cell* **20**, 2746-2762.
- Braybrook, S.A., and Harada, J.J.** (2008). LECs go crazy in embryo development. *Trends Plant Sci* **13**, 624-630.
- Breuninger, H., Rikirsch, E., Hermann, M., Ueda, M., and Laux, T.** (2008). Differential expression of WOX genes mediates apical-basal axis formation in the *Arabidopsis* embryo. *Dev Cell* **14**, 867-876.
- Butikofer, P., Malherbe, T., Boschung, M., and Roditi, I.** (2001). GPI-anchored proteins: now you see 'em, now you don't. *Faseb J* **15**, 545-548.
- Cao, Y., Tang, X., Giovannoni, J., Xiao, F., and Liu, Y.** (2012). Functional characterization of a tomato COBRA-like gene functioning in fruit development and ripening. *BMC Plant Biol* **12**, 211.
- Capaldi, R.A., Malatesta, F., and Darley-USmar, V.M.** (1983). Structure of cytochrome c oxidase. *Biochimica et biophysica acta* **726**, 135-148.
- Capron, A., Gourgues, M., Neiva, L.S., Faure, J.E., Berger, F., Pagnussat, G., Krishnan, A., Alvarez-Mejia, C., Vielle-Calzada, J.P., Lee, Y.R., Liu, B., and Sundaresan, V.** (2008). Maternal control of male-gamete delivery in *Arabidopsis* involves a putative GPI-anchored protein encoded by the LORELEI gene. *Plant Cell* **20**, 3038-3049.
- Caras, I.W., and Weddell, G.N.** (1989). Signal peptide for protein secretion directing glycopospholipid membrane anchor attachment. *Science* **243**, 1196-1198.

- Caras, I.W., Weddell, G.N., Davitz, M.A., Nussenzweig, V., and Martin, D.W., Jr.** (1987). Signal for attachment of a phospholipid membrane anchor in decay accelerating factor. *Science* **238**, 1280-1283.
- Casimiro, I., Marchant, A., Bhalerao, R.P., Beeckman, T., Dhooge, S., Swarup, R., Graham, N., Inze, D., Sandberg, G., Casero, P.J., and Bennett, M.** (2001). Auxin transport promotes Arabidopsis lateral root initiation. *Plant Cell* **13**, 843-852.
- Causier, B., Lloyd, J., Stevens, L., and Davies, B.** (2012). TOPLESS co-repressor interactions and their evolutionary conservation in plants. *Plant Signal Behav* **7**, 325-328.
- Chen, X., Naramoto, S., Robert, S., Tejos, R., Lofke, C., Lin, D., Yang, Z., and Friml, J.** (2012). ABP1 and ROP6 GTPase signaling regulate clathrin-mediated endocytosis in Arabidopsis roots. *Curr Biol* **22**, 1326-1332.
- Chen, Y.H., Li, H.J., Shi, D.Q., Yuan, L., Liu, J., Sreenivasan, R., Baskar, R., Grossniklaus, U., and Yang, W.C.** (2007). The central cell plays a critical role in pollen tube guidance in Arabidopsis. *Plant Cell* **19**, 3563-3577.
- Chiu, R.S., Nahal, H., Provart, N.J., and Gazzarrini, S.** (2012). The role of the Arabidopsis FUSCA3 transcription factor during inhibition of seed germination at high temperature. *BMC Plant Biol* **12**, 15.
- Darwin, F., and Darwin, C.** (1880). *The Power of Movement on Plants*.
- David, K., Carnero-Diaz, E., Leblanc, N., Monestiez, M., Grosclaude, J., and Perrot-Rechenmann, C.** (2001). Conformational dynamics underlie the activity of the auxin-binding protein, Nt-abp1. *J Biol Chem* **276**, 34517-34523.
- David, K.M., Couch, D., Braun, N., Brown, S., Grosclaude, J., and Perrot-Rechenmann, C.** (2007). The auxin-binding protein 1 is essential for the control of cell cycle. *Plant J* **50**, 197-206.
- Dharmasiri, N., Dharmasiri, S., and Estelle, M.** (2005). The F-box protein TIR1 is an auxin receptor. *Nature* **435**, 441-445.
- Eisenhaber, B., Bork, P., and Eisenhaber, F.** (2001). Post-translational GPI lipid anchor modification of proteins in kingdoms of life: analysis of protein sequence data from complete genomes. *Protein Engineering* **14**, 17-25.
- Eisenhaber, B., Schneider, G., Wildpaner, M., and Eisenhaber, F.** (2004). A sensitive predictor for potential GPI lipid modification sites in fungal protein sequences and its application to genome-wide studies for *Aspergillus nidulans*, *Candida albicans*, *Neurospora crassa*, *Saccharomyces cerevisiae* and *Schizosaccharomyces pombe*. *J Mol Biol* **337**, 243-253.
- Eisenhaber, B., Wildpaner, M., Schultz, C.J., Borner, G.H., Dupree, P., and Eisenhaber, F.** (2003). Glycosylphosphatidylinositol lipid anchoring of plant proteins. Sensitive prediction from sequence- and genome-wide studies for Arabidopsis and rice. *Plant Physiol* **133**, 1691-1701.
- Elkins, T., Hortsch, M., Bieber, A.J., Snow, P.M., and Goodman, C.S.** (1990). Drosophila fasciclin I is a novel homophilic adhesion molecule that along with fasciclin III can mediate cell sorting. *J Cell Biol* **110**, 1825-1832.
- Ellis, M., Egelund, J., Schultz, C.J., and Bacic, A.** (2010). Arabinogalactan-proteins: key regulators at the cell surface? *Plant Physiol* **153**, 403-419.
- Emanuelsson, O., Brunak, S., von Heijne, G., and Nielsen, H.** (2007). Locating proteins in the cell using TargetP, SignalP and related tools. *Nat Protoc* **2**, 953-971.
- Fan, L.M., Wang, Y.F., Wang, H., and Wu, W.H.** (2001). In vitro Arabidopsis pollen germination and characterization of the inward potassium currents in Arabidopsis pollen grain protoplasts. *J Exp Bot* **52**, 1603-1614.

- Ferguson, M.A., Homans, S.W., Dwek, R.A., and Rademacher, T.W.** (1988a). Glycosylphosphatidylinositol moiety that anchors *Trypanosoma brucei* variant surface glycoprotein to the membrane. *Science* **239**, 753-759.
- Ferguson, M.A., Homans, S.W., Dwek, R.A., and Rademacher, T.W.** (1988b). The glycosylphosphatidylinositol membrane anchor of *Trypanosoma brucei* variant surface glycoprotein. *Biochem Soc Trans* **16**, 265-268.
- Fujita, M., and Kinoshita, T.** (2010). Structural remodeling of GPI anchors during biosynthesis and after attachment to proteins. *FEBS Letters* **584**, 1670-1677.
- Fujita, M., and Kinoshita, T.** (2012). GPI-anchor remodeling: potential functions of GPI-anchors in intracellular trafficking and membrane dynamics. *Biochimica et biophysica acta* **1821**, 1050-1058.
- Gazzarrini, S., Tsuchiya, Y., Lumba, S., Okamoto, M., and McCourt, P.** (2004). The transcription factor FUSCA3 controls developmental timing in *Arabidopsis* through the hormones gibberellin and abscisic acid. *Dev Cell* **7**, 373-385.
- Gillmor, C.S., Lukowitz, W., Brininstool, G., Sedbrook, J.C., Hamann, T., Poindexter, P., and Somerville, C.** (2005). Glycosylphosphatidylinositol-anchored proteins are required for cell wall synthesis and morphogenesis in *Arabidopsis*. *Plant Cell* **17**, 1128-1140.
- Guilfoyle, T.J., and Hagen, G.** (2007). Auxin response factors. *Curr Opin Plant Biol* **10**, 453-460.
- Hamamura, Y., Nagahara, S., and Higashiyama, T.** (2012). Double fertilization on the move. *Curr Opin Plant Biol* **15**, 70-77.
- Harrison, S.J., Mott, E.K., Parsley, K., Aspinall, S., Gray, J.C., and Cottage, A.** (2006). A rapid and robust method of identifying transformed *Arabidopsis thaliana* seedlings following floral dip transformation. *Plant Methods* **2**, 19.
- Higashiyama, T., Yabe, S., Sasaki, N., Nishimura, Y., Miyagishima, S., Kuroiwa, H., and Kuroiwa, T.** (2001). Pollen tube attraction by the synergid cell. *Science* **293**, 1480-1483.
- Holder, A.A.** (1983). Carbohydrate is linked through ethanolamine to the C-terminal amino acid of *Trypanosoma brucei* variant surface glycoprotein. *Biochem J* **209**, 261-262.
- Holder, A.A., and Cross, G.A.** (1981). Glycopeptides from variant surface glycoproteins of *Trypanosoma Brucei*. C-terminal location of antigenically cross-reacting carbohydrate moieties. *Mol Biochem Parasitol* **2**, 135-150.
- Huber, O., and Sumper, M.** (1994). Algal-CAMs: isoforms of a cell adhesion molecule in embryos of the alga *Volvox* with homology to *Drosophila* fasciclin I. *EMBO J* **13**, 4212-4222.
- Jacobs, J., and Roe, J.L.** (2005). SKS6, a multicopper oxidase-like gene, participates in cotyledon vascular patterning during *Arabidopsis thaliana* development. *Planta* **222**, 652-666.
- Jones, A.M., and Venis, M.A.** (1989). Photoaffinity labeling of indole-3-acetic acid-binding proteins in maize. *Proc Natl Acad Sci U S A* **86**, 6153-6156.
- Kawagoe, K., Kitamura, D., Okabe, M., Taniuchi, I., Ikawa, M., Watanabe, T., Kinoshita, T., and Takeda, J.** (1996). Glycosylphosphatidylinositol-anchor-deficient mice: implications for clonal dominance of mutant cells in paroxysmal nocturnal hemoglobinuria. *Blood* **87**, 3600-3606.
- Kepinski, S., and Leyser, O.** (2005). The *Arabidopsis* F-box protein TIR1 is an auxin receptor. *Nature* **435**, 446-451.
- Ko, J.H., Kim, J.H., Jayanty, S.S., Howe, G.A., and Han, K.H.** (2006). Loss of function of COBRA, a determinant of oriented cell expansion, invokes cellular defence responses in *Arabidopsis thaliana*. *J Exp Bot* **57**, 2923-2936.

- Korasick, D.A., Enders, T.A., and Strader, L.C.** (2013). Auxin biosynthesis and storage forms. *J Exp Bot*.
- Krecek, P., Skupa, P., Libus, J., Naramoto, S., Tejos, R., Friml, J., and Zazimalova, E.** (2009). The PIN-FORMED (PIN) protein family of auxin transporters. *Genome Biol* **10**, 249.
- Kroj, T., Savino, G., Valon, C., Giraudat, J., and Parcy, F.** (2003). Regulation of storage protein gene expression in Arabidopsis. *Development* **130**, 6065-6073.
- Lalanne, E., Honys, D., Johnson, A., Borner, G.H., Lilley, K.S., Dupree, P., Grossniklaus, U., and Twell, D.** (2004). SETH1 and SETH2, two components of the glycosylphosphatidylinositol anchor biosynthetic pathway, are required for pollen germination and tube growth in Arabidopsis. *Plant Cell* **16**, 229-240.
- Laux, T., Wurschum, T., and Breuninger, H.** (2004). Genetic regulation of embryonic pattern formation. *Plant Cell* **16 Suppl**, S190-202.
- Leblanc, N., Perrot-Rechenmann, C., and Barbier-Brygoo, H.** (1999a). The auxin-binding protein Nt-ERabp1 alone activates an auxin-like transduction pathway. *FEBS Lett* **449**, 57-60.
- Leblanc, N., David, K., Grosclaude, J., Pradier, J.M., Barbier-Brygoo, H., Labiau, S., and Perrot-Rechenmann, C.** (1999b). A novel immunological approach establishes that the auxin-binding protein, Nt-abp1, is an element involved in auxin signaling at the plasma membrane. *J Biol Chem* **274**, 28314-28320.
- Li, H.J., Xue, Y., Jia, D.J., Wang, T., Hi, D.Q., Liu, J., Cui, F., Xie, Q., Ye, D., and Yang, W.C.** (2011). POD1 regulates pollen tube guidance in response to micropylar female signaling and acts in early embryo patterning in Arabidopsis. *Plant Cell* **23**, 3288-3302.
- Lobler, M., and Klamt, D.** (1985). Auxin-binding protein from coleoptile membranes of corn (*Zea mays* L.). I. Purification by immunological methods and characterization. *J Biol Chem* **260**, 9848-9853.
- Lotan, T., Ohto, M., Yee, K.M., West, M.A., Lo, R., Kwong, R.W., Yamagishi, K., Fischer, R.L., Goldberg, R.B., and Harada, J.J.** (1998). Arabidopsis LEAFY COTYLEDON1 is sufficient to induce embryo development in vegetative cells. *Cell* **93**, 1195-1205.
- Luerßen, H., Kirik, V., Herrmann, P., and Miséra, S.** (1998). FUSCA3 encodes a protein with a conserved VP1/ABI3-like B3 domain which is of functional importance for the regulation of seed maturation in Arabidopsis thaliana. *The Plant Journal* **15**, 755-764.
- Marton, M.L., Cordts, S., Broadhvest, J., and Dresselhaus, T.** (2005). Micropylar pollen tube guidance by egg apparatus 1 of maize. *Science* **307**, 573-576.
- Marton, M.L., Fastner, A., Uebler, S., and Dresselhaus, T.** (2012). Overcoming hybridization barriers by the secretion of the maize pollen tube attractant ZmEA1 from Arabidopsis ovules. *Curr Biol* **22**, 1194-1198.
- Mayor, S., and Riezman, H.** (2004). Sorting GPI-anchored proteins. *Nat Rev Mol Cell Biol* **5**, 110-120.
- McCormick, S.** (2004). Control of male gametophyte development. *Plant Cell* **16 Suppl**, S142-153.
- McDowell, M.A., Ransom, D.M., and Bangs, J.D.** (1998). Glycosylphosphatidylinositol-dependent secretory transport in *Trypanosoma brucei*. *Biochem J* **335 (Pt 3)**, 681-689.
- Messerschmidt, A., and Huber, R.** (1990). The blue oxidases, ascorbate oxidase, laccase and ceruloplasmin. Modelling and structural relationships. *Eur J Biochem* **187**, 341-352.

- Mu, J., Tan, H., Zheng, Q., Fu, F., Liang, Y., Zhang, J., Yang, X., Wang, T., Chong, K., Wang, X.J., and Zuo, J.** (2008). LEAFY COTYLEDON1 is a key regulator of fatty acid biosynthesis in Arabidopsis. *Plant Physiol* **148**, 1042-1054.
- Muniz, M., Morsomme, P., and Riezman, H.** (2001). Protein Sorting upon Exit from the Endoplasmic Reticulum. *Cell* **104**, 313-320.
- Nambara, E., Nambara, E., McCourt, P., and Naito, S.** (1995). A regulatory role for the ABI3 gene in the establishment of embryo maturation in Arabidopsis thaliana. *Development* **121**, 629-636.
- Okada, K., Ueda, J., Komaki, M.K., Bell, C.J., and Shimura, Y.** (1991). Requirement of the Auxin Polar Transport System in Early Stages of Arabidopsis Floral Bud Formation. *Plant Cell* **3**, 677-684.
- Okuda, S., Tsutsui, H., Shiina, K., Sprunck, S., Takeuchi, H., Yui, R., Kasahara, R.D., Hamamura, Y., Mizukami, A., Susaki, D., Kawano, N., Sakakibara, T., Namiki, S., Itoh, K., Otsuka, K., Matsuzaki, M., Nozaki, H., Kuroiwa, T., Nakano, A., Kanaoka, M.M., Dresselhaus, T., Sasaki, N., and Higashiyama, T.** (2009). Defensin-like polypeptide LUREs are pollen tube attractants secreted from synergid cells. *Nature* **458**, 357-361.
- Panigrahi, K.C., Panigrahy, M., Vervliet-Scheebaum, M., Lang, D., Reski, R., and Johri, M.M.** (2009). Auxin-binding proteins without KDEL sequence in the moss Funaria hygrometrica. *Plant Cell Rep* **28**, 1747-1758.
- Park, S., and Harada, J.J.** (2008). Arabidopsis embryogenesis. *Methods Mol Biol* **427**, 3-16.
- Peret, B., Swarup, K., Ferguson, A., Seth, M., Yang, Y., Dhondt, S., James, N., Casimiro, I., Perry, P., Syed, A., Yang, H., Reemmer, J., Venison, E., Howells, C., Perez-Amador, M.A., Yun, J., Alonso, J., Beemster, G.T., Laplace, L., Murphy, A., Bennett, M.J., Nielsen, E., and Swarup, R.** (2012). AUX/LAX genes encode a family of auxin influx transporters that perform distinct functions during Arabidopsis development. *Plant Cell* **24**, 2874-2885.
- Pierleoni, A., Martelli, P.L., and Casadio, R.** (2008). PredGPI: a GPI-anchor predictor. *BMC Bioinformatics* **9**, 392.
- Pittet, M., and Conzelmann, A.** (2007). Biosynthesis and function of GPI proteins in the yeast *Saccharomyces cerevisiae*. *Biochimica et biophysica acta* **1771**, 405-420.
- Poisson, G., Chauve, C., Chen, X., and Bergeron, A.** (2007). FragAnchor: a large-scale predictor of glycosylphosphatidylinositol anchors in eukaryote protein sequences by qualitative scoring. *Genomics Proteomics Bioinformatics* **5**, 121-130.
- Radford, H.E., and Mallucci, G.R.** (2010). The role of GPI-anchored PrP C in mediating the neurotoxic effect of scrapie prions in neurons. *Curr Issues Mol Biol* **12**, 119-127.
- Robert, S., Kleine-Vehn, J., Barbez, E., Sauer, M., Paciorek, T., Baster, P., Vanneste, S., Zhang, J., Simon, S., Covanova, M., Hayashi, K., Dhonukshe, P., Yang, Z., Bednarek, S.Y., Jones, A.M., Luschnig, C., Aniento, F., Zazimalova, E., and Friml, J.** (2010). ABP1 mediates auxin inhibition of clathrin-dependent endocytosis in Arabidopsis. *Cell* **143**, 111-121.
- Roudier, F., Schindelman, G., DeSalle, R., and Benfey, P.N.** (2002). The COBRA family of putative GPI-anchored proteins in Arabidopsis. A new fellowship in expansion. *Plant Physiol* **130**, 538-548.
- Roudier, F., Fernandez, A.G., Fujita, M., Himmelsbach, R., Borner, G.H., Schindelman, G., Song, S., Baskin, T.I., Dupree, P., Wasteneys, G.O., and Benfey, P.N.** (2005). COBRA, an Arabidopsis extracellular glycosyl-phosphatidyl inositol-anchored protein, specifically controls highly anisotropic expansion through its involvement in cellulose microfibril orientation. *Plant Cell* **17**, 1749-1763.

- Santner, A., and Estelle, M.** (2011). The ubiquitin-proteasome system regulates plant hormone signaling. *Plant J* **61**, 1029-1040.
- Santner, A., Calderon-Villalobos, L.I.A., and Estelle, M.** (2009). Plant hormones are versatile chemical regulators of plant growth. *Nat Chem Biol* **5**, 301-307.
- Santos Mendoza, M., Dubreucq, B., Miquel, M., Caboche, M., and Lepiniec, L.c.** (2005). LEAFY COTYLEDON 2 activation is sufficient to trigger the accumulation of oil and seed specific mRNAs in Arabidopsis leaves. *FEBS Letters* **579**, 4666-4670.
- Sardar, H.S., Yang, J., and Showalter, A.M.** (2006). Molecular interactions of arabinogalactan proteins with cortical microtubules and F-actin in Bright Yellow-2 tobacco cultured cells. *Plant Physiol* **142**, 1469-1479.
- Schiebl, C., Walther, A., Rescher, U., and Klammt, D.** (1997). Interaction of auxin-binding protein 1 with maize coleoptile plasma membranes in vitro. *Planta* **201**, 470-476.
- Schindelman, G., Morikami, A., Jung, J., Baskin, T.I., Carpita, N.C., Derbyshire, P., McCann, M.C., and Benfey, P.N.** (2001). COBRA encodes a putative GPI-anchored protein, which is polarly localized and necessary for oriented cell expansion in Arabidopsis. *Genes & Development* **15**, 1115-1127.
- Schmid, M., Davison, T.S., Henz, S.R., Pape, U.J., Demar, M., Vingron, M., Scholkopf, B., Weigel, D., and Lohmann, J.U.** (2005). A gene expression map of Arabidopsis thaliana development. *Nat Genet* **37**, 501-506.
- Schultz, C.J., Rumsewicz, M.P., Johnson, K.L., Jones, B.J., Gaspar, Y.M., and Bacic, A.** (2002). Using genomic resources to guide research directions. The arabinogalactan protein gene family as a test case. *Plant Physiol* **129**, 1448-1463.
- Sedbrook, J.C., Carroll, K.L., Hung, K.F., Masson, P.H., and Somerville, C.R.** (2002). The Arabidopsis SKU5 gene encodes an extracellular glycosyl phosphatidylinositol-anchored glycoprotein involved in directional root growth. *Plant Cell* **14**, 1635-1648.
- Seifert, G.J., and Roberts, K.** (2007). The biology of arabinogalactan proteins. *Annu Rev Plant Biol* **58**, 137-161.
- Sharma, P., Varma, R., Sarasij, R.C., Ira, Gousset, K., Krishnamoorthy, G., Rao, M., and Mayor, S.** (2004). Nanoscale Organization of Multiple GPI-Anchored Proteins in Living Cell Membranes. *Cell* **116**, 577-589.
- Shimomura, S.** (2006). Identification of a glycosylphosphatidylinositol-anchored plasma membrane protein interacting with the C-terminus of auxin-binding protein 1: a photoaffinity crosslinking study. *Plant Mol Biol* **60**, 663-677.
- Simon, S., and PetrãĖek, J.** (2011). Why plants need more than one type of auxin. *Plant Science* **180**, 454-460.
- Sindhu, A., Langewisch, T., Olek, A., Multani, D.S., McCann, M.C., Vermerris, W., Carpita, N.C., and Johal, G.** (2007). Maize Brittle stalk2 encodes a COBRA-like protein expressed in early organ development but required for tissue flexibility at maturity. *Plant Physiol* **145**, 1444-1459.
- Steffens, B., Feckler, C., Palme, K., Christian, M., Bottger, M., and Luthen, H.** (2001). The auxin signal for protoplast swelling is perceived by extracellular ABP1. *Plant J* **27**, 591-599.
- Swarup, R., and Peret, B.** (2012). AUX/LAX family of auxin influx carriers-an overview. *Front Plant Sci* **3**, 225.
- Takeuchi, H., and Higashiyama, T.** (2011). Attraction of tip-growing pollen tubes by the female gametophyte. *Curr Opin Plant Biol* **14**, 614-621.
- Tan, X., Calderon-Villalobos, L.I., Sharon, M., Zheng, C., Robinson, C.V., Estelle, M., and Zheng, N.** (2007). Mechanism of auxin perception by the TIR1 ubiquitin ligase. *Nature* **446**, 640-645.

- Thompson, J.D., Higgins, D.G., and Gibson, T.J.** (1994). CLUSTAL W: improving the sensitivity of progressive multiple sequence alignment through sequence weighting, position-specific gap penalties and weight matrix choice. *Nucleic Acids Res* **22**, 4673-4680.
- To, A., Valon, C., Savino, G., Guillemot, J., Devic, M., Giraudat, J., and Parcy, F.** (2006). A network of local and redundant gene regulation governs Arabidopsis seed maturation. *Plant Cell* **18**, 1642-1651.
- Tozeren, A., Sung, K.L., Sung, L.A., Dustin, M.L., Chan, P.Y., Springer, T.A., and Chien, S.** (1992). Micromanipulation of adhesion of a Jurkat cell to a planar bilayer membrane containing lymphocyte function-associated antigen 3 molecules. *J Cell Biol* **116**, 997-1006.
- Tomas, A., Paponov, I., and Perrot-Rechenmann, C.** (2010). AUXIN BINDING PROTEIN 1: functional and evolutionary aspects. *Trends Plant Sci* **15**, 436-446.
- Tomas, A., Braun, N., Muller, P., Khodus, T., Paponov, I.A., Palme, K., Ljung, K., Lee, J.Y., Benfey, P., Murray, J.A., Scheres, B., and Perrot-Rechenmann, C.** (2009). The AUXIN BINDING PROTEIN 1 is required for differential auxin responses mediating root growth. *PLoS One* **4**, e6648.
- Tsukamoto, T., and Palanivelu, R.** (2010). Loss of LORELEI function in the pistil delays initiation but does not affect embryo development in Arabidopsis thaliana. *Plant Signal Behav* **5**, 1487-1490.
- Tsukamoto, T., Qin, Y., Huang, Y., Dunatunga, D., and Palanivelu, R.** (2010). A role for LORELEI, a putative glycosylphosphatidylinositol-anchored protein, in Arabidopsis thaliana double fertilization and early seed development. *Plant J* **62**, 571-588.
- Ueda, M., Zhang, Z., and Laux, T.** (2011). Transcriptional activation of Arabidopsis axis patterning genes WOX8/9 links zygote polarity to embryo development. *Dev Cell* **20**, 264-270.
- Ugartechea-Chirino, Y., Swarup, R., Swarup, K., Peret, B., Whitworth, M., Bennett, M., and Bougourd, S.** (2012). The AUX1 LAX family of auxin influx carriers is required for the establishment of embryonic root cell organization in Arabidopsis thaliana. *Ann Bot* **105**, 277-289.
- Vogel, J.P., Raab, T.K., Schiff, C., and Somerville, S.C.** (2002). PMR6, a pectate lyase-like gene required for powdery mildew susceptibility in Arabidopsis. *Plant Cell* **14**, 2095-2106.
- Weitman, S.D., Lark, R.H., Coney, L.R., Fort, D.W., Frasca, V., Zurawski, V.R., Jr., and Kamen, B.A.** (1992). Distribution of the folate receptor GP38 in normal and malignant cell lines and tissues. *Cancer Res* **52**, 3396-3401.
- Wobus, U., and Weber, H.** (1999). Seed maturation: genetic programmes and control signals. *Curr Opin Plant Biol* **2**, 33-38.
- Woo, E.J., Marshall, J., Baulby, J., Chen, J.G., Venis, M., Napier, R.M., and Pickersgill, R.W.** (2002). Crystal structure of auxin-binding protein 1 in complex with auxin. *Embo J* **21**, 2877-2885.
- Woodward, A.W., and Bartel, B.** (2005). Auxin: regulation, action, and interaction. *Ann Bot* **95**, 707-735.
- Yadegari, R., and Drews, G.N.** (2004). Female gametophyte development. *Plant Cell* **16** Suppl, S133-141.
- Zanoni, I., Ostuni, R., Marek, L.R., Barresi, S., Barbalat, R., Barton, G.M., Granucci, F., and Kagan, J.C.** (2011). CD14 controls the LPS-induced endocytosis of Toll-like receptor 4. *Cell* **147**, 868-880.